2021

QUANTIFYING THE VALUE OF FOAM-BASED FLEXIBLE FLOATING SOLAR PHOTOVOLTAIC SYSTEMS

Koami Soulemane Hayibo
Michigan Technological University, khayibo@mtu.edu

QUANTIFYING THE VALUE OF FOAM-BASED FLEXIBLE FLOATING SOLAR PHOTOVOLTAIC SYSTEMS

By

Koami Soulemane Hayibo

A THESIS

Submitted in partial fulfillment of the requirements for the degree of

MASTER OF SCIENCE

In Electrical and Computer Engineering

MICHIGAN TECHNOLOGICAL UNIVERSITY

2021

This thesis has been approved in partial fulfillment of the requirements for the Degree of MASTER OF SCIENCE in Electrical and Computer Engineering.

Department of Electrical and Computer Engineering

Thesis Advisor:	*Joshua M. Pearce*
Committee Member:	*Paul L. Bergstrom*
Committee Member:	*David Watkins*
Department Chair:	*Glen E. Archer*

Table of Contents

List of figures

List of tables

Preface

This master's thesis is a collection of two papers that have been published in peer-reviewed journals. Chapter 2 is a review article that has been published in the academic journal *Renewable and Sustainable Energy Reviews* while Chapter 3 is an original research article that has been published in the academic journal *Energies*.

Title, citation, and authors' detail of the review article used for Chapter 2 are:

Title: A review of the value of solar methodology with a case study of the U.S. VOS

Citation: K. S. Hayibo and J. M. Pearce, "A review of the value of solar methodology with a case study of the U.S. VOS," (in en), *Renewable and Sustainable Energy Reviews,* vol. 137, p. 110599, 2021/03/01/ 2021, doi: 10.1016/j.rser.2020.110599.

Authors: Koami Soulemane Hayibo, Joshua M. Pearce

Authors Contributions

Hayibo: Wrote the manuscript draft; collected and reviewed articles; developed the VOS methodology; run simulations; analyzed data; plotted results; and discussed findings.

Pearce: Conceived and supervised research topic; reviewed, edited and submitted the manuscript for publication.

Title, citation, and authors' detail of the review article used for Chapter 3 are:

Title: Water Conservation Potential of Self-Funded Foam-Based Flexible Surface-Mounted Floatovoltaics

Citation: K. S. Hayibo, P. Mayville, R. K. Kailey, and J. M. Pearce, "Water Conservation Potential of Self-Funded Foam-Based Flexible Surface-Mounted Floatovoltaics," (in en), *Energies,* vol. 13, no. 23, p. 6285, 2020/01// 2020, doi: 10.3390/en13236285.

Authors: Koami Soulemane Hayibo, Pierce Mayville, Ravneet Kaur Kailey and Joshua M. Pearce

Authors Contributions

Hayibo: Wrote the manuscript draft; collected and reviewed articles; collected and cleaned data; developed the water evaporation model, developed temperature model; run

simulations on energy production and water-saving models; analyzed data; plotted results; and discussed findings.

Mayville: Wrote the manuscript draft; collected and cleaned data.

Kailey: Wrote the manuscript draft; collected and reviewed articles; and developed water evaporation model.

Pearce: Conceived and supervised research topic; reviewed, edited and submitted the manuscript for publication.

Acknowledgements

I would like to express my deepest gratitude to my advisor, Dr. Joshua Pearce, who offered me the opportunity to work and learn with him. I already had a certain interest in solar photovoltaic energy technologies before arriving at Michigan Technological University and working with Dr. Pearce has brought this interest to a whole new level.

I am very grateful to the Foreign Fulbright Program who offered me the opportunity to pursue a graduate degree in the United States and experience the American culture.

Special thanks to my committee members, Dr. Paul L. Bergstrom, and Dr. David Watkins for giving their invaluable time to make this work better.

I want to acknowledge the support of the SOLCAST team for granting free access to solar radiation data that was useful in completing this study.

I would like to extend my gratitude to my parents and siblings; especially my mother Afua Owusua for her unconditional love and care; my brother Koffi Hayibo for his continuous support; my sisters Afi and Kossiwa Hayibo, my brother Kossi Hayibo and my uncle Mouhamed Hayibor for always being there.

And to God Almighty, I am always grateful.

List of Symbols

Section 2: VOS calculation symbols

B	Burner tip fuel price	($/MMBtu)
C_D	Distribution capacity	(MW)
C_G	Utility generation capacity	(p.u.)
C_H	Health cost of natural gas	($/kWh)
C_{PV}	PV capacity for year 'n'	(kW)
C_T	Transmission capacity	(p.u.)
D	Utility Discount rate	(%)
D_E	Environmental discount rate	(%)
D_H	Heat rate degradation rate	(%)
D_{PV}	Degradation rate of PV	(%)
E	Environmental cost	($/MMBtu)
F	Utility discount factor	(%)
F_E	Environmental discount factor	(%)
h	Number of hours in the analysis period	-
H_C	Heat rate of combined cycle gas turbine	(Btu/kWh)
H_{CT}	Heat rate of peaker combustion turbine	(Btu/kWh)
H_n	Heat rate for year n	(Btu/kWh)
H_P	Heat rate of the plant	(Btu/kWh)
H_S	Solar heat rate	(Btu/kWh)
i	Number of years in analysis period	
I_C	Installation cost of combined cycle gas turbine	($/kW)
I_D	Investment on distribution capacity per year without PV	($)
I_{DP}	Investment on distribution capacity per year with PV	($)
I_P	Installation cost of peaker combustion turbine	($/kW)
K	Growth rate	(%)
M	Reserve capacity margin	(%)
n	nth year of analysis period	-
O	Output of the PV	(kWh)
PL_1	1st year load capacity	(kW)
PL_{10}	10th year load capacity	(kW)
Q	Distribution cost	($/kW)
S	PV fleet shape	(kW)
S_C	Solar capacity cost	($/kW)
U_C	Utility cost	($)
U_F	Utility fixed operation and maintenance cost	($/kW)
U_P	Utility price	($/kWh)
U_T	Utility transmission capacity cost	($/kW)
U_V	Utility variables operation and maintenance cost	($/kWh)
V_1	Avoided operation and maintenance fixed cost	($)
V_2	Avoided operation and maintenance variable cost	($)
V_3	Avoided fuel cost	($)

V_4	Avoided generation capacity cost	($)
V_5	Avoided reserve Capacity cost	($)
V_6	Avoided transmission capacity cost	($)
V_7	Avoided distribution cost	($)
V_8	Avoided environmental cost	($)
V_9	Avoided health liability	($)
VOS	Value of solar	($/kWh)

Section 3: FPV study symbols

P_a	Actual saturation vapor pressure	(kPa)
r_a	Aerodynamic resistance	(s/m)
ρ_a	Air density	(kg/m^3)
a	Albedo	-
h	Altitude	(m)
T_a	Average daily air temperature	(°C)
T_a	Average daily air temperature	(°C)
P	Average daily atmospheric pressure	(kPa)
T_d	Average daily dew temperature	(°C)
T_w	Average daily water temperature	(°C)
w_s	Average daily wind speed	(m/s)
R_{CS}	Clear sky radiation	(MJ/m^2/day)
C_f	Cloud coverage fraction	-
d_w	Effective depth of the lake	(m)
T_{eo}	Effective operating temperature	(°C)
η_{ref}	Efficiency at reference temperature	(%)
η_e	Electrical efficiency	(%)
ε	Emissivity of water	-
T_e	Equilibrium temperature	(°C)
R_{EX}	Extraterrestrial radiation	(MJ/m^2/day)
I_S	Global horizontal irradiation	(W/m^2)
R_S	Global horizontal irradiation	(MJ/m^2/day)
Cp_a	Heat capacity of air	(kJ/kg/°C)
Cp_w	Heat capacity of water	(MJ/kg/°C)
H_S	Heat storage flux	(MJ/m^2/day)
R_{IL}	Incoming longwave radiation	(MJ/m^2/day)
E_L	Lake evaporation	(mm)
λ	Latent heat of vaporization of water	(MJ/kg)
ϕ	Latitude	(rad)
$T_{a,max}$	Maximum daily air temperature	(°C)
Rh_{max}	Maximum daily relative humidity	(%)
$T_{w,max}$	Maximum daily water temperature	(°C)
P_w	Mean saturation vapor pressure	(kPa)
T_{uw}	Mean uniform temperature of water	(°C)

$T_{a,min}$	Minimum daily air temperature	(°C)
Rh_{min}	Minimum daily relative humidity	(%)
$T_{w,min}$	Minimum daily water temperature	(°C)
R_{NL}	Net longwave radiation	(MJ/m^2/day)
$R_{N,wb}$	Net radiation at wet-bulb temperature	(MJ/m^2/day)
R_{NS}	Net shortwave radiation	(MJ/m^2/day)
R_N	Net solar radiation	(MJ/m^2/day)
R_{OL}	Outgoing longwave radiation	(MJ/m^2/day)
$R_{OL,wb}$	Outgoing longwave radiation at wet-bulb temperature	(MJ/m^2/day)
P_{out}	Output power	(W)
A_P	Photovoltaic surface	(m^2)
η_P	Photovoltaic system efficiency	(%)
γ	Psychrometric constant	(kPa/°C)
T_{ref}	Reference temperature	(°C)
Δ_{wb}	Saturation vapor pressure curve at wet-bulb temperature	(kPa/K)
Δ	Slope of saturation vapor pressure curve	(kPa/°C)
σ	Stephan–Boltzmann constant	(MJ/m^2/K^4/day)
A	Surface of the lake	(m^2)
β	Temperature coefficient of the PV panel	(%/°C)
τ	Time constant	(day)
Δt	Time step	(h/day)
ρ_w	Water density	(kg/m^3)
T_{wb}	Wet-bulb temperature	(°C)
f_w	Wind function	(MJ/m^2/kPa/day)

Abstract

Distributed generation with solar photovoltaic (PV) technology is economically competitive if net metered in the U.S. Yet there is evidence that net metering is misrepresenting the true value of distributed solar generation so that the value of solar (VOS) is becoming the preferred method for evaluating economics of grid-tied PV. VOS calculations are challenging and there is widespread disagreement in the literature on the methods and data needed. To overcome these limitations, this thesis reviews past VOS studies to develop a generalized model that considers realistic future avoided costs and liabilities. The approach used here is bottom-up modeling where the final VOS for a utility system is calculated. The avoided costs considered are: plant O&M fixed and variable; fuel; generation capacity, reserve capacity, transmission capacity, distribution capacity, and environmental and health liability. The VOS represents the sum of these avoided costs. Each sub-component of the VOS has a sensitivity analysis run on the core variables and these sensitivities are applied for the total VOS. The results show that grid-tied utility customers are being grossly under-compensated in most of the U.S. as the value of solar eclipses the net metering rate as well as two-tiered rates. It can be concluded that substantial future work is needed for regulatory reform to ensure that grid-tied solar PV owners are not unjustly subsidizing U.S. electric utilities.

Even without regulatory reform PV is economic, yet to further accelerate PV deployment the economics of PV systems can be improved. One approach to doing this also provides a potential solution to the coupled water–energy–food challenges in land use with the concept of floating photovoltaics or floatovoltaics (FPV). In this thesis, a new approach to FPV is investigated using a flexible crystalline silicon-based FPV module backed with foam, which is less expensive than conventional pontoon-based FPV. This novel form of FPV is tested experimentally for operating temperature and performance and is analyzed for water-savings using an evaporation calculation adapted from the Penman–Monteith model. The results show that the foam-backed FPV had a lower operating temperature than conventional pontoon-based FPV, and thus a 3.5% higher energy output per unit power. Therefore, foam-based FPV provides a potentially profitable means of reducing water evaporation in the world's at-risk bodies of fresh water. The case study of Lake Mead found that if 10% of the lake was covered with foam-backed FPV, there would be enough water conserved and electricity generated to service Las Vegas and Reno combined. At 50% coverage, the foam-backed FPV would provide over 127 TWh of clean solar electricity and 633.22 million m^3 of water savings, which would provide enough electricity to retire 11% of the polluting coal-fired plants in the U.S. and provide water for over five million Americans, annually. Overall foam-backed FPV thus brings an even greater VOS than conventional PV and indicates that FPV will play a much larger role in our energy future.

1 Introduction

1.1 Contextualization

In the context of world energy production, solar photovoltaic (PV) energy has proven to be competitive in terms of energy pricing when compared to fossil fuel energy sources [1]. Continuous technical improvement of the existing technologies, development of new technologies, and coupling of solar PV technologies with other activities such as agriculture or water conservation will further drive down the cost of solar PV energy in the coming decades. One of the main advantages of solar photovoltaic energy is its distributed nature. Solar PV energy generation systems can be installed near the consumption site, therefore reducing the energy losses associated with transmission and distribution [2]. Furthermore, when compared to energy produced from fossil fuels, solar energy has been demonstrated to have far less environmental and health impact [3]. The Intergovernmental Panel on Climate Change (IPCC) has stated that the migration to renewable energy sources is central to mitigating climate change [4]. However, these advantages are often not reflected in the way distributed solar energy is valued. The most commonly used rate design by utilities to compensate solar customers throughout the United States (U.S.) is net metering. Net metering rate design provides at best a compensation equal to the retail price of electricity [5]. When the electricity production of the utility originates from fossil fuels, this means that the distributed solar electricity is valued at the same price or less than fossil fuels sources, therefore misrepresenting the true value of solar *(VOS)* [6-8].

On the other hand, one of the challenges solar PV systems need to overcome to become even more environmentally friendly and low cost is land-use. Land occupation can be a limit to the installed PV capacity, especially when the solar PV system's location conflicts with other essential activities such as agriculture [9]. There is new research geared towards reducing the land use impact of solar systems. A recent approach has investigated the combination of solar PV systems and agriculture called "agrivoltaics" [10], while several other studies are looking into the installation of solar PV systems on open water, called floating photovoltaic (FPV) or floatovoltaics, to solve the land-use challenges [11-17]. When a solar PV system is installed on a water surface, it will provide a boost in the energy production and contribute to the prevention of water loss due to evaporation [18-21]. Even though the racking used in floating solar PV systems is less expensive compared to land-based systems [22], the use of lower cost materials such as foam in floating PV systems can reduce the cost even more.

1.2 Goal and Scope

This study is part of a larger project that aims at investigating the economic and environmental viability of foam-based floating PV systems. The project has different components: the literature review of the value of solar, the after-market conversion of a

flexible photovoltaic panel into a flexible floating photovoltaic panel using foam-based racking, the experimental study of the energy production and water conservation potential of the foam-based FPV, the life cycle analysis of the FPV system, and the economic viability of the FPV systems using value of solar methodology.

The current study covers the review of value of solar and the experimental study of the energy production and water conservation potential of the foam-based FPV. The scope of the study is as follows:

- Value of Solar
    - Conduct a review of the existing methods used to calculate *VOS*;
    - Develop a generalized *VOS* model;
    - Study the VOS for the case of the United States using realistic values from the literature.
- Energy production and water conservation potential of foam-based FPV
    - Evaluate the water saving potential of the foam-based FPV using a modified Penman-Monteith model;
    - Develop an operating temperature model for the foam-based flexible FPV module;
    - Use the operating temperature model to study the energy production of the FPV module;
    - Apply the energy production model and the water conservation model to the case of Lake Mead.

Following these steps, it is expected to find a range of *VOS* design rates across the U.S. and compare those values with *VOS* and net metering values used in some states. On the other hand, the goal for studying the foam-based FPV modules is to establish the cooling effect of water on the modules, to evaluate the energy production of the modules, and to estimate the water saving capability of foam-based FPV systems.

1.3 Structure of the study

After the introduction, Chapter 2 of this study is dedicated to the review of value of solar methodology with a case study of the United States. In Chapter 2, the existing research on *VOS* is summarized and the formula used for different *VOS* components are detailed, and a sensitivity analysis is run using realistic values for the U.S. Chapter 3 focuses on the water conservation potential of self-funded foam-based flexible FPV. The water conservation model, the data collection procedure, the proposed FPV cell operating temperature model, and energy production model are described. Finally, Chapter 4 summarizes the findings, describes the challenges encountered during this study, and lists future work that could improve the study.

2 A review of the value of solar methodology with a case study of the U.S. VOS

2.1 Introduction

Solar photovoltaic (PV) technologies have had a rapid industrial learning curve [23-26], which has resulted in continuous cost reductions and improved economics [27, 28]. This constant cost reduction pressure has resulted in a spot price of polysilicon Chinese-manufactured PV modules of only US$0.18/W as of April 2020 [29]. There are several technical improvements, which are both already available and slated to drive the costs further down such as black silicon [30-32]. The International Renewable Energy Agency (IRENA) can thus confidently predict that PV prices will fall by another 60% in the next decade [33]. However, even at current prices, any scale of PV provides a levelized cost of electricity (LCOE) [34] lower than the net metered cost of grid electricity [35], and this will only improve with storage costs declining[36-40]. Specifically, PV already provides a lower levelized cost of electricity [34, 41, 42] than coal-fired electricity [35, 43, 44]. In addition, PV technology can be inherently distributed (e.g. each electricity consumer produces some or all of their electricity on site thus becoming 'prosumers'). Distributed generation with PV has several technical advantages, including improved reliability, reduced transmission losses [45, 46], enhanced voltage profile, reduced transmission and distribution losses [47], transmission and distribution infrastructures deferment, and enhanced power quality [48]. As PV prices decline, prices of conventional fossil fuel-based electricity production are increasing due to aging infrastructure [49-51], increased regulations (in some jurisdictions) [52-55], fossil fuel scarcity [56-58], and pollution costs [59-63]. Thus, PV represents a threat to conventional utility business models [64] and there is evidence that some utilities are manipulating rates to discourage distributed generation with solar [65], while others are embracing it such as in Austin, Texas or the state of Minnesota [66]. Rates structures vary widely throughout the U.S. [67-70] and there has been significant effort to determine the actual value of solar (*VOS*) electricity.

This shift towards *VOS* is fueled by criticisms of its predecessor [71], net metering, that is misrepresenting the true value of distributed solar generation [6-8]. *VOS* is more representative of the electricity cost because under a Value of Solar Tariff (VOST) scheme, the utility purchases part of, or the whole net solar photovoltaic electricity generation from its customers, therefore dissociating the VOST from the electricity retail price [7, 72]. Performing a complete *VOS* calculation, however, is challenging. One of the main challenges is data availability and accuracy [73, 74]. Three data challenges that have been identified by [74] are: 1) the time granularity of the solar irradiation data, 2) the origin of the data, modeled versus measured, and 3) the data measurement accuracy. Other challenges faced by utilities while assessing the *VOS* are which components to include in the calculations, and what calculation methods to assess the value of each component [5]. The possible components across the literature that are suggested to be included in a *VOS*

as avoided costs and solar benefits are: **energy production costs** (operation and maintenance) [67-69, 75-81], **electricity generation capacity costs** [6, 67-69, 75-81], **transmission capacity costs** [6, 67-69, 75-79, 81], **distribution capacity costs** [6, 67-69, 75-81], **fuel costs** [6, 67-69, 75, 78-81], **environmental costs** [67, 69, 75, 76, 78-81], **ancillary including voltage control benefits** [67, 75-77, 81], **solar integration costs** [69], **market price reduction benefits** [69, 78], **economic development value or job creation** [68, 69, 75, 78, 79], **health liability costs** [75, 78, 82]**,** and **value of increased security** [69, 75]. A guidebook has been developed by the United States' Interstate Renewable Energy Council (IREC) for the calculation of several of the *VOS* components [75]. These methods have been further developed by the U.S. National Renewable Energy Laboratory (NREL) [76]. NREL has provided more detailed calculation methods than the guidebook from the IREC with a different level of accuracy. The methods with a higher level of accuracy are more complicated to implement and require a higher level of data granularity. A qualitative study on *VOS* performed in 2014 suggested the inclusion of all relevant components in a *VOS* studies [82]. The calculation of the *VOS* can be done annually, as in the case of Austin Energy [6, 72], or can be fixed for a selected period, as per the case of Minnesota state's *VOS* (25 years) [67, 72]. There are recently an increasing number of studies looking into externality-based components of *VOS,* especially environmental costs and health liability costs [83-85]. This is because a country with high solar PV penetration rate provides a healthy population according to a German study [86]. An estimated average of 1,424 lives could be saved each summer in the Eastern United States, and $13.1 billion in terms of health savings if the total electricity generation capacity in the Eastern United States included 17% of solar PV [87]. For the entire U.S., if coal-fired electricity were replaced with solar generation, roughly 52,000 premature American deaths would be prevented from reduced air pollution alone [88]. Not surprisingly, the latest report from North Carolina Clean Energy Technology Center found out that there are policy changes on *VOS* across the United States with 46 states, in addition of D.C., considering making significant changes in their solar policies and transitioning to a *VOS* model in coming years [81].

This indicates *VOS* is the way of the future for grid integrated PV, but how exactly should solar be valued on the modern grid? In this study the *VOS* literature is reviewed, and a generalized model is developed taking realistic future avoided costs and liabilities into account from the literature. The approach used here is a bottom-up modeling where the final value of solar to a utility system is calculated. This model factors in the existing parameters, that have been identified in *VOS* studies in different U.S. jurisdictions. The approach starts from the existing formula to calculate the levelized cost of electricity from solar PV technology [34] and updates the formula by adding the avoided and opportunity costs and the effect of different externalities. The costs considered in the study are: avoided plant operation and maintenance (O&M) fixed cost; avoided O&M variable cost; avoided fuel cost; avoided generation capacity cost, avoided reserve capacity cost, avoided transmission capacity cost, avoided distribution capacity cost, avoided environmental cost, and the avoided health liability cost. The value of solar represents the sum of these costs.

Each sub-component of the *VOS* has a sensitivity analysis run on the core variables and these sensitivities are applied for the total *VOS*. The results are presented and discussed in the context of aligning policy and regulations with appropriate compensation for PV-asset owners and electric utility customers.

2.2 Methods and Theory

2.2.1 Avoided Plant O&M – Fixed Cost *(V_1)*

The use of solar energy results in a displacement of energy production from conventional energy sources. The avoided cost of plant operation and maintenance *(V_1)* (\$) depends on the energy saved by using solar PV for electricity generation instead of conventional energy generation processes. Equation (2.1) describes the calculation of the capacity of solar PV *(C_{PV})* (kW) throughout the lifetime of the solar PV system. During the first year of operation, the installed solar PV system is considered to not have suffered any degradation. Therefore, the capacity has a value of one. The degradation of the installed solar PV system is expressed by the degradation rate of PV *(D_{PV})* and for a marginal year *(n)*, the marginal capacity of the installed PV system for that year would be:

$$C_{PV} = (1 - D_{PV})^n \qquad \text{(kW)} \tag{2.1}$$

The fixed O&M cost is directly linked to the need for new conventional electricity generation plants. If the construction of new conventional generators in the location of interest can be avoided, there is no need to include the fixed O&M in the valuation of solar for this location. To calculate the value of the fixed O&M *(V_1)*, the value of the utility cost *(U_C)* (\$) needs to be known first. The utility cost depends on four parameters, the capacity of solar PV *(C_{PV})* mentioned above, the utility capacity *(C_G)* (per unit [p.u.]), the utility fixed O&M cost *(U_F)* (\$/kW), and the utility discount factor *(F)*. To calculate this utility cost, first the ratio of the capacity of solar to the utility capacity is calculated. This ratio is then multiplied by the utility fixed O&M cost. A discount is applied to the result by multiplying it by the utility discount factor [89]. The discount factor *(F)* depends on the year and can be calculated by using the discount rate *(D)*. The discount factor for year *(n)* is [67]:

$$F = \frac{1}{(1 + D)^n} \tag{2.2}$$

The discount rate used in the formula describes the uncertainty and the fluctuation of the value of money in time. The value of the discount rate differs when considered from a utility point of view or a societal point of view and can highly impact the utility cost. While considering the economics of solar PV systems, [75] has suggested the use of a discount

rate lower than the value used by the utility. This is because low discount rates are more suitable for projects that have a high initial investment cost and a low operation and end-of-life cost, such as solar PV systems.

$$U_C = U_F \times \frac{C_{PV}}{C_G} \times F \qquad (\$) \tag{2.3}$$

The avoided plant O&M fixed cost *(V_1)* is then calculated by summing the discounted utility cost for all the years included in the analysis period.

$$V_1 = \sum_0^i U_C \qquad (\$) \tag{2.4}$$

2.2.2 Avoided Plant O&M – Variable Cost *(V_2)*:

The utility cost for the avoided variable O&M cost *(V_2)* ($) is calculated by multiplying the utility variable O&M cost *(U_V)* ($/kWh) by the energy saved by using solar PV systems or the output of the solar PV system *(O)* (kWh), and the result is discounted by the discount factor *(F)*.

$$U_C = U_V \times O \times F \qquad (\$) \tag{2.5}$$

The avoided variable O&M *(V_2)* cost is the sum of the utility cost over the analysis period:

$$V_2 = \sum_0^i U_C \qquad (\$) \tag{2.6}$$

2.2.3 Avoided Fuel Cost *(V_3)*

Additionally, the calculation of the utility price *(U_P)* ($/kWh) requires the knowledge of the equivalent heat rate of a marginal solar. According to [90], the heat rate (Btu/kWh) describes how much fuel-energy, on average, a generator uses in order to produce 1kWh of electricity. It is typically used in the energy calculation of thermal-based plants and is therefore misleading for the calculation of solar energy production. Since the method evaluates the avoided cost from thermal-based plants, however, it is applied to solar PV generation. The heat rate *(H_S)* (Btu/kWh) of solar PV or displaced fuel heat rate during the first marginal year is calculated as:

$$H_S = \frac{\sum_0^h (H_p \times S)}{\sum_0^h S} \qquad (\text{Btu/kWh}) \tag{2.7}$$

In the equation above, the heat rate *(H_p)* (Btu/kWh) represents the real value of the utility plant's heat rate during the operation hours of the solar PV systems over the analysis period, and the parameter *(S)* (kW) describes the hourly PV fleet shape production over the hours *(h)* in the analysis period.

After the heat rate for the first year has been calculated, the heat rate for the succeeding years in the analysis period can be calculated by the following equation [67][45]:

$$H_n = H_S \times (1 - D_H)^n \qquad \text{(Btu/kWh)} \tag{2.8}$$

The primary use of heat rates is the assessment of the thermal conversion efficiency of fuel into electricity by conventional power plants. As a result, it is natural to deduce that the rate at which the heat rate (D_H) decreases corresponds to the efficiency loss rate of the power plant [91].

The utility price (U_P) depends on the heat rates and can be calculated once the heat rate is known as:

$$U_P = \frac{B \times H_n}{10^6} \qquad (\$/\text{kWh}) \tag{2.9}$$

Another parameter to account for is the burner tip price (B) ($/MMBtu). The burner tip price describes the cost of burning fuel to create heat in any fuel-burning equipment [92].

The avoided fuel cost (V_3) ($) is calculated in a similar way as the value of the fixed O&M. First, the utility cost is calculated by multiplying the value of the per unit PV output (O) by the utility price (U_P). The result is then discounted by the discount factor. The discount factor used in the case of the avoided fuel cost depends on the treasury yield [67]. The avoided fuel cost is obtained by summing up the utility cost over the analysis period.

$$U_C = U_P \times O \times F \qquad (\$) \tag{2.10}$$

$$\mathrm{V}_3 = \sum_0^i U_C \qquad (\$) \tag{2.11}$$

2.2.4 Avoided Generation Capacity Cost (V_4):

The installation of solar systems reduces the generation of electricity from new plants. This is represented by the avoided capacity cost. To calculate the avoided generation capacity cost, the solar capacity cost (S_C) ($/kW) needs to be known. Two variables are essential to evaluate the solar capacity cost, the cost of peaker combustion turbine (I_P) ($/kW) and the installed capital cost (I_C) ($/kW). The cost of peaker combustion turbine (I_P) is the cost associated with the operation of a turbine that functions only when the electricity demand is at its highest. The installed capital cost (I_C) describes the cost of combined cycle gas turbine updated by the cost based on the heat rate. The solar capacity can be calculated as follows [93]:

$$S_C = I_C + (H_S - H_C) \times \frac{I_P - I_C}{H_{CT} - H_C} \qquad (\$/\text{kW}) \tag{2.12}$$

H_{CT} (Btu/kWh) and H_C (Btu/kWh) are respectively the heat rate of the peaker combustion turbine, and the combined cycle gas turbine. After the calculation of the solar capacity cost *(S_C)*, the utility cost can be obtained by first, multiplying the ratio of solar PV capacity *(C_{PV})* and utility generation capacity *(C_G)* by the value of solar capacity cost *(S_C)*. Then, the result is discounted by the discount factor *(F)* to obtain the final value of the utility cost. And as in the previous cases the value of avoided generation capacity is the sum of the utility cost over the analysis period.

$$U_C = S_C \times \frac{C_{PV}}{C_G} \times F \qquad (\$) \tag{2.13}$$

$$\mathrm{V}_4 = \sum_0^i U_C \qquad (\$) \tag{2.14}$$

2.2.5 Avoided Reserve Capacity Cost *(V_5)*:

The calculation of the avoided reserve capacity cost *(V_5)* ($) follows the same pattern as the avoided cost of generation capacity. But in this case, the effective solar capacity, that is the ratio of the solar PV capacity *(C_{PV})* and utility generation capacity *(C_G)* is multiplied by the solar capacity cost, and then the result is multiplied by the reserve capacity margin *(M)* to obtain the utility costs. After that, the utility cost is discounted as previously described by the discount factor *(F)*. Then, the avoided reserve capacity is calculated by adding up the utility cost over the analysis period [76].

$$U_C = S_C \times \frac{C_{PV}}{C_G} \times M \times F \qquad (\$) \tag{2.15}$$

$$V_5 = \sum_0^i U_C \qquad (\$) \tag{2.16}$$

2.2.6 Avoided Transmission Capacity Cost *(V_6)*:

The avoided transmission capacity cost *(V_6)* ($) calculation is also performed similarly to the avoided generation capacity cost. This cost describes the losses that are avoided when electricity does not have to be transported on long distance because of installed solar systems. It is calculated by first multiplying the utility transmission capacity cost *(U_T)* ($/kW) by the solar PV capacity *(C_{PV})*. The result is then divided by the transmission capacity *(C_T)* (p.u.) and the discount factor *(F)* is applied to obtain the utility cost for a marginal year. The avoided transmission cost is calculated by the sum, over the years in the analysis period, of the corresponding utility costs [94].

$$U_C = U_T \times \frac{C_{PV}}{C_T} \times F \qquad (\$) \tag{2.17}$$

$$V_6 = \sum_0^i U_C \qquad (\$) \tag{2.18}$$

2.2.7 Avoided Distribution Capacity Cost *(V_7)*:

The two major variables that influence the avoided distribution capacity cost *(V_7)* ($) are the peak growth rate *(K)* and the system-wide costs. The system-wide costs account for several financial aspects of a distribution plant, which include overhead lines and devices, underground cables, line transformers, leased property, streetlights, poles, towers etc. [95].

All the deferrable system wide costs throughout a year have been summed up and the result divided by the yearly peak load increase in kW over a total period of a decade to obtain the distribution cost per growth of demand.

The ratio of the 10th year peak load *(PL_{10})* (kW) and the 1st year peak load *(PL1)* (kW) are used in the calculation of the growth rate *(K)* of demand. The expression of the growth rate *(K)* is as follows [67, 96]:

$$K = \left(\frac{PL_{10}}{PL_1}\right)^{\frac{1}{10}} - 1 \tag{2.19}$$

The distribution capital cost *(Q)* ($/kW) is utility owned data and depends on the utility, and the growth rate *(K)* that can be obtained by using the previous formula. An escalation factor is necessary to evaluate the distribution cost for deferral consecutive years [97].

After obtaining the distribution cost *(Q)* from the utility and the growth rate *(K)* is calculated, the distribution capacity *(C_D)* (kW) can be calculated from the growth rate. The result is then multiplied by the distribution cost and discounted by the discount factor *(F)* to get the discounted cost for a particular year. The discounted cost for the analysis period can in turn be used to calculate the investment during each year *(I_D)* ($) of the analysis period [67].

$$I_D = C_D \times Q \times F \qquad (\$) \tag{2.20}$$

When there is no other generation system than solar PV that comprised the installed capacity, the investment per year *(I_{DP})* ($) in terms of deferred distribution can be calculated from the investment deferred [67].

$$I_{DP} = C_D \times Q \times DF \qquad (\$) \quad \text{(in terms of deferred distribution)} \tag{2.21}$$

After obtaining the yearly investment without PV *(I_D)* and the yearly investment in terms of deferred distribution *(I_{DP})*, the utility cost can be obtained by dividing the difference between the yearly investment without PV and the yearly investment with PV by the distribution capacity *(C_D)*. This utility cost can be called the deferred cost per kW of solar. This deferred cost per kW of solar is discounted by the discount factor *(F)*, multiplied by

the solar PV capacity, and summed over the analysis period to obtain the avoided distribution capacity cost.

$$U_C = \frac{I_D - I_{DP}}{C_D} \times F \times C_{PV} \qquad (\$) \tag{2.22}$$

$$V_7 = \sum_0^i U_C \qquad (\$) \tag{2.23}$$

2.2.8 Avoided Environmental Cost *(V_8)*:

The four major pollutants that are considered in the calculation of the avoided environmental cost *(V_8)* ($) are: greenhouse gases (GHGs), sulfur dioxide, nitrogen oxide, and hazardous particulates [98].

The two parameters that influence the cost linked to CO_2 and other greenhouse gas emissions are the social cost of CO_2 and the gas emission factor [99]. With these two variables, the cost of avoided CO_2 can be calculated in dollars and then the real value linked to this cost is obtained by converting the previously calculated value in current value of dollars. This is done by multiplying the externality cost of CO_2 by the consumer price index (CPI) [100]. The obtained result is then multiplied by the general escalation rate for the following years [98]. The cost of CO_2 for every year is obtained by multiplying the previous value by pounds of CO_2 per kWh. The same logic is applied to the other pollutants to calculate the related costs and the cost related to all three categories of pollutant are added up to get the environmental cost *(E)* ($/MMBtu).

By multiplying the environmental cost by the solar heat rate *(H_S)*, the utility cost *(U_C)* is obtained. An environmental discount factor *(F_E)* is applied to the utility factor. The environmental discount factor *(F_E)* is defined as follows [101]:

$$F_E = \frac{1}{(1 + D_E)^n} \tag{2.24}$$

Here, D_E is the environmental discount rate taken from the Social Cost of Carbon report [99].

$$U_C = E \times H_S \times F_E \times O \qquad (\$) \tag{2.25}$$

$$V_8 = \sum_0^i U_C \qquad (\$) \tag{2.26}$$

2.2.9 Avoided health liability cost *(V_9)*:

The use of solar PV systems prevents part of the emissions of pollutants from getting into the air. This can in turn result in great health benefits. The harmful pollutants that greatly

impact human health are NO_x and SO_2. These two chemicals react with other compounds when they are released in the air to form a heavy and harmful product that is called particulate matter $PM_{2.5,}$ [102-104]. Particulate matter $PM_{2.5,}$ can cause diseases such as lung cancer and cardiopulmonary diseases [105]. It is difficult to evaluate the cost related to the avoided health liabilities and the saved lives. Several works have investigated the calculation of the cost of human health related to electricity production through fossil fuels [106-109]. Nevertheless, the most relevant approach is the work of [109] because the methods account for changes of the cost at a regional and plant level. This has been made possible because of data collected by EPA on the emission level of facilities through the Clean Air Markets Program. The result obtained by [109] is conservative as it does not include environmental impacts over the long term (e.g. climate change) [84, 86, 87, 110]. The calculation of the cost of health liability by [109] depends on the quantity of pollutants emitted (tons/year) during a year, the cost of a unit mass of emission for each pollutant in ($/tons), and the annual gross load (kWh/year).

The health cost of energy produced by fossil fuel sources *(C_H)* ($/kWh) obtained by [109] are used to calculate the utility cost. The utility cost *(U_C)* is the product of the health cost by the PV systems output *(O)*, that is discounted by the environmental discount factor *(F_E)*.

$$U_C = C_H \times O \times F_E \qquad (\$) \tag{2.27}$$

The avoided health liability cost *(V_9)* ($) is then calculated by:

$$V_9 = \sum_0^i U_C \qquad (\$) \tag{2.28}$$

2.2.10 Value of solar *(VOS)*

There are three different ways to represent the value of solar. It can be expressed either as the annual cost ($) over the analysis period or the lifetime of the installed solar photovoltaic system, or as the cost per unit of solar PV power installed ($/kW), or finally as the cost of generated electricity by the solar system ($/kWh) [76]. The most commonly used metric to express the *VOS* is the cost of electricity generated by the solar system ($/kWh) because it is user-friendly and is the same metric used by utilities on electricity bills [76]. To calculate the levelized value of *VOS* per kilowatt-hour of electricity produced, the sum of the value of all the avoided cost is calculated and then divided by the total amount of energy produced *(O)* during the analysis period discounted by the discount factor *(F)*.

$$VOS = \frac{V_1 + V_2 + V_3 + V_4 + V_5 + V_6 + V_7 + V_8 + V_9}{\sum_0^i (O \times F)} \qquad (\$/\text{kWh}) \tag{2.29}$$

Where:

- V_1: Avoided O&M fixed cost

- V_2: Avoided O&M variable cost
- V_3: Avoided fuel cost
- V_4: Avoided generation capacity cost
- V_5: Avoided reserve capacity cost
- V_6: Avoided transmission capacity cost
- V_7: Avoided distribution cost
- V_8: Avoided environmental cost
- V_9: Avoided health liability cost
- O: Output of the solar PV system
- F: Utility discount factor

2.3 Sensitivity

The calculation of *VOS* requires several parameters that come from different sources. Some parameters are location-dependent, while other parameters are state-dependent, and there are parameters that are utility-dependent. Many of these parameters can also change from one year to another. As a result, there are wide differences in the calculation of *VOS* across the literature [5]. The utility-related parameters that can change from one *VOS* calculation to another are the number of years in the analysis period *(i)*, the utility discount rate *(D)*, the utility degradation rate, the utility O&M fixed, and variable costs, the O&M cost escalation rate, the hourly heat rate (H_P), the heat rate degradation rate (D_H), the reserve capacity margin *(M)*, the transmission capacity cost (U_T), the peak load of year 1 (PL_1) and year 10 (PL_{10}), the distribution cost *(Q)*, the distribution cost escalation factor (G_D), and the distribution capacity (C_D). Parameters such as the cost of peaker combustion turbine (I_P), the cost of combine cycle gas turbine (I_C), the heat rate of peaker combustion turbine (H_{CT}), and the heat rate of combine cycle gas turbine (H_C) can be either obtained from the utility or from the U.S. Energy Information Agency. The solar PV fleet *(S)* can also be obtained from the utility or by simulation using the open source Solar Advisory Model (SAM) (https://github.com/NREL/SAM) [67]. Other variables that can affect the *VOS* but are not controlled by the utility are the PV degradation rate (D_{PV}), the environmental discount factor (F_E), the environmental cost of conventional energy, the health cost of conventional energy, and the cost of natural gas on the energy market. Table 2.1 summarizes high and low estimates of the values for the variables that are required to perform a *VOS* calculation and the *VOS* component they are used to calculate.

Table 2.1. Assumptions used for required variables for a VOS calculation.

Variable	**High estimate**	**Source**	**Low estimate**	**Source**	***VOS* components**
Degradation rate of PV (DPV) (%)	1	[111]	0.5	[75, 111, 112]	All components

Distribution capacity *(C_D)* (kW)	429,000	[113]	237,000	[113]	Avoided distribution cost *(V_7)*
Distribution cost *(Q)* ($/kW)	1,104	[113]	678	[113]	Avoided distribution cost *(V_7)*
Environment discount rate *(D_E)* (%)	2.5	[99]	5	[99]	Avoided environmental cost *(V_8)*
Environmental Cost *(E)* ($/metric tons of CO_2)	62-89	[99]	12-23	[99]	Avoided environmental cost *(V_8)*
Health cost of natural gas *(C_H)* ($/kWh)	0.025	[109]	0.025	[109]	Avoided health liability cost *(V_9)*
Heat rate degradation rate *(D_H)* (%)	0.2	[114]	0.05	[114]	• Avoided fuel cost *(V_3)* • Avoided environmental cost *(V_8)*
Heat rate of combined cycle gas *(H_C)* (Btu/kWh)	7,627	[115]			• Avoided generation capacity cost *(V_4)* • Avoided reserve capacity cost *(V_5)*
Heat rate of peaker combustion turbine *(H_{CT})* (Btu/kWh)	11,138	[115]			• Avoided generation capacity cost *(V_4)* • Avoided reserve capacity cost *(V_5)*
Installation capital cost of combined cycle gas turbine *(I_C)* ($/kW)	896	[116]			• Avoided generation capacity cost *(V_4)* • Avoided reserve capacity cost *(V_5)*
Installation cost of peaker combustion turbine *(I_P)* ($/kW)	1,496	[116]			• Avoided generation capacity cost *(V_4)* • Avoided reserve capacity cost *(V_5)*
Load Growth Rate *(K)* (%)	1.17	[117]	-0.94	[117]	Avoided distribution capacity cost *(V_7)*

Number of years in analysis period	30	[75]	25	PV industry warranties	All components
Reserve capacity margin *(M)* (%)	36	[118]	13	[118]	Avoided reserve capacity *(V_5)*
Solar Heat Rate *(H_S)* (Btu/kWh)	8,000	[72]			• Avoided fuel cost *(V_3)* • Avoided generation capacity cost *(V_4)* • Avoided reserve capacity cost *(V_5)* • Avoided environmental cost *(V_8)*
Transmission capacity cost *(U_T)* ($/kW)	130.535	[119]	17.895	[119]	Avoided transmission capacity *(V_6)*
Utility Discount rate *(D)* (%)	9	[75]	2.18	[75]	• Avoided plants O&M fixed cost *(V_1)* • Avoided plants O&M variable *(V_2)* • Avoided generation capacity cost *(V_4)* • Avoided reserve capacity cost *(V_5)* • Avoided transmission capacity cost *(V_6)* • Avoided distribution capacity cost *(V_7)*
Utility fixed O&M cost *(U_F)* ($/kW)	18.86	[113]	7.44	[113]	Avoided O&M fixed cost *(V_1)*
Utility variable O&M cost *(U_V)* ($/kWh)	0.01153	[113]	0.00216	[113]	Avoided O&M variable cost *(V_2)*

2.3.1 Number of years in analysis period

The number of years in the analysis period varies and can be as low as 20 years, and as high as 30 years or more [34, 75]. The typical warranty provided by solar panels manufacturer is 25 years. As a result, it is reasonable to set the lowest value of the analysis period to 25 years. Also, solar modules have proved to continue to reliably deliver energy 30 years after the installation of the system [75], therefore, 30 years has been set as the higher value of the analysis period in this study. Keyes et al. have pointed out that utility planning is often over shorter time periods (e.g. 10-20 years) [75]. However, economic decisions should be made over the entire life of the physical project not an arbitrary cutoff date [120] and there are existing methods to estimate the load growth on the utility side as it is usually done for conventional energy generators [72].

2.3.2 PV system degradation rate

The degradation rate of PV panels overtime depends on the location of operation as well as climate conditions (temperature, wind speed, dust, etc.). A statistical study conducted by the National Renewable Energy Laboratory [111] has found the value of the PV system degradation rate to be comprised between 0.5% and 1%. These two values are the boundaries that will be used as low and high values for the sensitivity analysis on the PV system degradation rate.

2.3.3 Utility discount rate

The discount rate is used to assess the change in money value overtime. This value can change depending not only on the location, but also on the utility. A discount rate value as high as 9% can be used or a value as low as the inflation rate might be used. The discount rates used by utilities are usually in the high range, but the social discount rate is closer to the inflation rate [75]. As a result, 9% will be considered as the high-end value of the discount rate while the current inflation rate of 2.18% will be considered for the lowest value. It is important to note that the value of the inflation rate changes with time and if this value is chosen as the discount rate it should be updated regularly for new calculations of the *VOS*. Also, the value of the inflation rate can be subjected to ongoing events. The value of the inflation rate of 2.18% was chosen at a date before the coronavirus outbreak in the United States that is ongoing. The outbreak has brought the inflation rate to as low as 0.25%. This value will not be used to run a sensitivity analysis because of the special conditions in which it occurred.

2.3.4 Environmental cost

The environmental cost associated with electricity production through conventional energy sources depends on the cost associated with the pollution from carbon dioxide (CO_2),

carbon monoxide (CO), nitrogen oxide (NO_x), and hazardous particulates (PM). The environmental cost of carbon dioxide dominates the cost of the other components. Different estimates of the CO_2 cost are given by the EPA [99]. The cost of CO, NO_x, and PM depends on state laws. The lowest value and highest value used for the cost of CO, NO_x, and PM were chosen from the state of Minnesota [121]. It has been hypothesized that if conventional energy sources are being used to produce electricity in the future, the effects on environment are going to worsen (e.g. lower quality fuel, higher embodied energies, etc.), and therefore the environmental cost will be expected to increase. This will be investigated by raising the environmental cost while analyzing the sensitivity of *VOS* to the environmental cost. This will show the trend of the impact of the environmental cost on the *VOS* and in the future, the values will need to be updated because the environmental cost is likely to exceed the maximum value used in this study.

2.3.5 Health liability cost

The health liability cost is a new calculated *VOS* component introduced by this study. This component has been mentioned by several studies but was not incorporated in the calculation due to lack of data for the evaluation [75, 84, 85, 122]. The health and mortality impacts of coal in particular are so severe that an ethical case can be made for the industry's elimination [123]. For example, Burney estimated that 26,610 American lives were saved between 2005 and 2016 by a conversion of coal-fired units to natural gas in the U.S. [124]. More lives would be saved, and non-lethal health impacts would be avoided with solar [88]. The values used here were obtained from the study of [109] that found the value of health impact cost of natural gas to be $0.025/kWh. As previously hypothesized, the use of fossil fuel energy sources in the future will increase the emissions, and the cost of health care has been escalating faster than inflation [124], thus increasing the cost of derived health liability. Several increase rates will be investigated. Although it should be pointed out the approach taken here was extremely conservative as the potential for climate/greenhouse gas emission liability [125, 126] was left for future work as discussed below.

2.3.6 Other parameters

The other parameters are utility related and in case of absence of utility data, generic values from the U.S. government agencies are used as indicated in Table 2.1 and run through realistic percent increases or decreases to determine their effect on the *VOS* components.

2.3.7 Sensitivity Analysis

A sensitivity analysis has been run on each of the nine *VOS* components as well as on the *VOS*. For each component, the sensitivity has been analyzed for some of its parameters wherever data was available. The evaluation of the variability of the *VOS* components has

been performed for each parameter. The sensitivity of a component to one of its parameters is determined by maintaining an average value of the other parameters and varying the studied parameter from its lowest value to its highest value. The different values that are obtained for the *VOS* component are then plotted to show its variation according to the parameter studied. A correlation study between the different parameters has not been conducted because there was no evident relationship between these parameters. Most of the parameters belong to utilities and there is no information on how they are chosen from one utility to another. An interaction study between the parameters and how their interaction affects the *VOS* components would be interesting for future studies where utility data are available.

A similar process has been used for the sensitivity analysis of the main *VOS*. The main *VOS*'s variability has been studied according to the nine *VOS* components. For each component for which the sensitivity of the *VOS* is analyzed, average values of the other components are maintained while the studied component's value is varied from its lowest value to its highest value.

2.4 Results and Discussion

The simulation results are plotted first for each *VOS* components. For each component, sensitivities on the different input variables have been investigated. Then the sensitivity of the overall *VOS* to each of the *VOS* components has been analyzed.

2.4.1 Avoided O&M fixed cost (V_1)

Figure 2.1 shows the results for the avoided O&M fixed cost (V_1). The sensitivity has been plotted for five parameters: the utility O&M fixed cost, the utility O&M cost escalation, the PV degradation rate, the utility discount rate, and the utility degradation rate. According to the results, the avoided O&M cost is highly sensitive to the utility O&M fixed cost and O&M cost escalation. When the utility O&M fixed cost increases, the avoided O&M cost increases accordingly, and an increase in the O&M escalation rate obviously increases the avoided O&M cost because it increases the utility fixed O&M cost over the analysis period. V_1 is also sensitive to the utility discount rate and decreases when the discount rate increases. This means that using a discount rate close to the social discount rate while conducting a *VOS* study will increase the avoided O&M cost while using a higher discount rate will lower the cost. This is in accordance with the recommendation of [75] to use of a discount rate lower than that of the utility in a distributed solar generation economic calculation. Also, the avoided O&M fixed cost is not very sensitive to the utility degradation rate or the PV degradation rate. Nevertheless, its value is slightly reduced when the PV degradation rate increases.

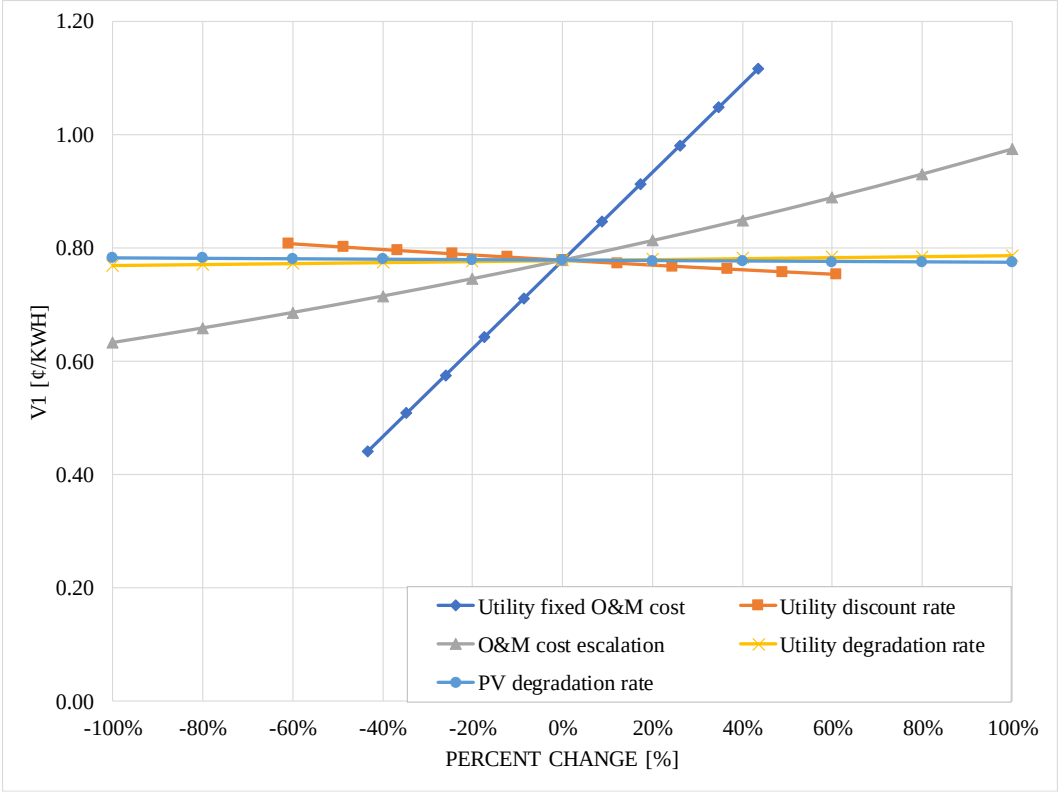

Figure 2.1. Sensitivity of avoided O&M fixed cost *(V_1)* in terms of LCOE (¢/kWh) to its parameters in percent change.

2.4.2 Avoided O&M variable cost *(V_2)*

The parameters for which the avoided O&M variable cost's *(V_2)* sensitivity has been studied are: the utility O&M variable cost, the utility O&M cost escalation, the PV degradation rate, and the utility discount rate. The sensitivity of the avoided O&M to its parameters are plotted in Figure 2.2. Figure 2.2 shows a similar variation trend of V_2 as compared to the case of the avoided fixed O&M cost. It is highly sensitive to the utility variable O&M cost, and the O&M cost escalation. The avoided variable O&M cost increases when the variable O&M, or the O&M cost escalation rate is increased but decreases with the increase of the discount rate or and the PV degradation rate.

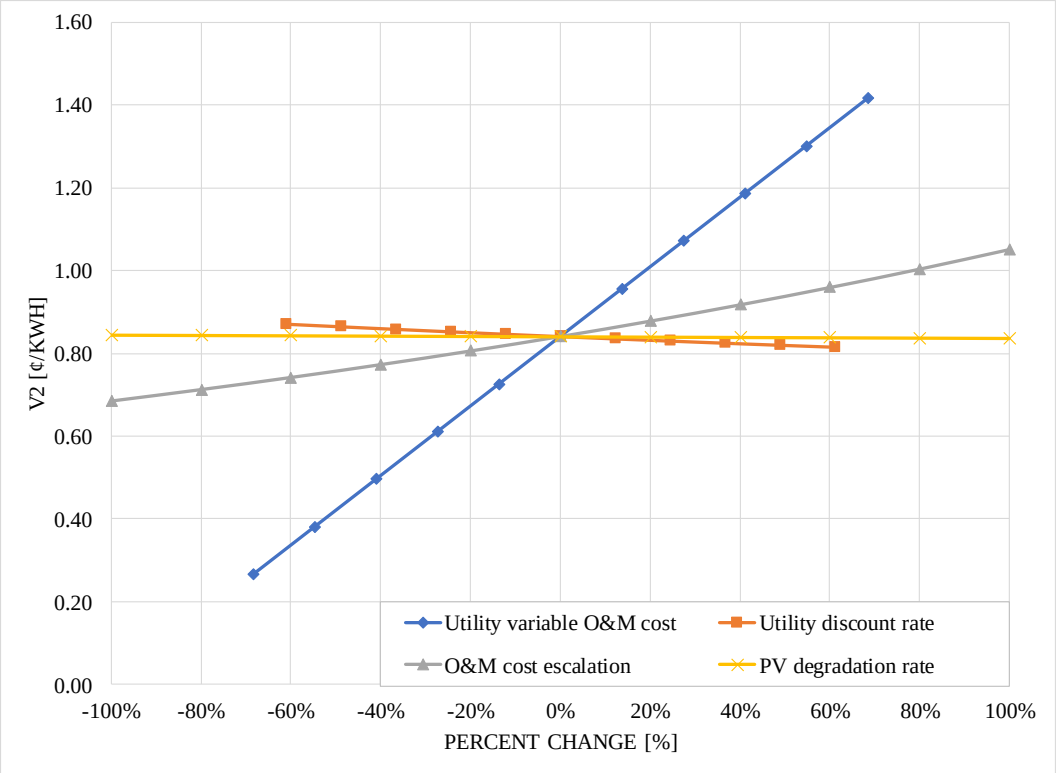

Figure 2.2. Sensitivity of avoided O&M variable cost *(V_2)* in terms of LCOE (¢/kWh) to its parameters in percent change.

2.4.3 Avoided fuel cost *(V_3)*

In the case of the avoided fuel cost *(V_3)*, the variables considered for the sensitivity analysis are the heat rate degradation rate, the natural gas price fluctuation rate and the PV degradation rate. While the avoided fuel cost has shown to be not very dependent on the heat rate degradation rate or the PV degradation rate, this value changes very quickly with a change in the natural gas price as in Figure 2.3. This is an important factor that should be carefully considered while conducting a *VOS* study because the price of natural gas is not fixed and varies according to several parameters that are not controlled by the utility, such as the economy, the weather, market supply and demand [127, 128]. The equivalent heat rate degradation rate expresses the degradation of the utility plant's efficiency over the analysis period, and when the efficiency decreases, there is a slight decrease in the avoided fuel cost. Another value for which the avoided fuel's sensitivity could have been studied is the equivalent heat rate for solar, which was not analyzed in detail here because of the lack of utility data. This is left for future work.

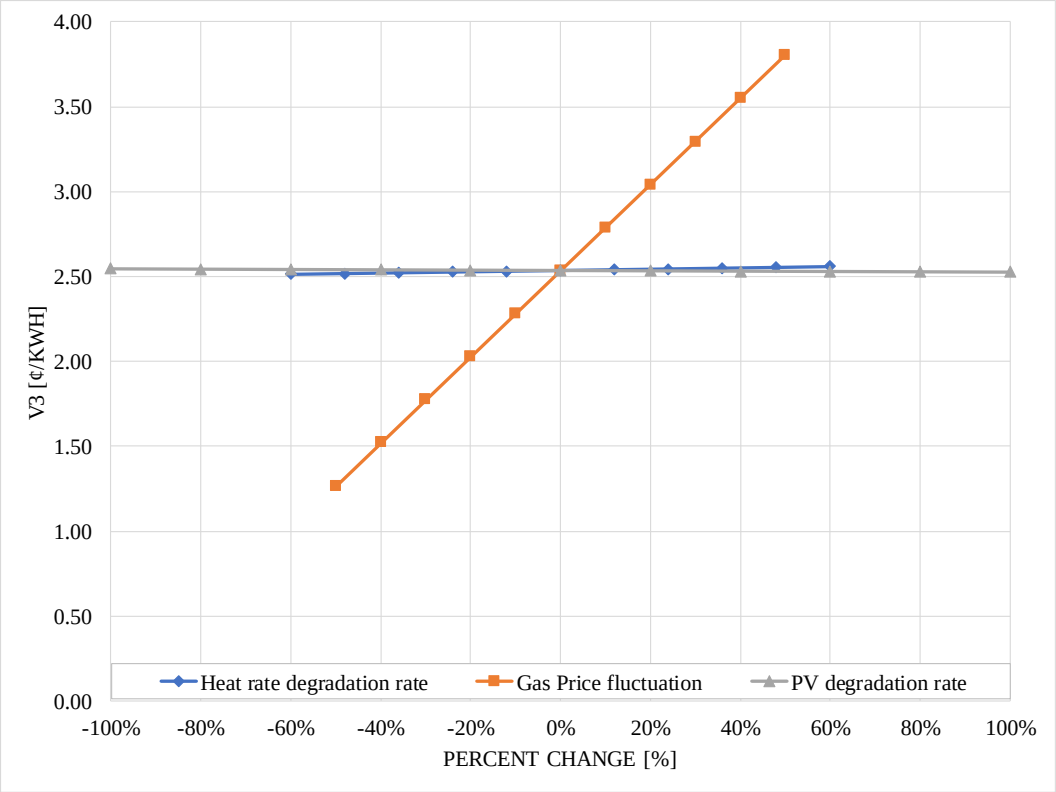

Figure 2.3. Sensitivity of avoided fuel cost (V_3) in terms of LCOE (¢/kWh) to its parameters in percent change.

2.4.4 Avoided generation capacity cost *(V_4)*

The sensitivity of the avoided generation capacity cost *(V_4)* has been plotted in Figure 2.4 for the discount rate, the utility degradation, and the PV degradation rate. The V_4 *VOS* component does not have a high variability to the PV degradation rate even though it shows a decreasing trend with the increase of PV degradation. But it reacts sharply to the utility degradation rate. This is because the generation capacity of the utility is highly impacted by the utility degradation. Also, as previously observed, when the discount rate grows far from the social discount rate, the avoided generation capacity cost decreases.

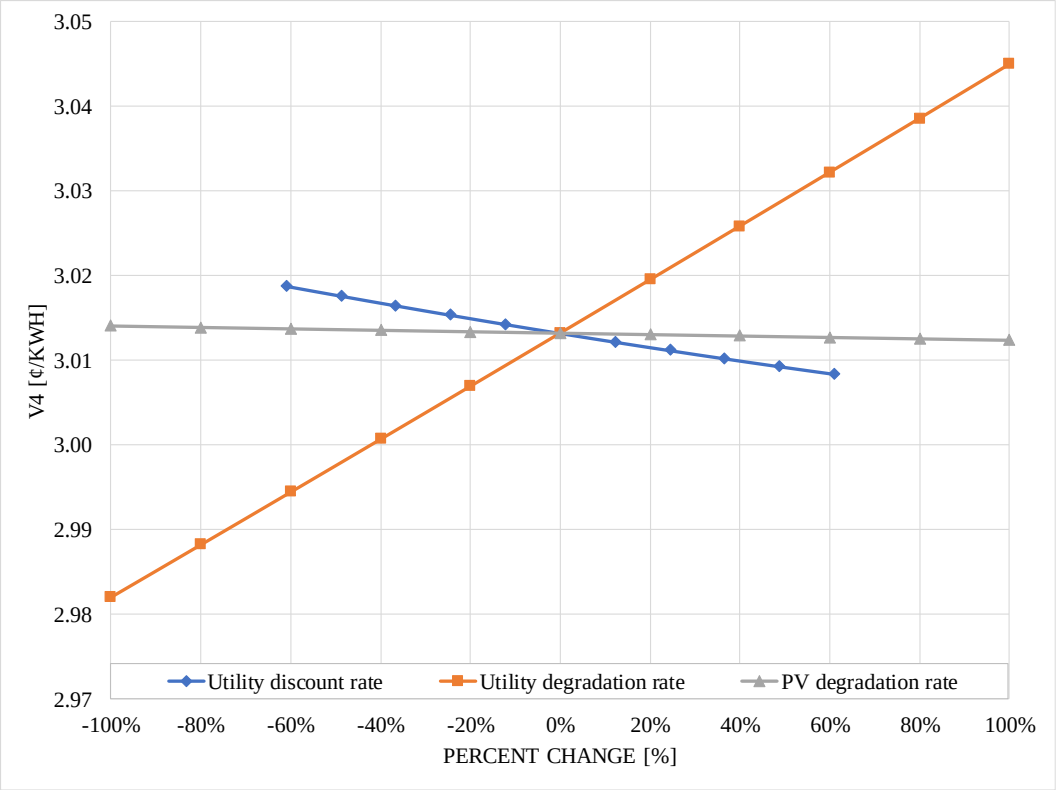

Figure 2.4. Sensitivity of avoided generation capacity cost *(V_4)* in terms of LCOE (¢/kWh) to its parameters in percent change.

2.4.5 Avoided reserve capacity cost *(V_5)*

The avoided reserve capacity cost *(V_5)* expresses the reserve component of the generation capacity; therefore, it can have a value of zero when there is no reserve capacity planned by the utility as shown in Figure 2.5. V_5 is highly sensitive to the reserve margin and the result shows that the more generation capacity is reserved, the more the avoided generation capacity cost increases. On the other hand, the avoided reserve capacity cost is not very sensitive to the discount rate compared to its sensitivity to the other parameters. V_5's value goes up when the utility degradation rate increases and goes down when the PV degradation rate increases.

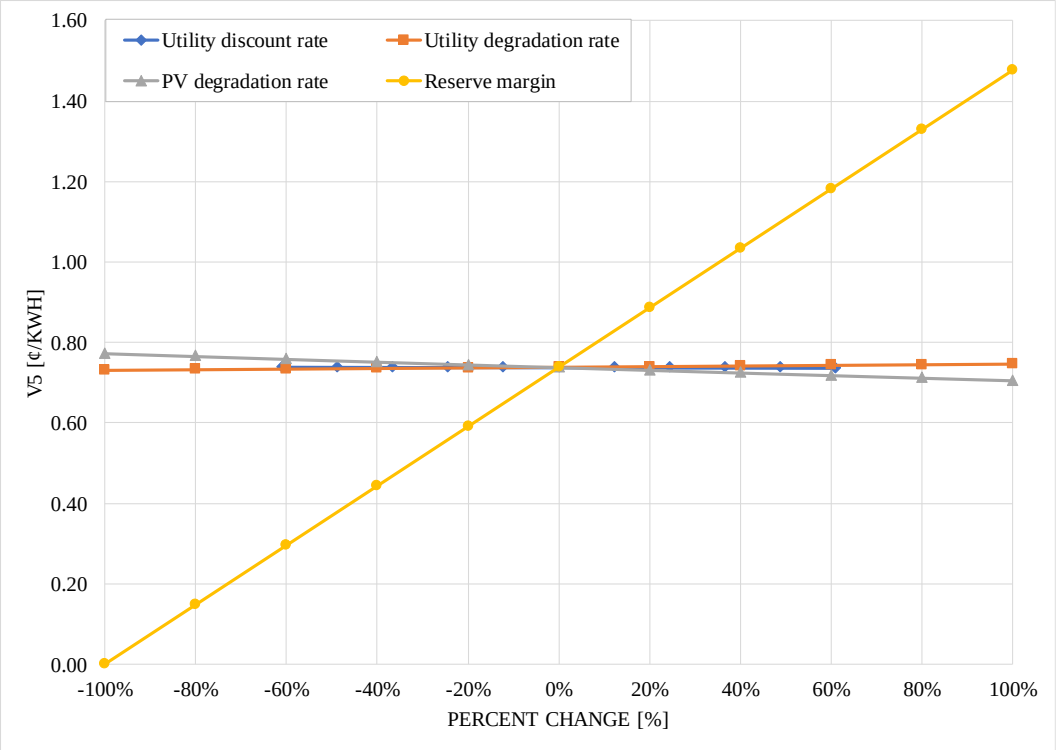

Figure 2.5. Sensitivity of avoided reserve capacity cost *(V_5)* in terms of LCOE (¢/kWh) to its parameters in percent change.

2.4.6 Avoided transmission capacity cost *(V_6)*

Three parameters have been analyzed in the sensitivity study of V_6: the discount rate, the transmission capacity cost, and the PV degradation rate. The parameter it is the most sensitive to is the transmission capacity cost. Obviously, when the transmission cost is low, the avoided cost associated will be low. The results shown in Figure 2.6 make it clear that the avoided transmission capacity cost does not change with the PV degradation rate or the discount rate. This is because the utility transmission capacity has been assumed to be constant over the analysis period, and the transmission capacity degradation rate has not been considered because utility data on this parameter was not available.

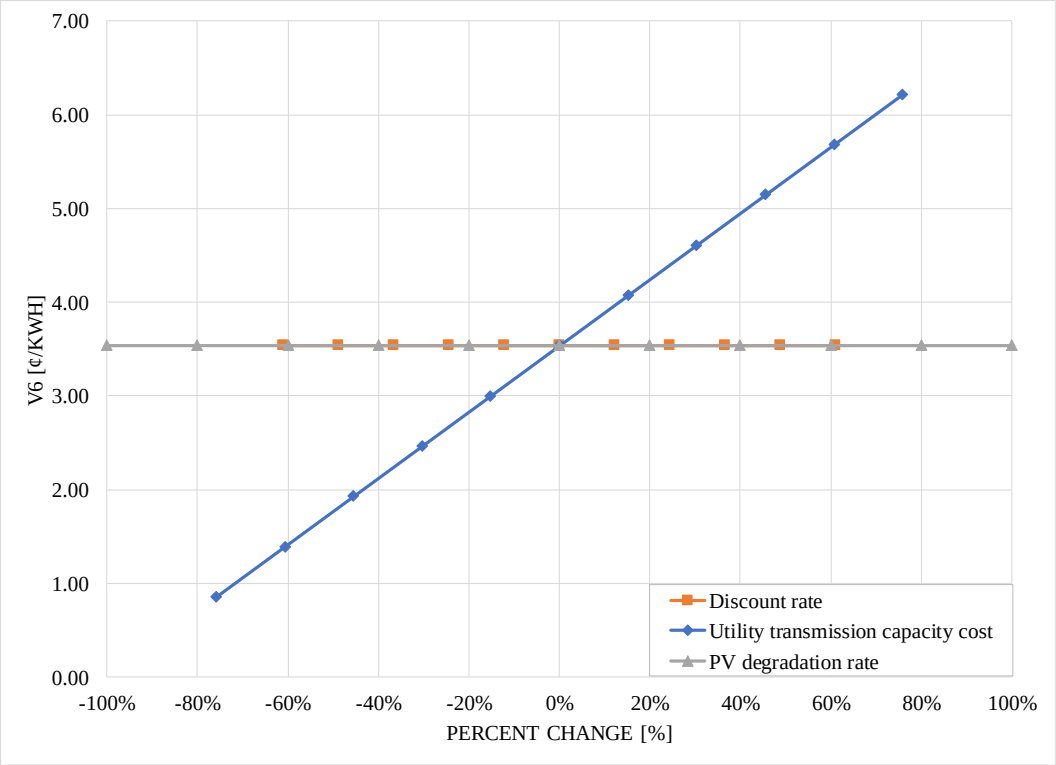

Figure 2.6. Sensitivity of avoided transmission capacity cost *(V_6)* in terms of LCOE (¢/kWh) to its parameters in percent change.

2.4.7 Avoided distribution capacity cost *(V_7)*

The avoided distribution capacity cost *(V_7)* is one of the most complicated *VOS* components to evaluate. As shown in Figure 2.7, its sensitivity has been studied for six variables: the load growth rate, the distribution capacity, the distribution capacity cost, the utility discount rate, the distribution cost escalation, and the PV degradation rate. But it depends on more than six parameters. The growth rate, for example is calculated from utility data, mainly, the load for the past ten years of operation [67, 129]. Here, the sensitivity has been analyzed on the growth rate directly to be as widely applicable as possible. Another parameter is the number of deferred years that is also a utility owned data.

The avoided distribution capacity cost naturally increases with the distribution capital cost. Figure 2.7 shows that the avoided distribution capacity cost does not fluctuate with the distribution capacity at all, but it is highly sensitive to the discount rate, the distribution cost, and the distribution cost escalation rate. It can even shift to a negative value when the discount rate is too low. This shows that choosing the discount during a *VOS* study must be a trade-off between the social discount rate and the utility discount rate. It is interesting to note that the avoided distribution capacity cost goes down when the distribution cost escalation is increasing. A possible explanation for this observation is that when a utility

has enough distribution capacity, it will purchase less power from solar PV systems owners, therefore the price goes down. The same reasoning can be used to explain the decreases of the cost when the load growth goes up. Finally, V_7 shows a slight decrease with the increase of the PV degradation rate.

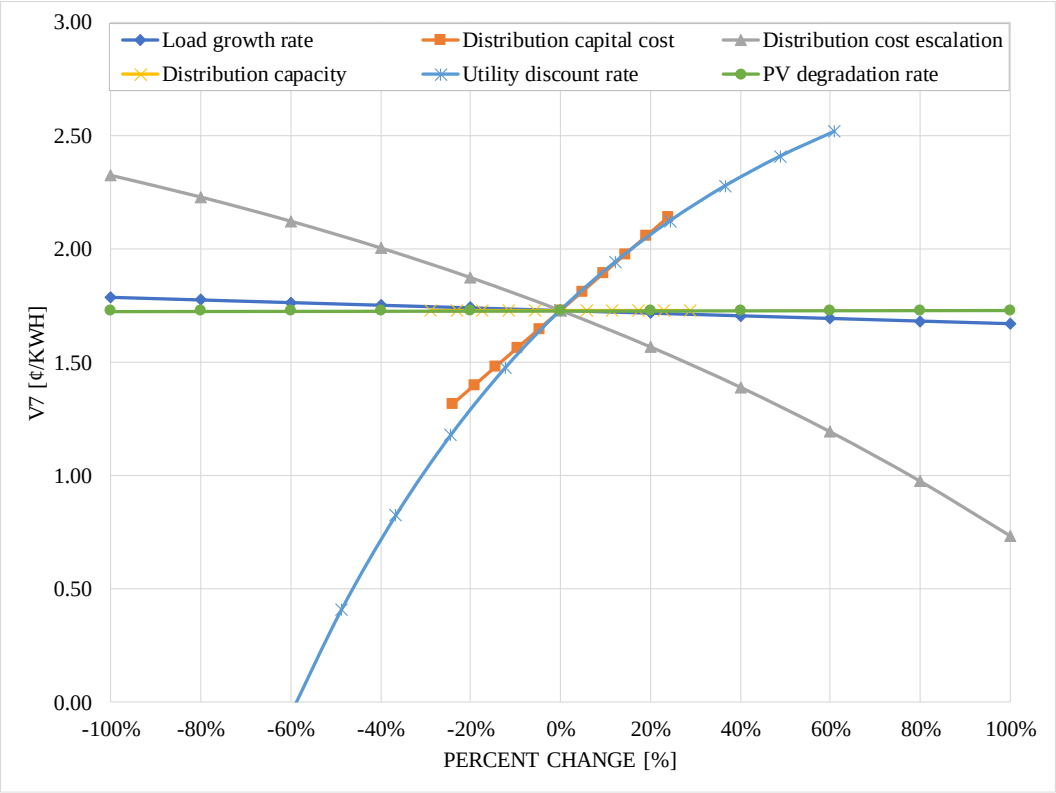

Figure 2.7. Sensitivity of avoided distribution capacity cost *(V_7)* in terms of LCOE (¢/kWh) to its parameters in percent change.

2.4.8 Avoided environmental cost *(V_8)*

The second most complicated component of the *VOS* calculation is the avoided environmental cost *(V_8)*. The sensitivity has been analyzed for the three environmental discount rate scenarios provided by the EPA [99]. For each scenario, a sensitivity analysis has been conducted on the environmental cost increase rate. V_8 will increase when the chosen environmental discount rate is low, but overall, each of the three EPA scenarios show an increase when the environmental cost increase rate goes up, as seen in Figure 2.8. This is useful to see how the avoided environmental costs might change in the future. Environmental externalities are volatile and changing quickly [84]. If it is assumed that in the future, the environmental impact of conventional energy production technologies will increase, then the costs of the environmental externalities will increase as well [122]. On

the other hand, an increase in distributed renewable energy generation could lead to a decrease or stabilization of the avoided environmental cost.

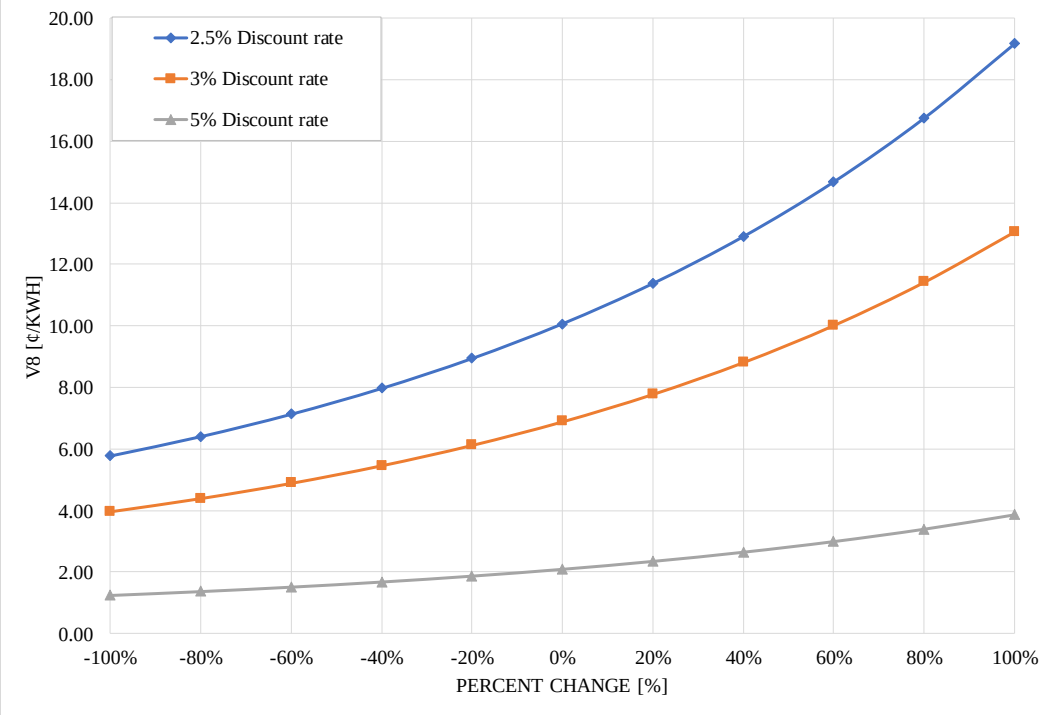

Figure 2.8. Sensitivity of avoided environmental cost *(V_8)* in terms of LCOE (¢/kWh) to the environmental cost increase rate in percent change, for different values of the discount rate.

2.4.9 Avoided health liability cost *(V_9)*

The avoided health liability cost, V_9, depends on three values, the health cost increase rate, the environmental discount rate, and the PV degradation. This cost does not fluctuate with the PV degradation rate but is very sensitive to the other two parameters. The environmental discount rate used here is the same as the environmental discount rate used in the evaluation of the avoided environmental cost's sensitivity study. As a result, the avoided health liability cost decreases when the environmental discount rate goes up as is the case for the avoided environmental cost.

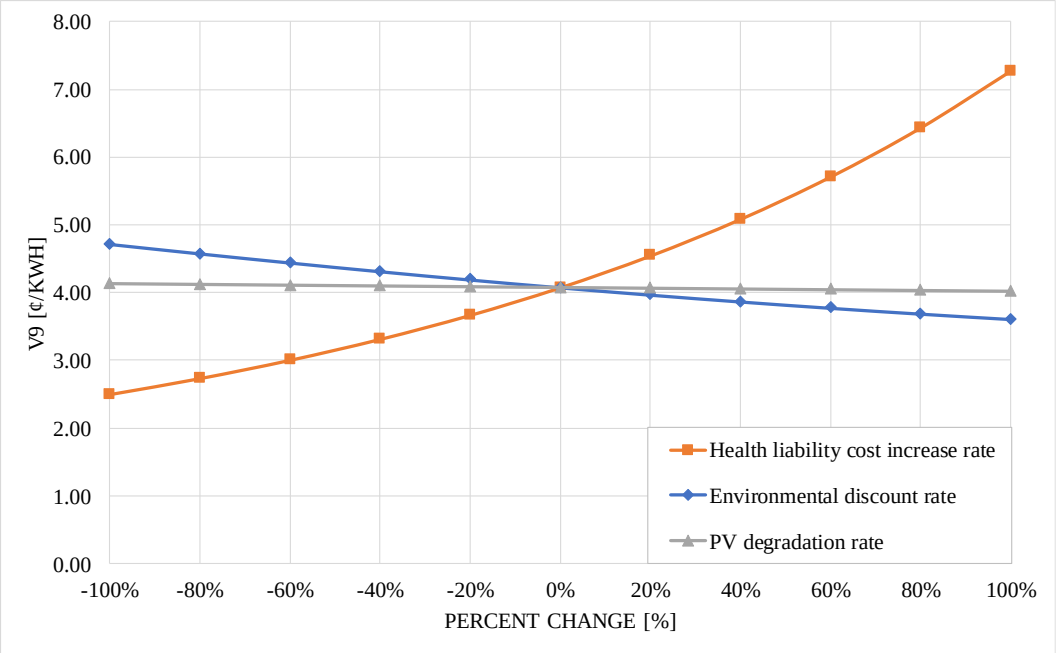

Figure 2.9. Sensitivity of avoided health liability cost *(V_9)* in terms of LCOE (¢/kWh) to its parameters in percent change.

2.4.10 Value of Solar *(VOS)*

After the sensitivity analysis of each *VOS* component, the main *VOS* value has been studied to find out how the impact of different components compare to one another and which components have more variability. Figure 2.10 shows that the *VOS* is, in decreasing order, sensitive to the avoided environmental cost *(V_8)*, avoided health liability cost *(V_9)*, avoided transmission capacity cost *(V_6)*, avoided fuel cost *(V_3)*, avoided distribution capacity cost *(V_7)*, avoided O&M variable cost *(V_2)*, avoided reserve capacity cost *(V_5)*, avoided O&M fixed cost *(V_1)*, and avoided generation capacity cost *(V_4)*.

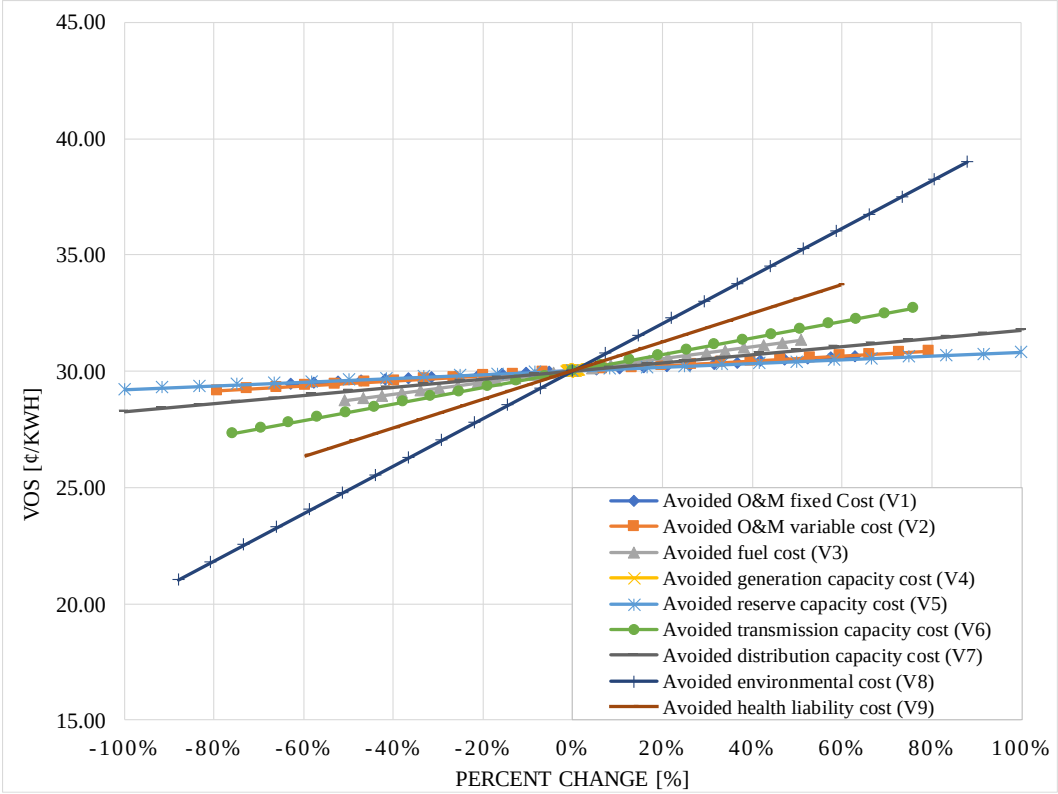

Figure 2.10. Sensitivity of *VOS* LCOE (¢/kWh) to all the components in this study, in percent change.

The contribution of each *VOS* component to the overall *VOS* depends on the case. The lowest *VOS* value calculated with the assumptions used in this study in term of LCOE is 9.37¢/kWh while the highest value calculated is 50.65¢/kWh. This variation observed in the *VOS* value comes from the fact that the parameters considered in this study are chosen to have the lowest and the highest value of *VOS*. The values of calculated *VOS* using utility data are highly likely to be located within this interval. It is also clear, based on the values shown in Figure 2.10, that the *VOS* exceeds the net metering rates (when they are even available) in the U.S. Thus, it can be concluded that even when grid-tied solar owners are provided with a full net metered rate for electricity fed back onto the grid, they are effectively subsidizing the electric utility/other customers.

For the low *VOS* value case shown in Figure 2.11, the avoided distribution cost *(V_7)*, and the avoided reserve capacity cost *(V_5)* has no contribution in the *VOS* value. The avoided generation capacity cost *(V_4)* and the avoided health liability cost *(V_9)* represent most of the *VOS* value followed by the avoided environmental cost *(V_8)* and avoided fuel cost *(V_3)*.

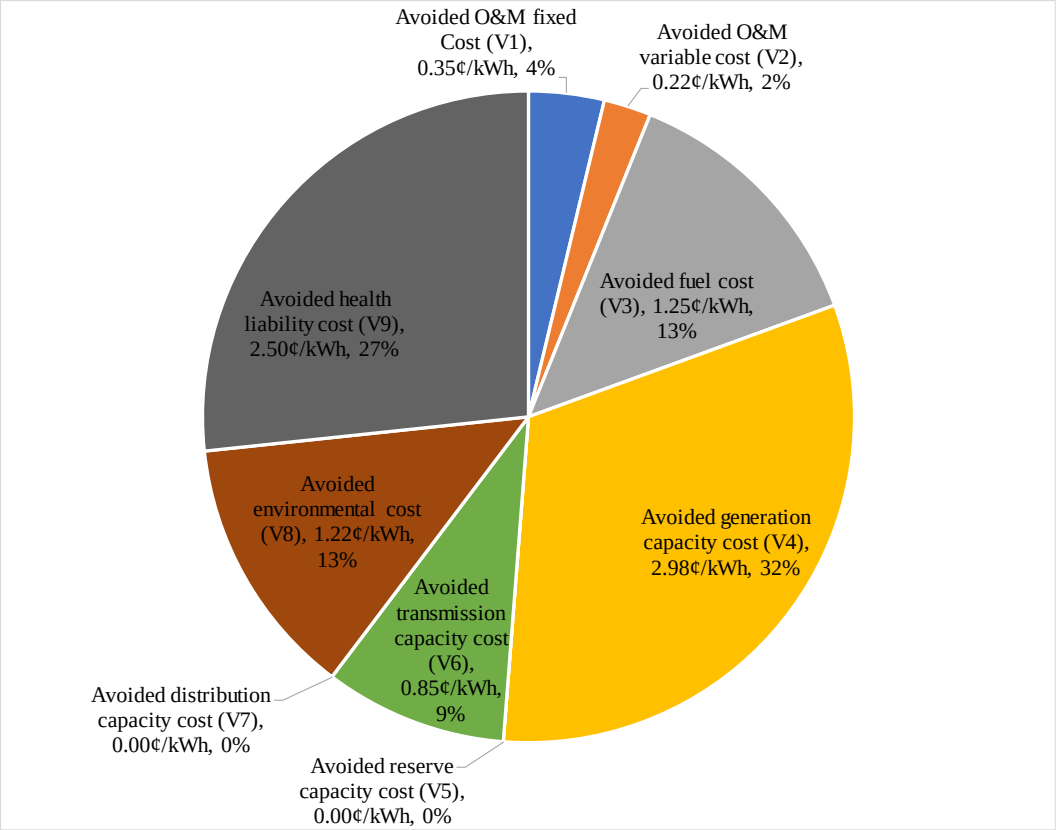

Figure 2.11. Contribution of each *VOS* component to the overall *VOS* LCOE – Low Cost Scenario.

The contribution of the avoided environmental *(V_8)* cost increases with the *VOS* value as it becomes the largest contributor to the overall value, followed by the health liability *(V_9)* cost as shown in Figure 2.12 representing a middle *VOS* value. The avoided generation capacity cost *(V_4)* is reduced as well as the contribution of the avoided fuel cost *(V_3)*.

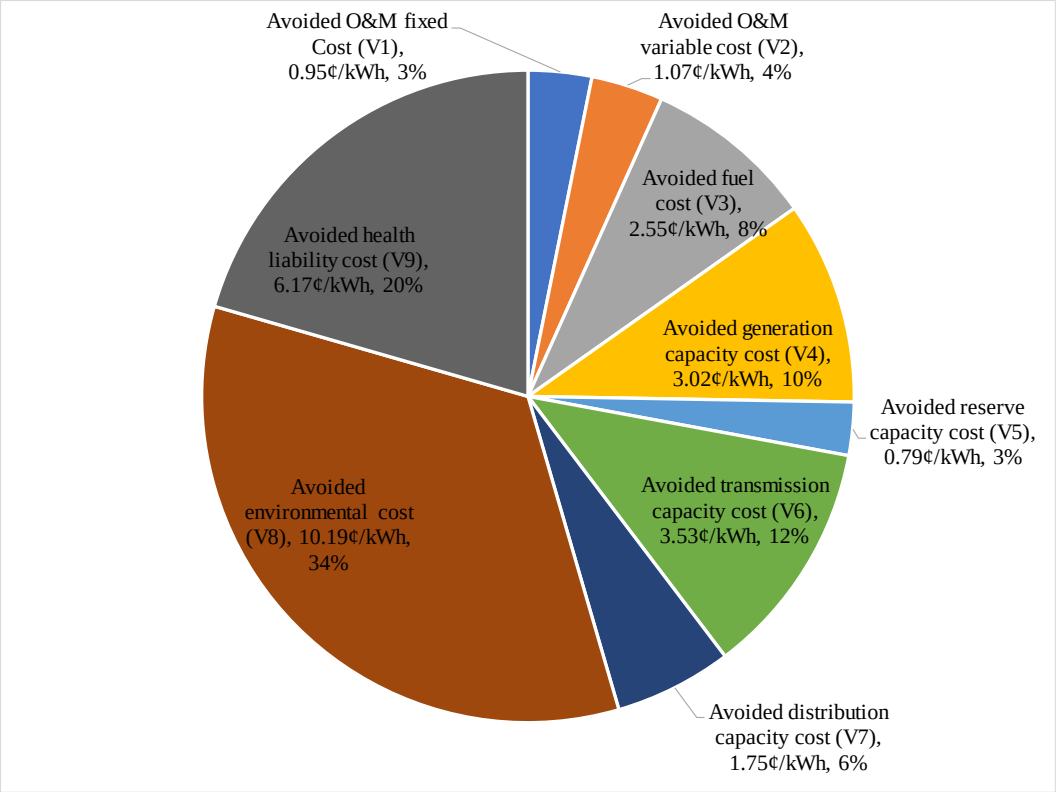

Figure 2.12. Contribution of each *VOS* component to the overall *VOS* LCOE – Middle Cost Scenario.

Figure 2.13 represents the contribution of each of the *VOS* components to the overall value in the case of the highest obtained value in the scope of this study. The avoided environmental cost *(V_8)*, avoided health liability cost *(V_9)*, and avoided transmission capacity cost *(V_6)* represent 69% of the total cost.

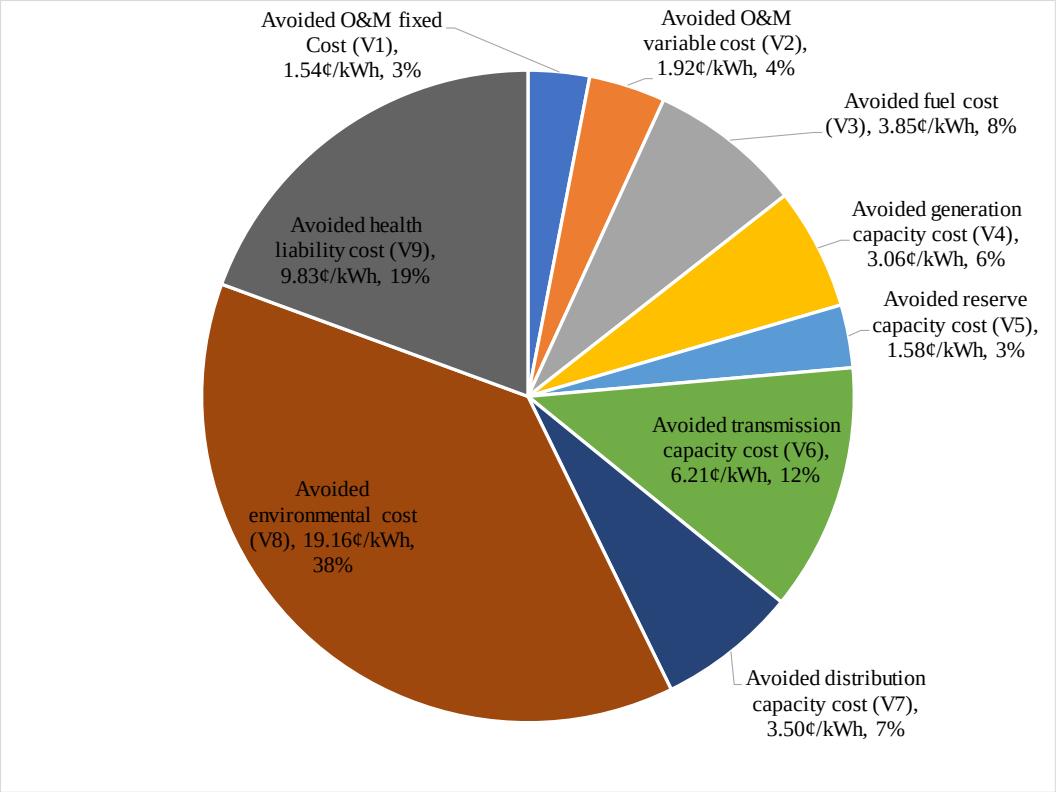

Figure 2.13. Contribution of each *VOS* component to the overall *VOS* LCOE – High Cost Scenario.

The evolution of the cost percentage contribution of each *VOS* throughout Figure 2.11, Figure 2.12, and Figure 2.13 shows the level of uncertainty of the *VOS* with respect to the corresponding component.

The lowest and highest LCOE *VOS* values obtained from the assumptions made in this study are, respectively, 9.37¢/kWh and 50.65¢/kWh. The existing *VOS* studies results fall into this interval. The sample calculation made by [67] for Minnesota is 13.5¢/kWh, while [68] calculated a *VOS* of 10.7¢/kWh for Austin Energy. These values are in the lower spectrum of the result of this study because of the considerations made. They incorporate fewer *VOS* components than the present study, and this study focuses on sensitivity, therefore higher values of parameters have been considered. Other results summarized by [69] have found the *VOS* to be 33.7¢/kWh in Maine, between 25.6 and 31.8¢/kWh in New Jersey and Pennsylvania [70], and 19.4¢/kWh in Washington, DC. In general, the *VOS* is much higher than the net metering costs and even the highest costs observed at the residential level [6, 80, 130]. The residential net metering rates are also the highest as compared to commercial and industrial rates, so the latter two are even more unjustly compensated for installing solar. Overall, this indicates that utilities are under-compensating customers with grid-connected PV systems if they are only paying net

metering rates, as displayed in Table 2.2. Table 2.2 shows a comparison between *VOS* rates and net metering rates in the U.S. states mentioned above, wherever data is available. As only a tiny fraction of utilities (3%) are paying full net metering rates anyway [65], there is a need for regulators to ensure that solar customers are being adequately compensated for the value of solar electricity they are sharing with the grid [64]. Substantial future work is needed to ensure that solar PV owners are not subsidizing non-solar electricity customers.

Table 2.2. Comparison of VOS rates and net metering rates for some U.S. States

State	**VOS**	**Net Metering**
Minnesota	13.5¢/kWh	
Austin (Texas)	10.7¢/kWh	Approximately 4 – 5¢/kWh (1.2 – 1.6$/kWh) [131]
Maine	33.7¢/kWh	12.16 – 14.66¢/kWh [132]
New Jersey	25.6 – 28¢/kWh	
Pennsylvania	28.2 – 31.8¢/kWh	Minimum value of (4¢/kWh) [133]
Washington D.C.	19.4¢/kWh	

2.5 Future Work

This study has covered a vast number of existing *VOS* components, but some components were not included in this study due to the lack of a reliable evaluation methodology. These components include the economic development cost, the avoided fuel hedge cost, and the avoided voltage regulation cost. These represent opportunities for future work once the evaluation methodologies have been developed. Also, there are some parameters sensitivities that would provide insights with multiple utility data sets. These parameters include the analysis period, the hourly solar heat rate and solar PV fleet, and the 10-years load profile. Future studies can focus on incorporating the sensitivities of these parameters into the model or can use the foundation of this model to build on new *VOS* studies according to a specific location and available data from utilities. Another limitation to this study is that it does not include the effect of the load match factor, and loss saving factor.

As the results show, the environmental and health costs can dwarf the technical costs and thereby determine the *VOS*. There are also second order effects that can be used to obtain a more accurate *VOS* values. For example, the negative impact of pollution from conventional fossil fuel electricity generation on crop yields [124] as well as PV production could also be considered in future work to give a more accurate V_8. In addition, as greater percentages of PV are applied to the grid, the avoided costs will change and there is a need for a dynamic *VOS* akin to dynamic carbon life-cycle analyses needed for real energy economics [134]. This complexity will be further enhanced by the introduction of PV and storage systems [135] as it will depend on size [136] and power flow management and scheduling [137, 138].

Perhaps the most urgent need for future work is accurate estimations of the value of avoided GHG liability costs because the magnitude of the potential liability [107,108] could overwhelm other subcomponents of the *VOS*. This is because as the realities of climate change have become more established, a method gaining traction to account for the negative externalities is climate litigation [125, 126, 139-149]. For utility *VOS* analysis this is particularly complex as it is difficult to know where to draw the box around environmental costs. As some studies have concluded there is liability for past emissions as well as for harm done in other nations [140]. Liability for disastrous events is also challenging to predict [144]. Combining both other nations and disaster creates liability potential that could become enormous with prioritization given to victims that are losing their land, culture, and lives due to climate change [145]. Tort-based lawsuits are already possible from a legal point of view [144], but there are other legal methods that could be used to reduce climate change such as public nuisance laws [146]. Some authors have argued a 'polluters pay principle' for carbon emissions [147]. Other studies have concluded that emitters such as conventional fossil fuel power plant operators should be forced to buy long-term insurance in order to cover their share of climate change costs for minimizing risks in case of insolvencies [148]. Determining what such insurance premiums should be is another area of substantial future work. Determining what the greenhouse gas liability costs are for conventional electricity generators (as well as potential avoided insurance costs) that can be avoided with PV is extremely challenging. These estimates will become easier with time as climate change impact studies become more granular, thereby assigning specific costs to specific amounts of emissions. In addition, realizing these climate liability costs in courtrooms will become more likely. As Krane points out, it is clear that as the negative impacts of climate change grow more pronounced, the fossil-fuel based electricity industry faces a future that will be less accepting of current practices and that will increase economic (and maybe even industry existential) risks [149]. Avoiding these risks has real value, which should be included in the *VOS* in the future.

2.6 Conclusions

This study demonstrated a detailed method for valuing the incorporation of solar PV-generated electricity into the grid and analyzed the sensitivity of each *VOS* component to its input parameters, and the overall sensitivity of the *VOS* to each of its components. Several components have been found to be sensitive to the utility discount rate, namely the avoided O&M fixed cost, avoided O&M variable cost, avoided generation capacity cost, and the avoided distribution capacity cost. Except for the avoided distribution capacity, the other components' values decrease with the increase of the utility discount rate. The distribution capacity is more sensitive to the discount rate than the other components. It increases with the discount rate and can be negative if the discount rate is very low. This has shown the necessity of carefully choosing the discount rate for *VOS* studies. Most of the *VOS* values do not have a high variability to the solar PV degradation rate even though its increase slightly reduces the value of each component and the overall *VOS*. The

environmental cost and the health liability cost are sensitive to the cost increase rate that can be tied to the emissions impact of the conventional energy sources. These two costs are likely to increase in the future with the worsening of the emission of fossil fuel sources and more information about its effects, which increases potential emissions liability for utilities. Finally, specific case studies could provide additional sensitivities on the few areas of the *VOS* that were not evaluated in this paper to create better *VOS* models. Overall, the results of this study indicate that grid-tied utility customers are being grossly undercompensated in most of the U.S. as the value of solar eclipses the net metering rate. Substantial future work is needed for regulatory reform to ensure that solar owners are not unjustly subsidizing U.S. electric utilities.

3 Water Conservation Potential of Self-Funded Foam-Based Flexible Surface-Mounted Floatovoltaics

3.1 Introduction

Water scarcity [150, 151], the energy crisis [152], and food scarcity [153, 154] are the largest currently coupled challenges [155] facing the global community, where they most severely affect the arid and semiarid regions of the world [156]. There is a wide scientific consensus that combustion of fossil fuels for energy is increasing atmospheric carbon dioxide (CO_2) concentrations and driving climate change [157]. This anthropogenic climate change is increasing globally averaged mean annual air temperatures and driving changes in precipitation, which are expected to continue and increase [158, 159]. The IPCC (Intergovernmental Panel on Climate Change) warns that the climate change over the next century will affect rainfall, river flows and sea levels all over the world [160], which will negatively impact agricultural yield [93]; particularly in already-malnourished sub-Saharan Africa. de Wit and Stankiewicz [161] predict rainfall in sub-Saharan Africa could drop by 10% causing surface drainage to drop 30–50% by midcentury, which would cause major water shortages. It is widely agreed that to prevent the worst of climate change, humanity needs to rapidly convert fossil fuel-based energy systems to renewable energy systems [162]. Solar photovoltaic (PV) technology is the most widely accessible, sustainable, and clean renewable source of energy that can be scaled to meet humanity's energy needs [163, 164]. To meet these needs, however, a substantial amount of land is still needed for PV to replace fossil fuels and this creates competition for limited land resources between food and energy [9]. A utility-scale PV plant land occupation varies between 20 km^2/GWh and 40 km^2/GWh depending on the type of solar panels used [165]. Despite life cycle carbon emissions [134], PV is more land efficient than all carbon capture and sequestration plans for coal [166], but with nearly a billion people already living undernourished, further reductions in agricultural land are not acceptable during a world food crisis [167].

A potential solution to these coupled water–energy–food challenges is the concept of floating photovoltaics, or floatovoltaics (FPV), which has been rapidly gaining a base in scientific literature [11-17]. FPV is growing fast and is expected to have an average growth rate of above 20% in the next five years due to extremely low costs (with an FPV bid recently coming in for a system in Thailand at under USD 0.50/Wp) [22]. FPV are easier to install and simpler to decommission than conventional PV systems and the racking costs are less, which lead to these overall cost savings [22]. As FPV are located near or immersed in water, the operational temperature is reduced, which raises the solar energy conversion efficiency [11, 15, 18, 168-171]. In regions where water scarcity is an issue, and particularly when this issue is likely to be aggravated by climate change, FPV can also be used to reduce water loss because it can reduce water evaporation by more than 70% [18-21]. The Penman–Monteith daily evaporation method indicates that FPV could even cut evaporation by as much as 90% [172]. Studies in China [173] and India [174, 175] have

all indicated massive potential water savings for both small and large FPV coverage areas. This is particularly important for preservation of water sources in arid and semi-arid regions, especially with water shortages in the region [176]. FPV, therefore, also holds substantial promise when coupled with existing hydro power to make dual use of the electrical infrastructure while improving the water resource itself [173, 177]. Similar advantages are to be expected for hybrid systems with pumped storage [178]. Finally, there is also evidence that FPV deployment reduces the PV degradation rate below 0.5% per year [179], which improves the levelized cost of solar electricity further.

FPV research has focused on several system design strategies [180]:

(1) Tilted arrays of solid modules (normally on top of pontoon structures) [20, 181-183];
(2) Submerged PV modules (with and without a pontoon) [13, 168, 170, 171, 184];
(3) Micro-encapsulated phase change material (MEPCM)-based pontoon modules [185-187];
(4) Thin-film PV (no ridged pontoon supporting structure) [13, 15, 188].

The thin-film FPV design has the advantage of reducing racking costs even more so than pontoon style FPV, as it clearly stops more evaporation and gains an advantage by the operational temperature being lower. However, the temperature coefficients are better for amorphous silicon (a-Si:H) thin film materials than those of crystalline silicon (c-Si) so the benefits of the water cooling are muted for a-Si:H-based FPV.

In this study, a new approach is used with a flexible crystalline silicon module on a similar foam system to that described by Pierce et al. [188] for a-Si:H FPV. This approach enables a larger solar electric output gain (or FPV boost), and as solar is largely already profitable, there is an opportunity for the electricity production value of c-Si flexible foam-backed FPV to subsidize a means of water conservation by cutting water evaporation losses. To build on past FPV work and investigate the potential of FPV coupled to hydro power in the U.S., the water saving potential at Lake Mead using FPV is investigated in this study. Lake Mead is an artificial reservoir created by the United States government to run the Hoover Dam, which was built in 1935[189, 190]. This novel form of FPV is analyzed for water-saving potential using an evaporation calculation adapted from the Penman–Monteith daily evaporation model [191] that is approved by the Food and Agriculture Organization of the United Nations (FAO) [192]. An energy production analysis is performed and an open source spreadsheet is developed to simulate the evaporation and the energy yield of the flexible FPV [193], as well as to investigate the impact of using passive water-cooled FPV, where the cooling potential was measured experimentally for a foam-based FPV. The potential is determined for a case study based on the coverage of FPV ranging from 10% to 50% [194] of Lake Mead. The results are compared to “conventional” tilted pontoon-style FPV and are discussed in the context of the energy–water–food nexus.

3.2 Materials and Methods

3.2.1 Data Collection

3.2.1.1 Lake Evaporation Data

Most of the weather data used in this study were collected on Lake Mead through buoys installed by the United States National Oceanic and Atmospheric Administration's National Data Buoy Center (NOAA-NDBC) [195]. The rest of the data were obtained from open-access weather data made available by the McCarran International Airport's weather station in Las Vegas [196], and from SOLCAST, a solar data provider [197].

The main characteristics of the lake differ slightly from one study to another and depend on the year the study was conducted. In this study, the lake characteristics' values used for the evaporation calculation are taken from the National Park Service (NPS) website [198]. According to the NPS, as of 2010, the lake has a maximum surface area of 159,866 acres (647 million m^2), and a maximum capacity of 29,686,054 acre-feet (36,617 million m^3). The mean depth of the lake is estimated to be 55.5 m by the National Park Service [190]. The average elevation of the lake is 328.574 m above sea water level. The weather buoy used to collect the data is located in the North Boulder Basin of the lake at a geographical position of latitude 36.087 N and longitude 114.728 W. The temperature sensor for air temperature collection is located at a height of 2 m above the lake surface while the anemometer is at 3 m above. Additionally, the atmospheric pressure sensor is located at 330.574 m above sea water level or 2 m above the lake surface, and the water temperature is measured at 0.5 m below the lake surface [199]**.**

The buoy installed in Lake Mead's North Boulder basin by the NOAA-NDBC has been capturing different types of variables since 2016, which are stored in a historical database on the agency's website. Among the data required to conduct an evaporation calculation using the Penman–Monteith model, the wind speed (w_s), the atmospheric pressure (P), the maximum ($T_{w,max}$), minimum ($T_{w,min}$), and daily mean (T_w) water temperature; and the air temperature were obtained from the NOAA-NDBC historical database. The rest of the data were not captured by the buoy; therefore, alternative methods have been used to gather the required data. According to Moreo and Swancar, when data are not available for the study location, nearby airport weather data can be used instead [189]. In this study, the nearest airport close to Lake Mead is the Las Vegas Airport. The relative humidity (Rh) data have thus been obtained from the Weather Underground website that has made data from the Las Vegas Airport available. The remaining variable is the daily incoming solar irradiation or global horizontal irradiation (R_S) that has been obtained from SOLCAST's historical database [197]. This variable is also used for the solar energy production modeling.

The raw data from the NOAA-NDBC database were collected with an interval of 10 min starting at 00 h 00 min each day while the data from the Las Vegas Airport were measured with an 1 hour interval starting at 00 h 56 min each day. Since daily data were required for the calculation, a mean daily value has been calculated for each variable. First, the data obtained from the NOAA-NDBC were cleaned by keeping only hourly data at the beginning of the hour (00 min) in order to match the data from Las Vegas Airport. A MATLAB code [200] was developed to perform this operation. Then, the same code was used to strip the missing data from the data table. A line of data was considered missing from the data table if one or more of the variables were not recorded by either the NOAA-NDBC station sensors or the Las Vegas Airport station sensors. After that, the data were reported in a spreadsheet that was used to calculate the mean daily value of the wind speed (w_s), the atmospheric pressure (P), the water temperature (T_w) and the air temperature (T_a) by averaging the hourly data for each day. Another method used in the literature to calculate daily mean weather data is to calculate the average of the maximum and minimum value of the day [201]. However, studies have shown that if data are available, it is best to calculate the mean daily temperature by averaging the hourly values [202, 203]. The spreadsheet was also used to retrieve the maximum ($T_{w,max}$), and minimum ($T_{w,min}$) daily temperatures as well as the maximum (Rh_{max}), and minimum (Rh_{min}) daily relative humidity. The number of missing data points was 246 hourly data. Instead of having total hourly data of 8760 points, 8514 data points were used for this study after the data cleaning process. There was no more than 3 missing data points for a single day except for 5 specific days that are the 4th, 60th, 97th, 318th, and 347th day of the year 2018. These 5 days were, respectively, missing 4, 4, 10, 5, and 16 data points. The days with the highest number of missing data were the 97th and 347th day of the year. Since there are only two such days among the 365 that populated the year 2018, it has been considered that it will not have a significant impact on the results. Therefore, the available data were representative in estimating the mean daily values of the variables for each day.

3.2.1.2 FPV Panel Data Collection

In a previous study, it was found that polyethylene (PE) foam was the most cost-effective way to add buoyancy to flexible solar modules [188]. This study uses this after-market conversion method to convert SunPower SPR-E-Flex PVs into FPVs [204]. The density of the green polyethylene 1.2 lb ½" (12.7 mm) was used to determine the area of foam needed to make the panel rise by approximately 10 mm above the water's surface [205] using the calculations detailed in [188]. The foam was cut into about 50 mm by 240 mm sections that were placed evenly on the backside of module. The sections were then adhered using 3 M 5200 fast-set waterproof adhesive. Each foam piece had a line of adhesive caulked onto its perimeter and through the center. Then, the foam piece was pressed on the surface of the panel to adhere it, see Figure 3.1. The FPV with PV control was deployed in Chassell Bay, MI during the summer of 2020 to determine operational temperature and performance. This resulted in the FPV floating directly above the water surface, but still enabling wave action to clear the modules as shown in Figure 3.2.

(a) (b)

Figure 3.1. Cut away view showing adhesive underneath foam attached to c-Si-based flexible photovoltaic (PV) module: (a) top view and (b) orthogonal view.

Figure 3.2. Closeup of floating photovoltaic/floatovoltaic (FPV) corner after deployment, showing water coverage from a modest wave (top left).

The NanoDAQ monitoring board used in [188] was used in this study to measure module power and temperature of both the control (flat land-based mounted dry PV set at zero degree tilt angle) and wet FPV (floating on lake surface). The thermistors used for measuring temperature were held in place on the panels using 3M VHB tape. The air and water temperature were also measured with thermistors. The SunPower panels came with MC4 connectors installed on 12 AWG (2 mm^2) wires. MC4 connectors were added to the 14 AWG (1.6 mm^2) wires coming from the NanoDAQ, including the load wires. An additional hole was made in the NanoDAQ waterproof case and sealed using 3M 5200 to use the battery's USB port to power it. An AC load with a timer was used to drain the battery during mid-day to ensure there was a load to produce the power measurement. The schematic of the wiring diagram for the experimental set up is shown in Figure 3.3.

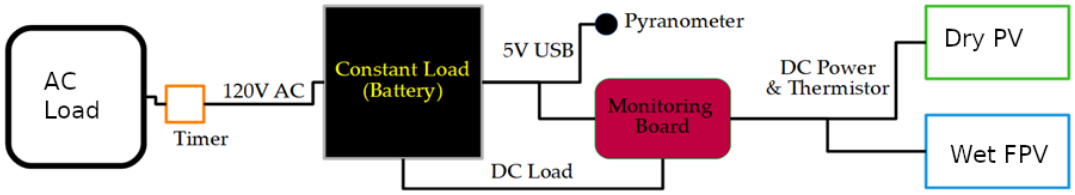

Figure 3.3. Wiring diagram for NanoDAQ monitoring board.

The FPV utilized mooring similar to that used in [188] except for the inclusion of a buoy. The wet FPV was moored by using an anchor and a towing ring on land. A rope was looped through the grommets in the solar PV and overhand loop knots were tied to secure the FPV in place. Energy generation of dry PV and wet FPV, temperature of air, water, PV, and FPV were recorded in 15 min increments.

3.2.2 Water Evaporation Modeling

The Penman–Monteith model used in this study is a data intensive water evaporation model because it requires the measurement of several weather data. Some of the data can be calculated, but the accuracy of the model is increased if they are measured. The Penman–Monteith model was originally designed to calculate the evapotranspiration losses from leaves' and canopies' surfaces [191]. However, the method has been adapted in several studies to estimate the evaporation of surface water [206-209]. One important thing to note regarding the use of the Penman–Monteith evapotranspiration model for lake evaporation is the use of water temperature instead of air temperature in some of the parameters' calculations: the outgoing longwave radiation, the partial vapor pressure at the water surface and slope of the temperature saturation water vapor curve. The original Penman–Monteith model estimates the evapotranspiration of crops; therefore, the model only uses the air temperature in its implementation. The use of water temperature instead of air temperature has been validated in several lake evaporation studies [206, 208, 209].

The Penman–Monteith [191] equation adapted to open water surfaces is [208, 209]:

$$E_L = \frac{1}{\lambda} \times \frac{\left(\Delta \times (R_N - H_S) + 86400 \times \rho_a \times Cp_a \times {}^{(P_w - P_a)}/_{r_a}\right)}{\Delta + \gamma} \quad (\text{mm} \cdot \text{day}^{-1}) \qquad (3.1)$$

where E_L (mm/day) is the daily evaporation rate and Cp_a (kJ/kg/°C) and ρ_a (kg/m^3) are, respectively, the heat capacity, and the density of air. The other parameters in the Penman–Monteith equation are: the latent heat of vaporization (λ) (MJ/kg), the slope of the saturation vapor pressure curve (Δ) (kPa/°C), the net daily solar radiation (R_N) (MJ/m^2/day), the daily heat storage flux (H_S) (MJ/m^2/day), the mean saturation vapor

pressure (P_w) (kPa), the actual vapor pressure of the air (P_a) (kPa), the aerodynamic resistance (r_a) (s/m), and the the psychrometric constant (γ) (kPa/°C). These parameters need to be calculated and depend on several weather data. The weather data needed to calculate these parameters are comprised of: the daily maximum ($T_{a,max}$) (°C) and daily minimum ($T_{a,min}$) (°C) air temperature; the daily maximum ($T_{w,max}$) (°C), daily minimum ($T_{w,min}$) (°C), and daily mean water temperature (T_w) (°C); the daily maximum (Rh_{max}) (%), and daily minimum relative humidity (Rh_{min}) (%); the daily mean dew temperature (T_d) (°C), the daily mean atmospheric pressure (P) (kPa); the daily mean wind speed (w_s) (m/s) at a height of 2 m above the water surface; and the daily incoming solar radiation (R_S) (MJ/m^2/day). The other parameters that are needed to calculate the components in the evaporation model of Penman–Monteith include: the altitude of the lake's location (h) (m); the surface area (A) (m^2), and the effective depth (d_w) (m) of the lake reservoir; and the latitude of the location of the water surface (ϕ) (rad).

When all the listed parameters are available, the computation of the lake water evaporation using the Penman–Monteith model starts with the calculation of the mean saturation vapor pressure (P_w) (kPa), and the actual vapor pressure of the air (P_a) (kPa) [192, 201, 207]:

$$P_w = \frac{1}{2} \times 0.6108 \times \left(\exp\left(\frac{17.27 \times \mathrm{T_{w,max}}}{\mathrm{T_{w,max}} + 237.3}\right) + \exp\left(\frac{17.27 \times \mathrm{T_{w,min}}}{\mathrm{T_{w,min}} + 237.3}\right)\right) \quad \text{(kPa)} \qquad (3.2)$$

$$P_a = \frac{1}{2} \times 0.6108 \times \left(\frac{Rh_{min}}{100} \times \exp\left(\frac{17.27 \times T_{w,max}}{T_{w,max} + 237.3}\right) + \frac{Rh_{max}}{100} \times \exp\left(\frac{17.27 \times T_{w,min}}{T_{w,min} + 237.3}\right)\right) \quad \text{(kPa)} \qquad (3.3)$$

After the calculation of the two vapor pressures, the slope of the saturation vapor pressure curve (Δ) (kPa/°C) is calculated [192, 201, 207]:

$$\Delta = \frac{4096 \times P_w}{(T_w + 237.3)^2} \quad (\mathrm{kPa \cdot {}^\circ C^{-1}}) \qquad (3.4)$$

Then, the latent heat of vaporization (λ) (MJ/kg), which depends on the water temperature, is calculated [192, 207]:

$$\lambda = 2.501 - 0.002361 \times T_w \quad (\mathrm{kPa \cdot {}^\circ C^{-1}}) \qquad (3.5)$$

From the latent heat of vaporization, the psychrometric constant (γ) (kPa/°C) can be deduced [192, 201],

$$\gamma = \frac{Cp_a \times P}{R_{MW} \times \lambda} \quad (\mathrm{kPa \cdot {}^\circ C^{-1}}) \qquad (3.6)$$

In Equation (3.6), R_{MW} = 0.622 and is equal to the molecular weight of water vapor over the molecular weight of dry air.

After that, the wind function f_w (MJ/m^2/kPa/day) is needed to estimate the aerodynamic resistance of the water surface. The formula used to calculate the wind function is proposed by McJannet et al. [210]. The formula was found to work well with the Penman–Monteith evaporation model. The wind function calculation by McJannet's formula depends on the wind speed as well as on the surface area of the lake.

$$f_w = (2.36 + 1.67 \times w_s) \times A^{-0.05} \quad (\mathrm{MJ \cdot m^{-2} \cdot kPa^{-1} \cdot day^{-1}}) \tag{3.7}$$

Once the wind function is known, a combination of the Penman–Monteith model equations presented in the works of Zotarelli et al. and Finch et al. gives the value of the aerodynamic resistance (s/m) [201, 209]:

$$r_a = \frac{\rho_a \times Cp_a \times 86400}{1000 \times \gamma \times f_w} \quad (\mathrm{s \cdot m^{-1}}) \tag{3.8}$$

The two remaining terms are the net solar radiation (R_N) (MJ/m^2/day) and the change in water heat storage flux (H_S) (MJ/m^2/day). The net solar radiation's calculation depends on the net longwave radiation (R_{NL}) (MJ/m^2/day) and the net shortwave radiation (R_{NS}) (MJ/m^2/day) [192, 201, 207].

$$R_N = R_{NS} - R_{NL} \quad (\mathrm{MJ \cdot m^{-2} \cdot day^{-1}}) \tag{3.9}$$

The net shortwave radiation is calculated using the albedo (a) and the measured incoming solar radiation (R_S) (MJ/m^2/day) [192, 201, 207-209]:

$$R_{NS} = (1 - a) \times R_S \quad (\mathrm{MJ \cdot m^{-2} \cdot day^{-1}}) \tag{3.10}$$

The net longwave radiation is calculated by taking the difference between the outgoing longwave radiation (R_{OL}) (MJ/m^2/day) and the incoming longwave radiation (R_{IL}) (MJ/m^2/day). The incoming longwave radiation is given by the Equation (3.11) [211, 212]

$$R_{IL} = \sigma \left(C_f + (1 - C_f) \left(1 - \left(0.261 \times \exp(-7.77 \times 10^{-4} T_a^2) \right) \right) \right) (T_a + 273.15)^4 \quad (\mathrm{MJ \cdot m^{-2} \cdot day^{-1}}) \tag{3.11}$$

In Equation (3.11), σ [MJ/m^2/T^4/day] is the Stefan–Boltzmann's constant, T_a is the daily mean air temperature and C_f is the cloud coverage fraction that has been estimated as follows [213]:

$$\begin{aligned} C_f &= 1.1 - R_{Ratio} \; ; \; R_{Ratio} \leq 0.9 \\ C_f &= 2(1 - R_{Ratio}) \; ; \; R_{Ratio} > 0.9 \end{aligned} \tag{3.12}$$

The parameter R_{Ratio} is the ratio of the incoming solar radiation (R_S) to the clear sky radiation R_{CS} (MJ/m^2/day). The clear sky radiation is calculated using Equation (3.13) [209, 212, 213]:

$$R_{CS} = (0.75 + 2 \cdot 10^{-5} \times h) \times R_{EX} \qquad (\mathrm{MJ \cdot m^{-2} \cdot day^{-1}}) \tag{3.13}$$

The extraterrestrial radiation R_{EX} (MJ/m^2/day) depends on the latitude of the lake, the sunset hour angle, the solar declination angle, the solar constant, and the inverse relative distance from the sun to earth. This calculation is a well-known procedure that has been detailed in the guide for crop evapotranspiration calculations by the FAO [192]. The outgoing longwave radiation depends on the water surface temperature and is calculated as:

$$R_{OL} = \varepsilon \times \sigma \times (T_w + 273.15)^4 \qquad (\mathrm{MJ \cdot m^{-2} \cdot day^{-1}}) \tag{3.14}$$

T_w (°C) is the mean daily water temperature and ε is the emissivity of the water surface. The emissivity of water surface varies between 0.95 and 0.99 for water temperatures below 55 °C [214]. An average value of ε = 0.97 has been used in this study. The net longwave radiation is therefore:

$$R_{NL} = R_{IL} - R_{OL} \qquad (\mathrm{MJ \cdot m^{-2} \cdot day^{-1}}) \tag{3.15}$$

The water heat storage flux (H_S) (MJ/m^2/day) expresses the change in the heat stored in the water from one day to another. The heat storage flux calculation methods used in two different studies by Abtew et al., and Finch et al. are suitable for shallow water bodies evaporation [207, 209]. Since Lake Mead is a deep lake, the equilibrium temperature approach proposed by de Bruin has been used instead. In this approach, an equilibrium temperature is used to estimate a mean daily uniform temperature of the water body for each day [215]. The heat storage flux's formula using de Bruin's method is [212, 215-217]:

$$H_S = \rho_w C p_w d_w \times {\left(T_{uw,j} - T_{uw,j-1}\right)}/{\Delta t} \qquad (\mathrm{MJ \cdot m^{-2} \cdot day^{-1}}) \tag{3.16}$$

The constants' values ρ_w (kg/m^3), Cp_w (MJ/kg/°C), d_w (m) are, respectively, the density of water, the heat capacity of water, and the depth of the lake. $T_{uw,j}$ and $T_{uw,j-1}$ are, respectively, the mean uniform water temperature for day (j), and day ($j–1$). Δt is the time step for the temperature estimation. The mean uniform water temperature ($T_{uw,j}$) depends on the equilibrium temperature (T_e) (°C) and the time constant (τ) (day):

$$T_{uw,j} = T_e + \left(T_{uw,j-1} - T_e\right) \times \exp\left({-1}/{\tau}\right) \qquad (°\mathrm{C}) \tag{3.17}$$

$$T_e = T_{wb} + \frac{R_{N,wb}}{4 \times \sigma \times (T_{wb} + 273.15)^3 + f_w \times (\Delta_{wb} + \gamma)} \qquad (°\mathrm{C}) \tag{3.18}$$

$$\tau = \frac{\rho_w \times Cp_w \times d_w}{4 \times \sigma \times (T_{wb} + 273.15)^3 + f_w \times (\Delta_{wb} + \gamma)} \qquad \text{(day)} \qquad (3.19)$$

$R_{N,wb}$ (MJ/m^2/day), T_{wb} (°C), and Δ_{wb} (kPa/K) are, respectively, the net radiation at the wet-bulb temperature, the wet-bulb temperature, and the slope of the saturation vapor pressure curve at the wet-bulb temperature. The wet-bulb temperature (T_{wb}) is calculated using the following equation [212, 217]:

$$T_{wb} = \frac{0.00066 \times 100 \times T_a + {(4098 \times P_a \times T_d)}/{(T_d + 237.3)^2}}{0.00066 \times 100 + {(4098 \times P_a \times T_d)}/{(T_d + 237.3)^2}} \qquad (°C) \qquad (3.20)$$

The saturation vapor pressure curve at the wet-bulb temperature Δ_{wb} (kPa/K) is calculated by:

$$\Delta_{wb} = \frac{4096 \times 0.6108 \times \exp\left(\frac{17.27 \times T_{wb}}{T_{wb} + 237.3}\right)}{(T_{wb} + 237.3)^2} \qquad (\text{kPa} \cdot \text{K}^{-1}) \qquad (3.21)$$

The net radiation ($R_{N,wb}$) at the wet-bulb temperature is:

$$R_{N,wb} = (1 - a) \times R_S + \left(R_{IL} - R_{OL,wb}\right) \qquad (\text{MJ} \cdot \text{m}^{-2} \cdot \text{day}^{-1}) \qquad (3.22)$$

In Equation (3.22), $R_{OL,wb}$ (MJ/m^2/day) is the outgoing longwave radiation at the wet-bulb temperature and is calculated by:

$$R_{OL,wb} = C_f \times \sigma \times \left((T_a + 273.15)^4 + 4 \times (T_a + 273.15)^3 \times (T_{wb} - T_a)\right) \qquad (\text{MJ} \cdot \text{m}^{-2} \cdot \text{day}^{-1}) \qquad (3.23)$$

After the calculation of all parameters, the lake evaporation's value (E_L) can be calculated using Equation (3.1).

3.2.3 Energy Production Modeling

The power output of a PV module (P_{out}) (W) is calculated by applying different losses to the incoming solar irradiance and is given by:

$$P_{out} = I_S \times A_P \times \eta_P \qquad (\text{W}) \qquad (3.24)$$

where I_S (W/m^2) is the incoming solar irradiance, A_P (m^2) is the effective area of the solar panel, and η_P (%) is the efficiency of the PV system. In this study, the efficiency of the

system includes the electrical efficiency of the module, which is dependent on the operating temperature, the shading losses, the soiling and hotspot losses, and the mismatch losses. Additionally, the solar irradiation component used is the global horizontal irradiation because the inclination of the panels is 0°. The power output is calculated hourly and summed up to determine the energy production of the system over a year.

3.2.3.1 FPV Operating Temperature

The energy produced by a photovoltaic system depends on the electrical efficiency of the modules. The electrical efficiency of the modules (η_e) changes with the operating temperature of the cell and is calculated using Equation (3.25) [179, 218]:

$$\eta_e = \eta_{ref} \times \left[1 - \beta \times \left(T_{eo} - T_{ref}\right)\right] \qquad (\%) \qquad (3.25)$$

where η_{ref} (%), β_{ref} (%/°C), T_{eo} (°C), and T_{ref} (°C) are, respectively, the reference efficiency of the panel, the temperature coefficient of the panel, the effective operating temperature of the panel, and the reference temperature.

The data collected from the FPV test bed are used to determine the effective operating temperature (T_{eo}) of the FPV. The model describing the temperature dependence on the ambient temperature and the solar power in nominal operating cell temperature (NOCT) conditions is a linear model [218-220]:

$$T_{cell} = T_{me} + k \times I_S \qquad (°C) \qquad (3.26)$$

T_{Cell} (°C) is the operating temperature of the solar cells, k (°C. m^2/W) is the coefficient of the relationship, I_S (W/m^2) is the solar irradiance, and T_{me} (°C) is the ambient temperature of the location of the solar module. This model is well-adapted for offshore, roof or ground mounted, PV systems but needs to be modified to accurately describe FPV systems. A study conducted by Kamuyu et al. [179] has proposed a solar cell temperature calculation in FPV using the air temperature, the water temperature, the solar irradiance, and the wind speed. Kamuyu et al.'s study focused on FPV mounted at a tilt angle relative to the water's surface where the air temperature and wind speed played a larger role in determining the module temperature than the water temperature. In this study, because the modules are on/under the water surface, wind speed is neglected, and the water temperature plays the dominant role in module temperature. Thus, the Kamuyu approach for pontoon-based FPV was adapted and used here with experimental data for solar flux, air temperature, water temperature, and module temperature. The approach used was a multilinear variable regression. The regression has three independent variables that are the solar irradiance (I_S), the water temperature (T_w), and the air temperature (T_a). The last variable of the regression, the FPV module's effective operating temperature (T_{eo}), depends on the previous three. The goal of the regression is to find a linear relationship between the module's effective operating temperature (T_{eo}), and the three independent variables in the form of:

$$T_{eo} = \alpha_0 + \alpha_1 T_w + \alpha_2 T_a + \alpha_3 I_S \qquad (°C), \tag{3.27}$$

where α_0 is a constant term; α_1, α_2, and α_3 are the regression coefficients relative to the water temperature, air temperature, and solar irradiance, respectively.

The solar module temperature dataset from the test bed has been stored in a MATLAB column vector, and the independent variables have been stored within a MATLAB numeric matrix to which an additional unit column has been added at the beginning to account for the coefficient α_0. Then, the regression is performed using a dedicated MATLAB function called "regress" [221]. The "regress" function performs a multivariable regression on experimental data and outputs the coefficients of the regression as well as other values such as the R-squared value of the regression and the residuals. The experimentally obtained coefficients are used in the case study of Lake Mead to estimate the effective operating module temperatures that are, in turn, used in the energy yield simulation.

3.2.3.2 Other Loss Factors

This study focuses on the FPV system; therefore, the other factors considered are only related to the panels. In the case of a complete system design, losses from other equipment such as the inverter or transformer need to be considered. Other factors that could impact the efficiency of the floating solar PV modules are the same as conventional land-based PV systems. These factors are solar irradiance losses, shading losses, soiling, mismatch losses, and DC cabling losses [194, 222, 223].

The foam-based support as well as the PV are mounted flat on the water surface (e.g., tilt angle = 0 degrees); therefore, they are not exposed to the optimum amount of solar irradiation for any location other than those on the equator. A study conducted by Jacobson et al. has provided an estimate of the optimal tilt for fixed tilt solar PV systems for different locations throughout the world [224]. The loss due to the tilt angle has been considered in this study and only the global horizontal irradiation for the energy yield calculation is used.

The impact of shading losses on FPV is low because water surfaces are flat and there are no nearby obstacles that could cause a direct shade to the modules. In the case of foam-based FPV, there is no mutual shade between the modules either because the mounting systems are flat on the water surface. Lake Mead is located in a mountainous region; therefore, far horizon shading may occur during certain times of the day or the year but is expected to be minimal. A detailed shading losses analysis has not been conducted during this study and an estimated value of zero percent has been used.

Soiling can be significant on FPV panels. Soiling in the case of FPV systems is mostly due to bird dropping or algae growth [188]. According to a report on FPV systems by the World Bank Group, nesting birds have been found to prefer the use of FPV modules as a nesting

place [194]. In the report of the World Bank Group, however, the floating systems used were inclined; thus, allowing the presence of sheltered places where the birds were nesting. In the case of foam-based FPV, it has been assumed that the effect of birds will be lower because the modules are mounted directly on the water surface and the mounting system offers no sheltered space for nesting. A detailed study of the impact of birds nesting on foam-based FPV panels would be interesting for future studies. In addition, by ensuring the FPV are above the water surface, the growth of algae on the front surface of the FPV can be minimized.

Mismatch losses and DC cable losses can be higher in FPV systems due to the relative movement of the modules on the water surface, but an optimum design can minimize these losses [194].

3.2.3.3 Parameters Used for Energy Yield Simulation

The energy production model simulates a floating solar PV system on the surface of Lake Mead. The area covered by the solar PV installation is described in Section 2.4. The values used for the energy production simulation as well as the sources of the values are given in Table 3.1.

Table 3.1. Energy modeling simulation parameters

Parameters	**Value**	**Source**
Solar PV temperature model	(Equation (3.27))	This study
Reference efficiency of the module	23%	[204]
Module inclination	0°	This study
Shading losses	0%	This study
Soiling	3%	[194]
Mismatch losses	6%	[223]
DC cable losses	3%	[223]

3.2.4 Water Savings Capability and Efficiency of the System

The water savings capability of the FPV system investigated in this study has been estimated to be 90% of the volume of water corresponding to the surface covered by the FPV. This assumption is supported by previous studies that found that covering water surfaces with pontoon-based FPV could reduce the evaporation losses by more than 90% [172, 225]. Thus, the resulting values are extremely conservative as here the FPV covers the entire water surface and is not a tilted FPV mount as in [172, 225]. When planning an FPV installation on a water surface, the percentage coverage of the water by the solar systems depends on the type of activities that are being performed on the body of water. According to the World Bank Group, the FPV system should not cover more than 50% of the water surface if used for fishing and not more than 60% if the water body is not used

for fishing [194]. Therefore, a sensitivity analysis will be run on the coverage percentage to investigate the energy production and water saving capability of the foam-based FPV system in this study from 10% to 50% in 10% increments because Lake Mead is used for fishing. Then, the water saving capability is estimated by multiplying the water evaporation rate and the surface coverage. The result is adjusted by 90%. The cost of water saved annually is estimated using the average water cost in Nevada where Lake Mead serves as a clean water source. The cost of water according to Las Vegas Valley Water District ranges from USD 0.35/m^3 to 1.37/m^3 for a family size residential home, according to the size of the installed water meter [226]. On the other hand, the wholesale electricity rate of the power produced at the Hoover Dam, located in Nevada, is USD 0.02/kWh [227, 228]. These values are used to estimate the lowest and highest potential energy revenues of the foam-based FPV system.

3.3 Results

3.3.1 Water Evaporation

The results from the water evaporation model simulation at Lake Mead show an evaporation rate estimate of 1957 mm in 2018. This result is in agreement with the results of the study conducted by Moreo and Swancar [189] on Lake Mead during the period of March 2010 through February 2012 using the eddy covariance evaporation method. The study estimated the lake evaporation from March 2010 to February 2011, and from March 2011 to February 2012. According to the two authors, the evaporation rate for the first study period had a minimum value of 1958 mm and a maximum value of 2190 mm; while the minimum value was 1787 mm and the maximum value was 1975 mm for the second study period. The result obtained in this present study is located within the result interval of Moreo and Swancar's study. Another early study by Westenburg et al. provided the evaporation data for Lake Mead from 1997 to 1999 [229]. The average evaporation rate for that period was 2281 mm per year.

Figure 3.4a shows the monthly results of the evaporation rates simulation using 2018 data. The evaporation rate is low in the winter and increases in summer. The evaporation rate at the peak of the summer, in June, is approximately five times more than the lowest evaporation rate of the winter, in December. Figure 3.4b shows the daily evaporation estimates throughout the year.

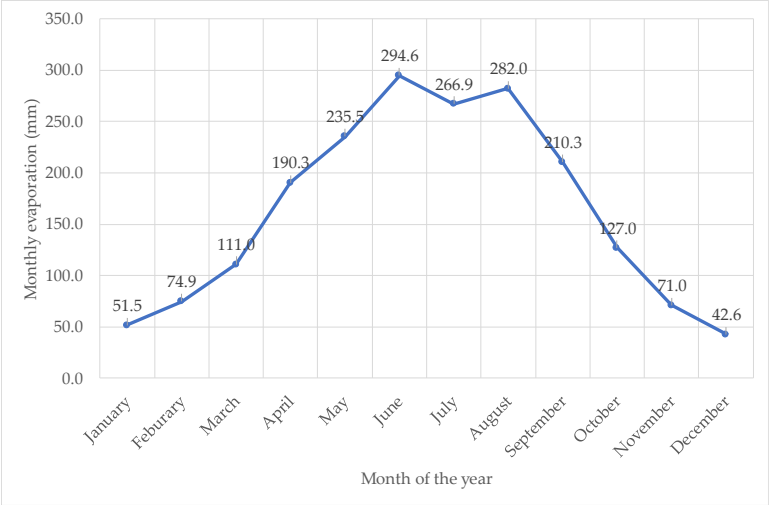

(a)

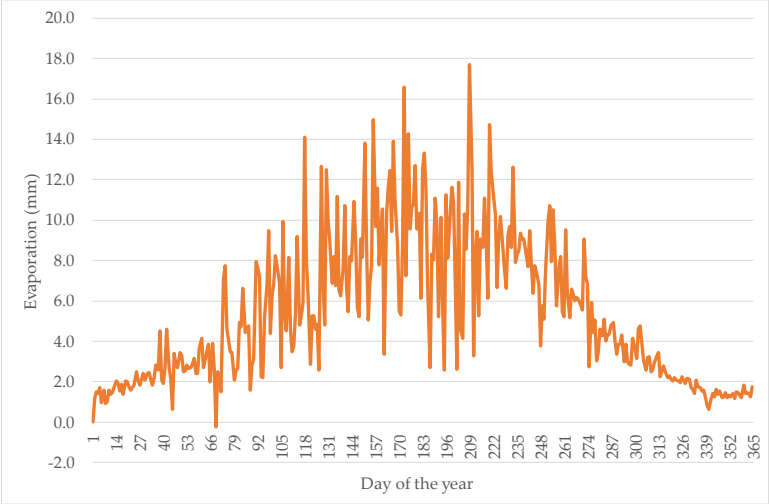

(b)

Figure 3.4. Water evaporation simulation results for Lake Mead: (a) simulated evaporation values (mm) for each month of the year 2018; (b) simulated evaporation values (mm) for each day of the year 2018.

3.3.2 Energy Production

3.3.2.1 FPV Operating Temperature Model

The multilinear regression on the collected data yielded the coefficients α_0, α_1, α_2, and α_3, which describe the relationship between the FPV effective operating temperature (T_{eo}) and the independent variables: the water temperature (T_w), the air temperature (T_a), and the solar irradiance (I_S). The regression coefficients have been obtained with an R-squared

value of 0.8276. Figure 3.5 shows the statistical results of the regression. The R-squared value combined with the random distribution of the residuals' plot on Figure 3.5b show that there is a linear relationship between T_{eo} and the independent variables.

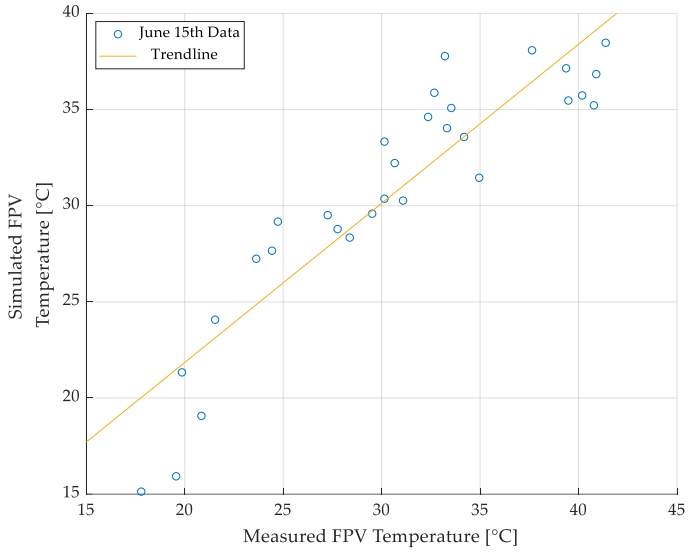

(a)

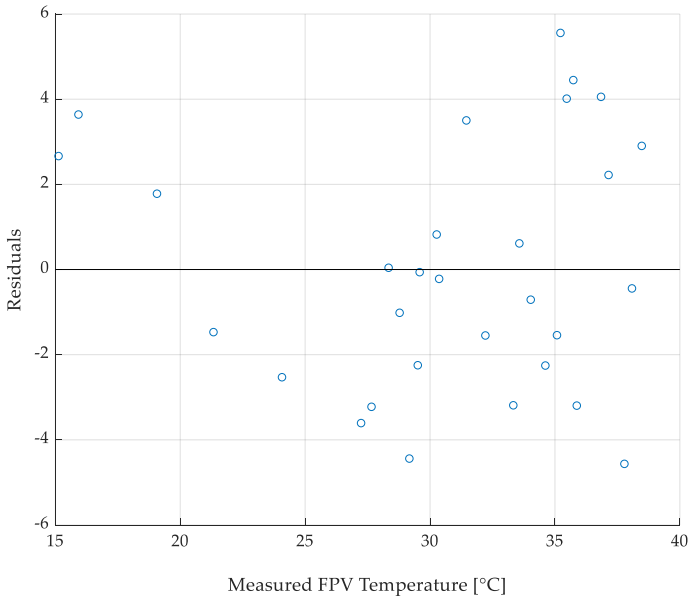

(b)

Figure 3.5. Multilinear regression results of the FPV panels' effective operating temperature (Teo): (a) simulated FPV temperature plotted against the measured temperature for 15 June 2020; (b) residuals' distribution plotted against the simulated FPV temperature for 15 June 2020.

Equation (3.28) is proposed as a model that represents the effective operation temperature of FPV mounted on a foam-based support.

$$T_{eo} = -13.2554 - 0.0875 \times T_w + 1.2645 \times T_a + 0.0128 \times I_S \quad (°C) \qquad (3.28)$$

Figure 3.6 shows the simulated operating temperature using the proposed model, the operating temperature of a titled aluminum pontoon-based mount FPV model based on the original Kamuyu et al.'s model (for pontoon-based tilted FPV), and the measured operating temperature for June 15 2020. The simulated temperature is at times higher or lower than the measured temperature, but the overall trend of the two temperature profiles matches. The model proposed in this study is compared to the unadapted tilted FPV model and the current model (which is an adaptation of Kamuyu et al.'s model for foam-backed flat-surface FPV) and provides a better description of a foam-based FPV panel's operating temperature. The proposed model in this study has a similar profile to Kamuyu's model, and the proposed model provides a better description of the foam-based solar module's behavior.

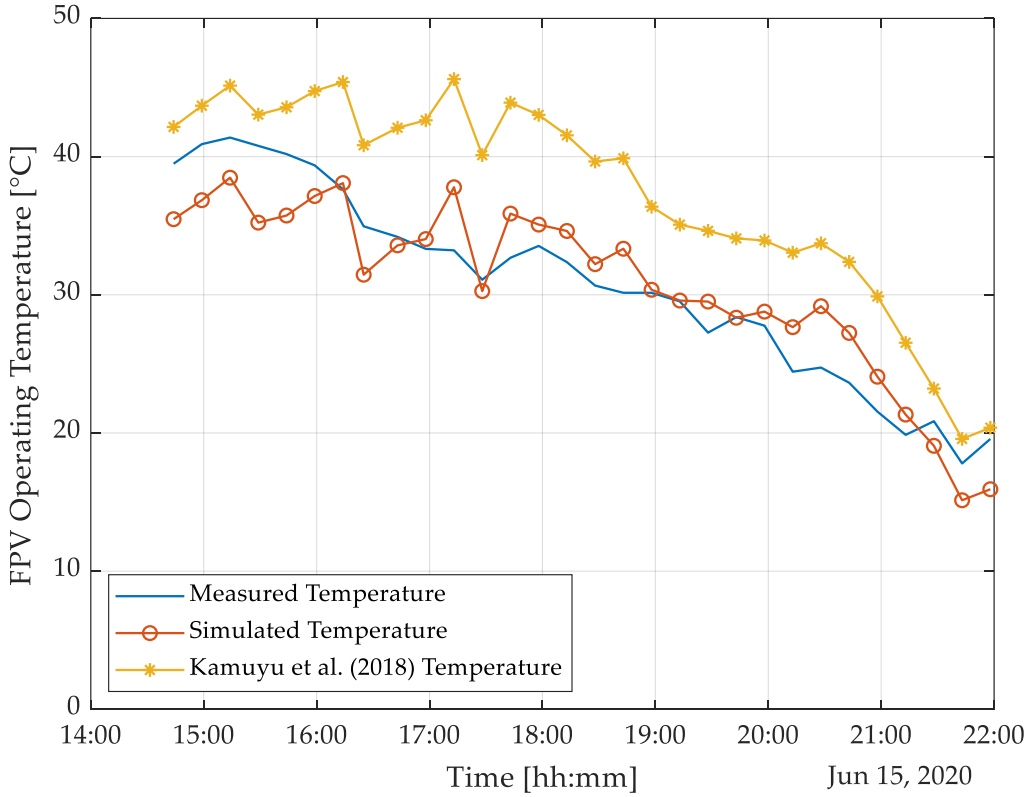

Figure 3.6. Measured FPV operating temperature compared to simulated FPV operating temperature for 15 June 2020.

The temperature profile of a foam-based FPV panel installed on Lake Mead has been simulated using the proposed FPV operating temperature model and compared to a pontoon-based FPV as described by Kamuyu's model in Figure 3.7.

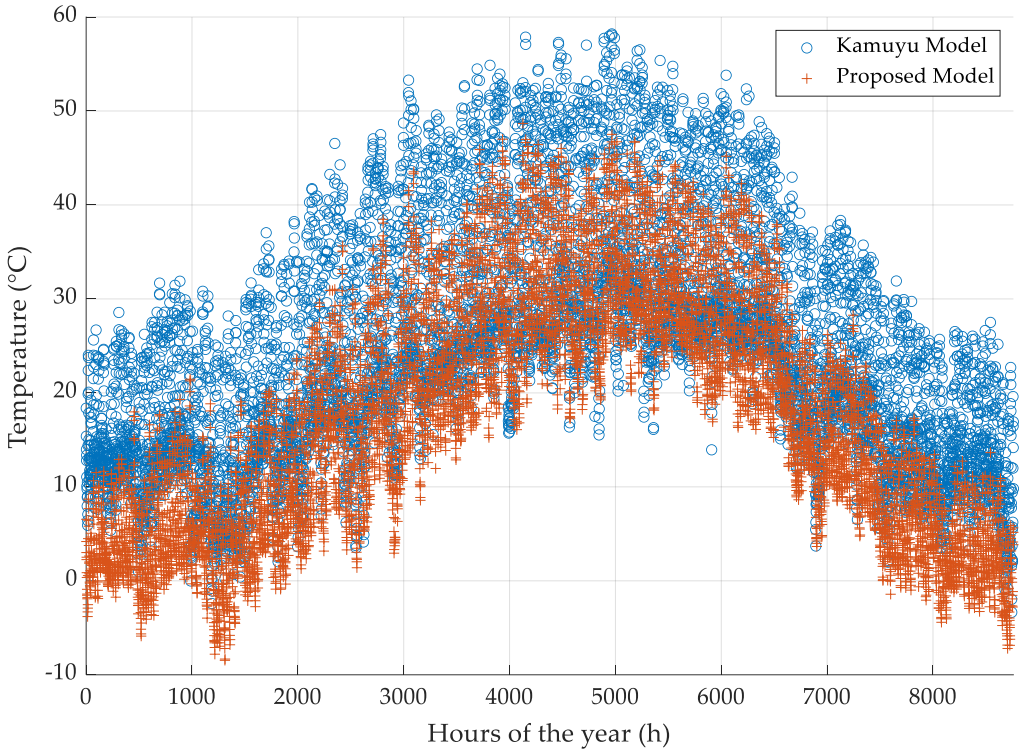

Figure 3.7. Operation temperature of an FPV installed on the surface of Lake Mead. (+) Operating temperature using the proposed model in this study for foam-based FPV. (o) Operating temperature using a pontoon-based tilted FPV described by Kamuyu's model.

The maximum temperature obtained with the model proposed in this study is 48.7 °C and the minimum temperature is −8.5 °C. On the other hand, the maximum temperature and the minimum temperature obtained if the FPV system was tilted are, respectively, 58.2 °C and −3.4 °C. Overall, the temperature model used here based on experimental data during the summer months predicts a lower temperature when the panels are in direct contact with the water surface.

3.3.2.2 Energy Yield and Water Savings of an FPV System Installed on Lake Mead

The temperature profile is used to estimate the electrical efficiency of the solar panel, which is in turn used to simulate the energy yield of an FPV system installed on Lake Mead with historical weather data. The energy yield has been simulated by assuming a coverage of

the lake surface (640 km^2) between 10 and 50% in 10% increments. The results are shown in detail for the 10% coverage case and the total energy production is shown for the other cases.

Figure 3.8 shows the comparison between the monthly energy production obtained using the proposed model and the energy production of a tilted FPV for 10% coverage of the lake's surface. As can be seen in Figure 3.8, and as expected from Figure 3.7, the proposed model predicts a slightly higher energy production, about 3.5%, which is correlated with the lower operating temperature of the modules**.** The maximum energy per month production is 3.2 TWh and occurs in the month of June, while the minimum energy per month production is 1.1 TWh and occurs in December.

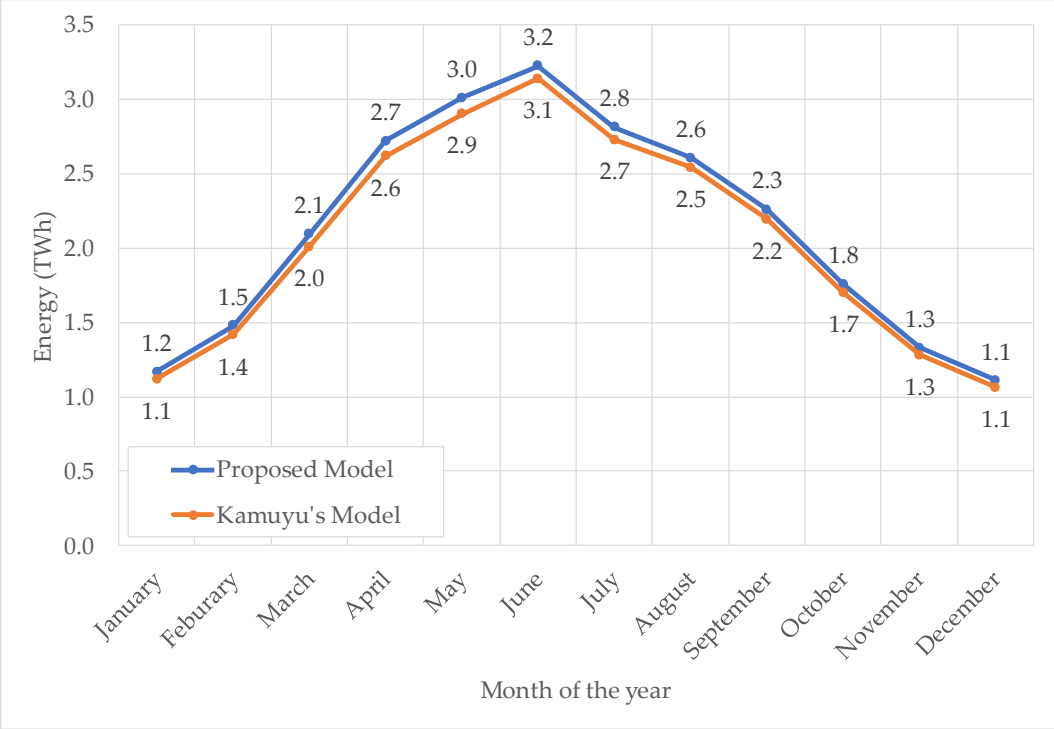

Figure 3.8. Monthly energy yield of a simulated foam-based FPV system installed on 10% of Lake Mead's surface using historical data from 2018. Comparison between the proposed model (c-Si flexible foam-backed FPV) and a tilted FPV based on Kamuyu's model (c-Si aluminum mount FPV).

Figure 3.9 shows the result for the daily energy simulation when 10% of Lake Mead's surface is covered with a foam-based solar FPV system. The maximum daily energy production is 570 MWh on 6 January while the minimum daily production is 21 MWh on 18 June.

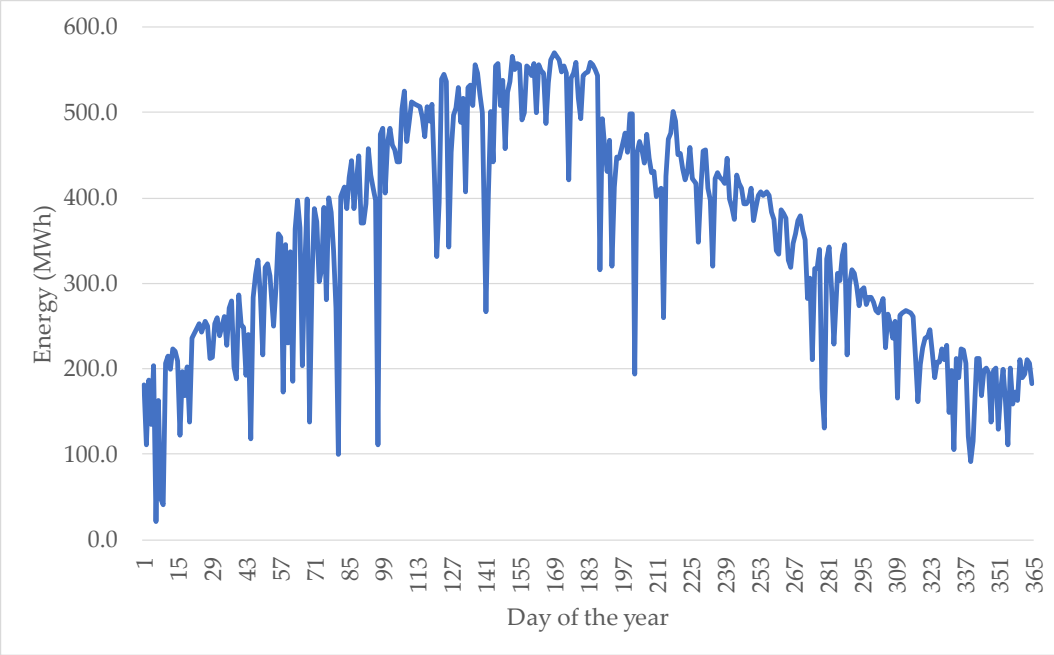

Figure 3.9. Daily energy production results using the temperature model proposed in this study for 10% coverage of Lake Mead's surface.

Figure 3.10 shows the simulated annual energy production, and the water saving capabilities of a foam-based solar FPV system installed on the surface of Lake Mead as a function of coverage area from 10–50%. For a coverage of 10%, the annual production using collected temperature data is 25.59 TWh, corresponding to a saved water volume of 126.64 million m^3. When the percentage coverage is increased, the energy production is increased linearly. For a coverage of 50% of the lake's surface, it is possible to harvest 127.93 TWh of electrical energy and save 633.22 million of m^3 of water using foam-based FPV panels.

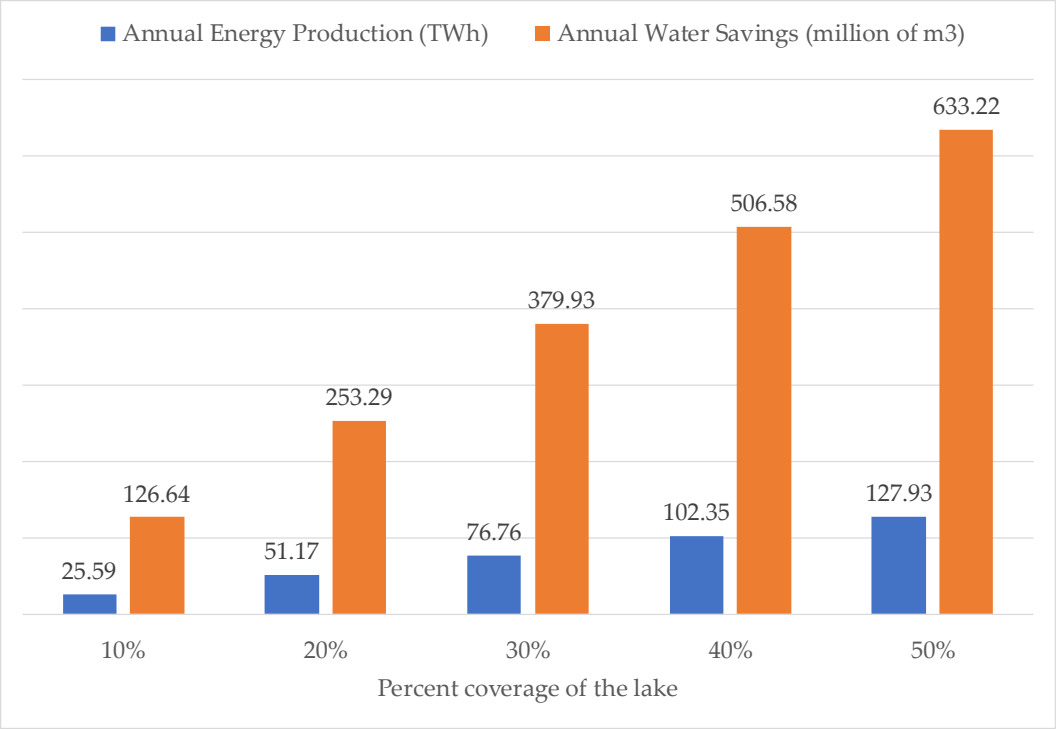

Figure 3.10. Simulated annual energy production (TWh) and water saving capability (millions of m3) of a foam-based solar FPV system installed on Lake Mead's surface using historical temperature data and the proposed model depending on the percentage coverage of the lake's surface.

Table 3.2 shows the annual water and energy savings estimates related to the water savings and energy production from the FPV. With houses with the least water consumption, the cost of the water saved is estimated to be USD 44 million when 10% of the lake surface is covered, and USD 220 million when 50% of the lake surface is covered. On the other hand, when the consumers' water consumption is on the high side, these costs increase, amounting to USD 172 million when 10% of the lake is covered and USD 861 million when 50% is covered. Furthermore, the results for the energy production show that USD 0.5 billion of energy can be generated when 10% of the lake surface is covered. The value of the energy generated when 50% of the lake surface is covered is estimated as USD 2.6 billion.

Table 3.2. Estimation of the yearly cost of water saved and energy produced using water and energy cost range from Nevada for an FPV system covering 10–50% of Lake Mead's surface.

Lake Surface Percent Coverage	**Water Savings at \$0.35/m^3 (Millions of \$)**	**Water Savings at \$1.37/m^3 (Millions of \$)**	**Energy Revenues at 2¢/kWh (Billions of \$)**
10%	43.99	172.19	0.51

20%	87.98	344.37	1.02
30%	131.97	516.56	1.54
40%	175.96	688.75	2.05
50%	219.95	860.94	2.56

The relative values of the water and energy provided by the foam-based FPV indicate that the electricity production from the FPV could be used to subsidize water conservation in arid and semi-arid areas. Thus, FPV could be a self-funded water conservation approach.

3.4 Discussion

The water evaporation calculation performed in this study predicts a significant water saving potential for foam-based FPV systems on Lake Mead. The evaporation calculation using historical data has shown an annual evaporation estimate of 1957.6 mm for the lake. The result of the calculation performed in this study is in agreement with previous evaporation studies on Lake Mead [189, 229]. The simulation results show annual water savings ranging from 126.64 to 633.22 million m^3 depending on the percentage of the lake surface covered by the FPV system. According to the United States Environmental Protection Agency (US EPA), each American uses, on average, 88 gallons of water per day, resulting in an annual water consumption of 32,120 gallons or 121.59 m^3 per capita [230]. The amount of water saved using foam-based FPV on Lake Mead will therefore be enough to supply water to more than five million Americans in the case that 50% of the lake surface is covered. This would make a significant impact on the cities near Lake Mead. The value is more than the four million population of the second largest city in the country, Los Angeles [231] or the entire population of Nevada of 3.1 million [232]. When 10% of the lake is covered by FPV panels, the amount of water saved is enough to supply water to the populations of both Henderson (320,189) and Las Vegas (651,319) or Las Vegas and Reno (255,601) in Nevada [233]. According to an analysis performed by Barsugli et al., Lake Mead has a 50% percent chance of going dry between 2035 and 2047 if nothing is done to stop the current draw down and evaporation rate of the lake [234]. Other studies on the management of the lake have resulted in the same conclusion [235, 236]. These studies have shown the need for new ways to mitigate lake evaporation not only on Lake Mead, but on other lakes in the world, especially those located in arid environments. Floating solar photovoltaic technology provides a solution to limit evaporation of water surfaces and provide electrical energy for the surrounding populations.

The energy production analysis has yielded an annual energy production ranging from 25.9 TWh to 127.93 TWh for a coverage of the lake of 10%, and 50%, respectively. The energy production profile is in accordance with a previous FPV study conducted by Kamuyu et al. [179], showing an improvement of 10% from a ground-mount system. This is confirmed by the study of Pierce et al., who determined that the energy production improvement of an FPV systems is 5–10% compared to a ground-mount system for mono and

polycrystalline silicon [188]. This is due to the cooling effect of the water on the FPV modules. According to the United States Energy Information Agency (US EIA), the average American household electricity consumption is 10,649 kWh per year. This means that the energy production of an FPV system covering 10% of Lake Mead has the capacity to power more than two million American homes [237]. This is more than the electricity needed to power the homes in Las Vegas, Henderson and Reno combined. On the other hand, the total electricity consumption in the U.S. according to 2018 statistics is 4178 TWh. This implies that the electricity production from a solar FPV system covering 50% of Lake Mead can supply 3% of the total electricity consumed in the U.S. and can replace more than 11% of the coal-fired power plants operating in the country; thus, contributing in a significant way to the reduction in the national carbon dioxide emissions [238] and the concomitant air pollution-related mortality [88, 124, 239, 240]. This study is in agreement with past work showing enormous potential for FPV on water bodies in the U.S. [241].

The results of this study show that there are several benefits to implementing a foam-based FPV solar plant. Foam-based FPV avoids the issues related to land use in ground-mounted solar PV [242] and since the floating device is made of low-cost material, the racking cost is lower than other raft racking FPV technologies [188]. In addition, FPV systems in general have the potential to form agrivoltaic type systems [243] by merging with aquaculture to form aquavoltaics [244, 245]. The flexible foam-backed FPV approach used here even makes mobile FPV possible. The FPV approach demonstrated here is less expensive than conventional pontoon-based FPV and has a slightly higher energy output per W because of the modules' close proximity to the water. FPV racking in general is less costly than conventional ground mounted PV. Thus, as PV is already often the least costly method for new electricity production, it provides a potentially profitable means of reducing water evaporation in the world's dwindling bodies of fresh water. Overall, the results of this study appear extremely promising. Solar FPV is a fairly new technology that is growing at a tremendous rate, but for it to reach its full potential, future work is needed to explore policies that sustain the development of this technology while also minimizing negative externalities. To accomplish this, a full life cycle analysis (LCA) study is needed on this technology.

Future work is also needed to experimentally verify the results of this study in different locations throughout the world. In addition, future work is needed to investigate fouling (and means to prevent it) in different bodies of water. More data should also be collected to further refine the temperature model and improve the energy production accuracy of the results shown here. Foam-based technology used as a floating device needs to be investigated more in order to have a commercially viable mass-produced FPV foam racking. The work shown here and completed previously was accomplished using after-market alterations of flexible PV modules. It should be pointed out that economic calculations used here assumed a 25-year lifetime for the PV modules. Although they are rated for extreme environments, guaranteed to resist corrosion and waterproof, the flexible SunPower modules only carry a 5-year warranty rather than the industry standard 25–30

year warranty. Future work to test the long-term performance of such systems is needed to ensure the reliability and safety of a foam-backed FPV as described in this article. In addition, future technical work is needed to investigate the potential for making flexible modules rated for high voltages that would be more appropriate for utility scale systems such as described in this study. The cost of the FPV racking would be further reduced by integrating bulk purchased foam into the PV manufacturing process. In addition, closed loop, circular economy [246-248] and industrial symbiosis [249] could be applied to the FPV manufacturing process. This would be expected to further reduce the cost of the FPV as well but may also necessitate policy intervention to ensure end of life recycling [250]. The polyethylene foam used here could be fabricated from recycled plastic waste [251-253], thereby further improving the environmental balance sheet for foam-backed FPV. Future studies can potentially look into the long-term stability of foam in water by analyzing the effect of different qualities of water on this material. Another aspect of foam-based rack where future work is needed is the mooring technology used to secure the FPV. Finally, the environmental impacts of the floating solar systems on marine life have not been fully established [194] and will be an interesting subject for future studies. These impacts include the effect of the FPV system on water temperature and stratification in the lake, as well as the effects of the system on oxygen transfer and dissolved oxygen levels in the lake.

3.5 Conclusions

This study introduced a new approach to FPV using a flexible crystalline silicon module backed with foam, which is less expensive than conventional pontoon-based FPV racking and land-based PV racking. The results show that the foam-backed FPV had a lower operating temperature than conventional pontoon-based fixed tilt out-of-water FPV and thus a higher energy output per unit power because of the modules' close proximity to the water. Thus, because PV costs are now normally the least costly method of new electricity production, the hypothetical large-scale foam-based FPV provides a potentially profitable means of reducing water evaporation in the world's at-risk bodies of fresh water.

The case study of Lake Mead found that if 10% of the lake was covered with foam-backed FPV, there would be more than enough solar electricity generated to power the homes in Las Vegas, Henderson and Reno combined and enough water savings for Las Vegas and Reno. At 50% lake coverage, the foam-backed FPV would provide over 127 TWh of clean solar electricity and 633.2 million m^3 of water savings, which would provide enough electricity to retire 11% of the polluting coal-fired plants in the U.S. and water for over five million Americans, annually.

4 Conclusions

This thesis has established a methodology to estimate the value of solar, has developed a cell operating temperature model of FPV modules proving the cooling effect of water on foam-based FPV modules, and has shown the water conservation potential of foam-based FPV systems. The case study of the value of solar in the U.S. has resulted in a possible *VOS* range from 9.37¢/kWh to 50.65¢/kWh showing that current net metering design rates are under-compensating solar owners. The FPV case study for Lake Mead has shown on the other hand that there is a great economic potential, water saving potential, and energy gain potential when foam-based flexible floating solar PV panels are installed on the surface of a water body, which would be expected to drive the VOS even higher.

The main challenge that was encountered during this thesis was data availability. When conducting a *VOS* study data from utility is often required and this data have been found to be difficult to acquire. On the other hand, an FPV model study requires a significant amount of weather data, some of which can be found through open-source satellite data. However, the best way to acquire data for an in-depth FPV study is to take measurements on-site, which is time-consuming.

This thesis paves the way to the following future research areas:

- Environmental life cycle assessment of a flexible foam-based floating solar PV module;
- Application of the *VOS* study on a floating PV system;
- *VOS* policy implications;
- *VOS* applications to other countries;
- Long-term stability of the foam-based rack in an aquatic environment;
- Further investigations on the mooring technology;
- Low-cost open source water data collection datalogger;
- Optimized electrical design of a standalone FPV system;
- Optimized electrical design of a grid connected FPV system;
- Power cogeneration potential of coupling a foam-based FPV system to a hydropower generation unit.
- Experimental and theoretical investigation of distributed flexible foam-based FPV as pool covers;
- Experimental and theoretical investigation of distributed flexible foam-based FPV as cottage power;
- Experimental and theoretical investigation of distributed flexible foam-based FPV as means of electrification for sustainable development;
- Experimental and theoretical investigation of centralized flexible foam-based FPV on large lakes and the oceans;
- Distributed manufacturing of flexible foam-based FPV;

- FPV-based policy for water conservation;
- Experimental flexible foam-based FPV aquavoltaics;
- Commercial viability of the foam-based FPV system.
- Environmental impact of a foam-based FPV system on water temperature and stratification in the lake;
- Effects of a foam-based FPV system on oxygen transfer and dissolved oxygen levels in the lake

5 Reference List

[1] IRENA. "Renewables Increasingly Beat Even Cheapest Coal Competitors on Cost." https://www.irena.org/newsroom/pressreleases/2020/Jun/Renewables-Increasingly-Beat-Even-Cheapest-Coal-Competitors-on-Cost (accessed.

[2] US EPA. "Distributed Generation of Electricity and its Environmental Impacts." United States Environmental Protection Agency. https://www.epa.gov/energy/distributed-generation-electricity-and-its-environmental-impacts (accessed 01-19, 2021).

[3] A. Shahsavari and M. Akbari, "Potential of solar energy in developing countries for reducing energy-related emissions," *Renewable and Sustainable Energy Reviews*, vol. 90, pp. 275-291, 2018, doi: 10.1016/j.rser.2018.03.065.

[4] "Renewable energy sources and climate change mitigation: special report of the Intergovernmental Panel on Climate Change," in "Choice Reviews Online," 0009-4978, 1523-8253, 2012/07/01 2012, vol. 49. Accessed: 2021/01/19/19:14:24. [Online]. Available: http://choicereviews.org/review/10.5860/CHOICE.49-6309

[5] T. Stanton, "Review of State Net Energy Metering and Successor Rate Designs," National Regulatory Research Institute, 2019 2019.

[6] K. R. Rábago *et al.*, "DESIGNING AUSTIN ENERGY'S SOLAR TARIFF USING A DISTRIBUTED PV VALUE CALCULATOR," Austin, TX, USA, Technical Report 2012 2012. [Online]. Available: http://www.rabagoenergy.com/files/value-of-solar-rate.pdf

[7] J. Farrell, "Minnesota's Value of Solar," Institute for Local Self-Reliance, Minnesota, USA, Technical Report 2014/04// 2014. [Online]. Available: /wp-content/uploads/2014/04/MN-Value-of-Solar-from-ILSR.pdf

[8] A. Poullikkas, "A comparative assessment of net metering and feed in tariff schemes for residential PV systems," (in en), *Sustainable Energy Technologies and Assessments*, vol. 3, pp. 1-8, 2013/09/01/ 2013, doi: 10.1016/j.seta.2013.04.001.

[9] K. Calvert, J. M. Pearce, and W. E. Mabee, "Toward renewable energy geo-information infrastructures: Applications of GIScience and remote sensing that build institutional capacity," (in en), *Renewable and Sustainable Energy Reviews*, vol. 18, pp. 416-429, 2013/02// 2013, doi: 10.1016/j.rser.2012.10.024.

[10] A. S. Pascaris, C. Schelly, and J. M. Pearce, "A First Investigation of Agriculture Sector Perspectives on the Opportunities and Barriers for Agrivoltaics," *Agronomy*, vol. 10, no. 12, 2020, doi: 10.3390/agronomy10121885.

[11] S. Yasmeena and G. T. R. Das, "A Review on New Era of Solar Power Systems: Floatovoltaic Systems or Floating Solar Power Plants," *JIC,* vol. 3, no. 1, pp. 1-8, 2015/01/15/ 2015, doi: 10.26634/jic.3.1.3419.

[12] Z. A. A. Majid, M. H. Ruslan, K. Sopian, M. Y. Othman, and M. S. M. Azmi, "Study on Performance of 80 Watt Floating Photovoltaic Panel," *J MECH ENG SCI,* vol. 7, no. 1, pp. 1150-1156, 2014/12/30/ 2014, doi: 10.15282/jmes.7.2014.14.0112.

[13] K. Trapani and D. L. Millar, "The thin film flexible floating PV (T3F-PV) array: The concept and development of the prototype," (in en), *Renewable Energy,* vol. 71, pp. 43-50, 2014/11/01/ 2014, doi: 10.1016/j.renene.2014.05.007.

[14] E. M. d. Sacramento, P. C. M. Carvalho, J. C. de Araújo, D. B. Riffel, R. M. d. C. Corrêa, and J. S. Pinheiro Neto, "Scenarios for use of floating photovoltaic plants in Brazilian reservoirs," *IET Renewable Power Generation,* vol. 9, no. 8, pp. 1019-1024, 2015 2015, doi: 10.1049/iet-rpg.2015.0120.

[15] K. Trapani and M. R. Santafé, "A review of floating photovoltaic installations: 2007–2013," (in en), *Progress in Photovoltaics: Research and Applications,* vol. 23, no. 4, pp. 524-532, 2015 2015, doi: 10.1002/pip.2466.

[16] S. S. Patil, M. M. Wagh, and N. N. Shinde, "A review on floating solar photovoltaic power plants," *Int. J. Sci. Eng. Res,* vol. 8, no. 6, pp. 789-794, 2017/06// 2017. [Online]. Available: https://www.ijser.org/researchpaper/A-Review-on-Floating-Solar-Photovoltaic-Power-Plants.pdf.

[17] N. M. Kumar, J. Kanchikere, and P. Mallikarjun, "Floatovoltaics: Towards improved energy efficiency, land and water management," *International Journal of Civil Engineering and Technology*, vol. 9, no. 7, pp. 1089-1096, 2018 2018. [Online]. Available: https://www.researchgate.net/profile/Nallapaneni_Manoj_Kumar2/publication/326675843_Floatovoltaics_Towards_improved_energy_efficiency_land_and_water_management/links/5b5d7413aca272a2d672c9e5/Floatovoltaics-Towards-improved-energy-efficiency-land-and-water-management.pdf.

[18] C. Ferrer-Gisbert, J. J. Ferrán-Gozálvez, M. Redón-Santafé, P. Ferrer-Gisbert, F. J. Sánchez-Romero, and J. B. Torregrosa-Soler, "A new photovoltaic floating cover system for water reservoirs," (in en), *Renewable Energy,* vol. 60, pp. 63-70, 2013/12/01/ 2013, doi: 10.1016/j.renene.2013.04.007.

[19] A. McKay, "Floatovoltaics: Quantifying the Benefits of a Hydro-Solar Power Fusion," Pomona College, 2013.

[20] M. R. Santafé, P. S. Ferrer Gisbert, F. J. Sánchez Romero, J. B. Torregrosa Soler, J. J. Ferrán Gozálvez, and C. M. Ferrer Gisbert, "Implementation of a photovoltaic floating cover for irrigation reservoirs," (in en), *Journal of Cleaner Production*, vol. 66, pp. 568-570, 2014/03/01/ 2014, doi: 10.1016/j.jclepro.2013.11.006.

[21] P. Sharma, B. Muni, and D. Sen, "Design parameters of 10 KW floating solar power plant," presented at the National Conference on Renewable Energy and Environment (NCREE-2015), 2015, 2015. [Online]. Available: https://www.iarjset.com/upload/2015/si/ncree-15/IARJSET%2017%20P127.pdf.

[22] F. Haugwitz, "Floating solar PV gains global momentum," (in en-US), *pv magazine International*, PV Magazine 2020/09/22/ 2020. [Online]. Available: https://www.pv-magazine.com/2020/09/22/floating-solar-pv-gains-global-momentum/.

[23] C. F. Yu, W. G. J. H. M. van Sark, and E. A. Alsema, "Unraveling the photovoltaic technology learning curve by incorporation of input price changes and scale effects," (in en), *Renewable and Sustainable Energy Reviews*, vol. 15, no. 1, pp. 324-337, 2011/01/01/ 2011, doi: 10.1016/j.rser.2010.09.001.

[24] S. Hong, Y. Chung, and C. Woo, "Scenario analysis for estimating the learning rate of photovoltaic power generation based on learning curve theory in South Korea," (in en), *Energy*, vol. 79, pp. 80-89, 2015/01/01/ 2015, doi: 10.1016/j.energy.2014.10.050.

[25] A. J. C. Trappey, C. V. Trappey, H. Tan, P. H. Y. Liu, S.-J. Li, and L.-C. Lin, "The determinants of photovoltaic system costs: an evaluation using a hierarchical learning curve model," (in en), *Journal of Cleaner Production*, vol. 112, pp. 1709-1716, 2016/01/20/ 2016, doi: 10.1016/j.jclepro.2015.08.095.

[26] I. Mauleón, "Photovoltaic learning rate estimation: Issues and implications," (in en), *Renewable and Sustainable Energy Reviews*, vol. 65, pp. 507-524, 2016/11/01/ 2016, doi: 10.1016/j.rser.2016.06.070.

[27] D. Feldman, G. Barbose, R. Margolis, R. Wiser, N. Darghouth, and A. Goodrich, "Photovoltaic (PV) Pricing Trends: Historical, Recent, and Near-Term Projections," National Renewable Energy Laboratory, Golden, CO, USA, Technical Report DOE/GO-102012-3839, 2012/11// 2012. [Online]. Available: https://www.nrel.gov/docs/fy13osti/56776.pdf

[28] G. L. Barbose, N. R. Darghouth, D. Millstein, K. H. LaCommare, N. DiSanti, and R. Widiss, "Tracking the Sun X: The Installed Price of Residential and Non-Residential Photovoltaic Systems in the United States," Lawrence Berkley National Laboratory, Technical Report LBNL-2001062, 2017/09// 2017. [Online].

Available: https://eta-publications.lbl.gov/sites/default/files/tracking_the_sun_10_report.pdf

[29] "PVinsights," (in en), 2020/04/06/ 2020. [Online]. Available: http://pvinsights.com/.

[30] M. Kroll *et al.*, "Black silicon for solar cell applications," in *Proc.SPIE*, 2012/05/02/ 2012, vol. 8438, Brussels, Belgium: International Society for Optics and Photonics, doi: 10.1117/12.922380. [Online]. Available: https://doi.org/10.1117/12.922380

[31] A. Barron, "Cost reduction in the solar industry," *Materials Today*, vol. 18, pp. 2-3, 2015//02/ 2015, doi: 10.1016/j.mattod.2014.10.022.

[32] C. Modanese, H. Laine, T. Pasanen, H. Savin, and J. Pearce, "Economic Advantages of Dry-Etched Black Silicon in Passivated Emitter Rear Cell (PERC) Photovoltaic Manufacturing," *Energies*, vol. 11, p. 2337, 2018//09/ 2018, doi: 10.3390/en11092337.

[33] Reuters, "Solar costs to fall further, powering global demand - Irena," (in en), *Reuters*, 2017/10/23/ 2017. [Online]. Available: https://www.reuters.com/article/singapore-energy-solar-idUSL4N1MY2F8.

[34] K. Branker, M. J. M. Pathak, and J. M. Pearce, "A review of solar photovoltaic levelized cost of electricity," (in en), *Renewable and Sustainable Energy Reviews*, vol. 15, no. 9, pp. 4470-4482, 2011/12/01/ 2011, doi: 10.1016/j.rser.2011.07.104.

[35] C. Richard, "New wind and solar cheaper than existing coal and gas," 2018/08// 2018. [Online]. Available: https://www.windpowermonthly.com/article/1491146/new-wind-solar-cheaper-existing-coal-gas.

[36] E. Tervo, K. Agbim, F. DeAngelis, J. Hernandez, H. K. Kim, and A. Odukomaiya, "An economic analysis of residential photovoltaic systems with lithium ion battery storage in the United States," (in en), *Renewable and Sustainable Energy Reviews*, vol. 94, pp. 1057-1066, 2018/10/01/ 2018, doi: 10.1016/j.rser.2018.06.055.

[37] H. Liu, D. Azuatalam, A. C. Chapman, and G. Verbič, "Techno-economic feasibility assessment of grid-defection," (in en), *International Journal of Electrical Power & Energy Systems*, vol. 109, pp. 403-412, 2019/07/01/ 2019, doi: 10.1016/j.ijepes.2019.01.045.

[38] W.-P. Schill, A. Zerrahn, and F. Kunz, "Solar Prosumage: An Economic Discussion of Challenges and Opportunities," in *Energy Transition: Financing Consumer Co-*

Ownership in Renewables, J. Lowitzsch Ed. Cham: Springer International Publishing, 2019, pp. 703-731.

[39] J. von Appen and M. Braun, "Strategic decision making of distribution network operators and investors in residential photovoltaic battery storage systems," (in en), *Applied Energy*, vol. 230, pp. 540-550, 2018/11/15/ 2018, doi: 10.1016/j.apenergy.2018.08.043.

[40] H. M. Marczinkowski and P. A. Østergaard, "Residential versus communal combination of photovoltaic and battery in smart energy systems," (in en), *Energy*, vol. 152, pp. 466-475, 2018/06/01/ 2018, doi: 10.1016/j.energy.2018.03.153.

[41] C. S. Lai and M. D. McCulloch, "Levelized cost of electricity for solar photovoltaic and electrical energy storage," (in en), *Applied Energy*, vol. 190, pp. 191-203, 2017/03/15/ 2017, doi: 10.1016/j.apenergy.2016.12.153.

[42] M. H. Kang and A. Rohatgi, "Quantitative analysis of the levelized cost of electricity of commercial scale photovoltaics systems in the US," (in en), *Solar Energy Materials and Solar Cells*, vol. 154, pp. 71-77, 2016/09/01/ 2016, doi: 10.1016/j.solmat.2016.04.046.

[43] International Renewable Energy Agency, *Renewable power generation costs in 2017*. Abu Dhabi, UAE(in en), 2018, p. 160.

[44] D. Dudley, "Renewable Energy Will Be Consistently Cheaper Than Fossil Fuels By 2020, Report Claims," (in en), *Forbes*, 2018/01// 2018. [Online]. Available: https://www.forbes.com/sites/dominicdudley/2018/01/13/renewable-energy-cost-effective-fossil-fuels-2020/.

[45] B. Banerjee and S. M. Islam, "Reliability based optimum location of distributed generation," (in en), *International Journal of Electrical Power & Energy Systems*, vol. 33, no. 8, pp. 1470-1478, 2011/10/01/ 2011, doi: 10.1016/j.ijepes.2011.06.029.

[46] L. Liu, H. Bao, and H. Liu, "Siting and sizing of distributed generation based on the minimum transmission losses cost," in *2011 IEEE Power Engineering and Automation Conference*, 2011/09// 2011, vol. 3, Wuhan, China, pp. 22-25, doi: 10.1109/PEAM.2011.6135006. [Online]. Available: https://ieeexplore.ieee.org/document/6135006

[47] N. M. Saad *et al.*, "Impacts of Photovoltaic Distributed Generation Location and Size on Distribution Power System Network," (in en), *IJPEDS*, vol. 9, no. 2, p. 905, 2018/06/01/ 2018, doi: 10.11591/ijpeds.v9.i2.pp905-913.

[48] P. P. Barker and R. W. De Mello, "Determining the impact of distributed generation on power systems. I. Radial distribution systems," in *2000 Power Engineering Society Summer Meeting*, 2000 2000, vol. 3, Seattle, WA, USA: IEEE, pp. 1645-1656, doi: 10.1109/PESS.2000.868775. [Online]. Available: http://ieeexplore.ieee.org/document/868775/

[49] R. E. Brown and H. L. Willis, "The economics of aging infrastructure," *IEEE Power and Energy Magazine*, vol. 4, no. 3, pp. 36-43, 2006/05// 2006, doi: 10.1109/MPAE.2006.1632452.

[50] Z. Li and J. Guo, "Wisdom about age [aging electricity infrastructure]," *IEEE Power and Energy Magazine*, vol. 4, no. 3, pp. 44-51, 2006/05// 2006, doi: 10.1109/MPAE.2006.1632453.

[51] H. L. Willis and R. R. Schrieber, *Aging power delivery infrastructures*, 2nd ed. ed. (Power engineering ; 35). Boca Raton: CRC Press/Taylor & Francis (in eng), 2017, p. 820.

[52] D. Pudasainee, J.-H. Kim, and Y.-C. Seo, "Mercury emission trend influenced by stringent air pollutants regulation for coal-fired power plants in Korea," (in en), *Atmospheric Environment*, vol. 43, no. 39, pp. 6254-6259, 2009/12/01/ 2009, doi: 10.1016/j.atmosenv.2009.06.007.

[53] M. Celebi, F. Graves, and C. Russell, "Potential Coal Plant Retirements: 2012 Update," (in en), *The Battle Group*, p. 13, 2012/10// 2012.

[54] M. Rallo, M. A. Lopez-Anton, M. L. Contreras, and M. M. Maroto-Valer, "Mercury policy and regulations for coal-fired power plants," (in en), *Environ Sci Pollut Res*, vol. 19, no. 4, pp. 1084-1096, 2012/05/01/ 2012, doi: 10.1007/s11356-011-0658-2.

[55] M. B. Gerrard and S. Welton, "US Federal Climate Change Law in Obama's Second Term," *Transnational Environmental Law*, vol. 3, no. 1, pp. 111-125, 2014/04// 2014, doi: 10.1017/S2047102514000016.

[56] E. De Cian, F. Sferra, and M. Tavoni, "The influence of economic growth, population, and fossil fuel scarcity on energy investments," (in en), *Climatic Change*, vol. 136, no. 1, pp. 39-55, 2016/05/01/ 2016, doi: 10.1007/s10584-013-0902-5.

[57] E. Kriegler *et al.*, "RoSE: Roadmaps Towards Sustainable Energy Futures and Climate Protection: A Synthesis of Results from the Rose Project," *The RoSE Project of the Potsdam Institute for Climate Impact Research*, 2013/01/01/ 2013. [Online]. Available: https://ecommons.udayton.edu/phy_fac_pub/8.

[58] D. J. Murphy, "The implications of the declining energy return on investment of oil production," *Philosophical Transactions of the Royal Society A: Mathematical, Physical and Engineering Sciences*, vol. 372, no. 2006, p. 20130126, 2014/01/13/ 2014, doi: 10.1098/rsta.2013.0126.

[59] E. J. Wilson, S. J. Friedmann, and M. F. Pollak, "Research for Deployment: Incorporating Risk, Regulation, and Liability for Carbon Capture and Sequestration," *Environ. Sci. Technol.*, vol. 41, no. 17, pp. 5945-5952, 2007/09/01/ 2007, doi: 10.1021/es062272t.

[60] D. Burtraw, K. Palmer, A. Paul, B. Beasley, and M. Woerman, "Reliability in the U.S. electricity industry under new environmental regulations," (in en), *Energy Policy*, vol. 62, pp. 1078-1091, 2013/11/01/ 2013, doi: 10.1016/j.enpol.2013.06.070.

[61] L. F. Pratson, D. Haerer, and D. Patiño-Echeverri, "Fuel Prices, Emission Standards, and Generation Costs for Coal vs Natural Gas Power Plants," *Environ. Sci. Technol.*, vol. 47, no. 9, pp. 4926-4933, 2013/05/07/ 2013, doi: 10.1021/es4001642.

[62] J. Linn, E. Mastrangelo, and D. Burtraw, "Regulating Greenhouse Gases from Coal Power Plants under the Clean Air Act," *Journal of the Association of Environmental and Resource Economists*, vol. 1, no. 1/2, pp. 97-134, 2014/03/01/ 2014, doi: 10.1086/676038.

[63] D. Burtraw, J. Linn, K. Palmer, and A. Paul, "The Costs and Consequences of Clean Air Act Regulation of CO_2 from Power Plants," *The American Economic Review*, vol. 104, no. 5, pp. 557-562, 2014 2014. [Online]. Available: https://www.jstor.org/stable/42920998.

[64] E. Prehoda, J. M. Pearce, and C. Schelly, "Policies to Overcome Barriers for Renewable Energy Distributed Generation: A Case Study of Utility Structure and Regulatory Regimes in Michigan," (in en), *Energies*, vol. 12, no. 4, p. 674, 2019/01// 2019, doi: 10.3390/en12040674.

[65] C. Schelly, E. P. Louie, and J. M. Pearce, "Examining interconnection and net metering policy for distributed generation in the United States," (in en), *Renewable Energy Focus*, vol. 22-23, pp. 10-19, 2017/12/01/ 2017, doi: 10.1016/j.ref.2017.09.002.

[66] NREL, "Value-of-Solar Tariffs | State, Local, and Tribal Governments | NREL," 2019/05// 2019. [Online]. Available: https://www.nrel.gov/state-local-tribal/basics-value-of-solar-tariffs.html.

[67] B. L. Noris, M. C. Putnam, and T. E. Hoff, "Minnesota Value of Solar: Methodology," Clean Power Research, Technical Report 2014/01/30/ 2014. [Online]. Available: https://www.cleanpower.com/wp-content/uploads/MN-VOS-Methodology-2014-01-30-FINAL.pdf

[68] Clean Power Research, "2014 Value of Solar at At Austin Energy," Clean Power Research, Austin, TX, USA, Technical Report 2013/10/21/ 2013. [Online]. Available: http://www.austintexas.gov/edims/document.cfm?id=199131

[69] A. Holm, J. J. Cook, A. Y. Aznar, J. W. Coughlin, and B. Mow, "Distributed Solar Photovoltaic Cost-Benefit Framework Study: Considerations and Resources for Oklahoma," Technical Report NREL/TP-7A40-72166, 1561512, 2019/09/05/ 2019. Accessed: 2020/02/07/14:27:45. [Online]. Available: http://www.osti.gov/servlets/purl/1561512/

[70] R. Perez, B. L. Norris, and T. E. Hoff, "The Value of Distributed Solar Electric Generation to New Jersey and Pennsylvania," Clean Power Research, Technical Report 2012/11// 2012. [Online]. Available: https://www.nj.gov/emp/pdf/cleanrenewablepower/MSEIA-Final-Benefits-of-Solar-Report-2012-11-01(1).pdf

[71] A. Brown and J. Bunyan, "Valuation of Distributed Solar: A Qualitative View," (in eng), *The Electricity Journal*, vol. 27, no. 10, pp. 27-48, 2014 2014, doi: 10.1016/j.tej.2014.11.005.

[72] M. Taylor, J. McLaren, K. Cory, T. Davidovich, J. Sterling, and M. Makhyoun, "Value of Solar. Program Design and Implementation Considerations," National Renewable Energy Lab. (NREL), Golden, CO (United States), Golden, CO, USA, Technical Report NREL/TP-6A20-62361, 2015/03/01/ 2015. Accessed: 2020/04/04/19:10:23. [Online]. Available: https://www.osti.gov/biblio/1215005

[73] F. D. Munoz and A. D. Mills, "Endogenous Assessment of the Capacity Value of Solar PV in Generation Investment Planning Studies," (in en), *IEEE Transactions on Sustainable Energy*, vol. 6, no. 4, pp. 1574-1585, 2015/10/01/ 2015, doi: 10.1109/tste.2015.2456019.

[74] D. Gami, R. Sioshansi, and P. Denholm, "Data Challenges in Estimating the Capacity Value of Solar Photovoltaics," *IEEE Journal of Photovoltaics*, vol. 7, no. 4, pp. 1065-1073, 2017/07// 2017, doi: 10.1109/JPHOTOV.2017.2695328.

[75] J. B. Keyes and K. R. Rábago, "A REGULATOR'S GUIDEBOOK: Calculating the Benefits and Costs of Distributed Solar Generation," Interstate Renewable Energy Council, Inc., Technical Report 2013/10// 2013. [Online]. Available:

https://irecusa.org/publications/a-regulators-guidebook-calculating-the-benefits-and-costs-of-distributed-solar-generation/

[76] P. Denholm *et al.*, "Methods for Analyzing the Benefits and Costs of Distributed Photovoltaic Generation to the U.S. Electric Utility System," National Renewable Energy Laboratory, Golden, CO, USA, Technical Report NREL/TP-6A20-62447, 1159357, 2014/09/01/ 2014. Accessed: 2020/03/03/04:37:24. [Online]. Available: http://www.osti.gov/servlets/purl/1159357/

[77] G. Blackburn, C. Magee, and V. Rai, "Solar Valuation and the Modern Utility's Expansion into Distributed Generation," (in en), *The Electricity Journal*, vol. 27, no. 1, pp. 18-32, 2014/01/01/ 2014, doi: 10.1016/j.tej.2013.12.002.

[78] D. Pitt and G. Michaud, "Assessing the Value of Distributed Solar Energy Generation," (in eng), *Current Sustainable/Renewable Energy Reports*, vol. 2, no. 3, pp. 105-113, 2015 2015, doi: 10.1007/s40518-015-0030-0.

[79] S. Harari and N. Kaufman, "Assessing the Value of Distributed Solar," (in en), *Yale Center for Business and the environment*, p. 21, 2017 2017.

[80] A. C. Orrell, J. S. Homer, and Y. Tang, "Distributed Generation Valuation and Compensation," Technical Report PNNL-27271, 1561273, 2018/02/14/ 2018. Accessed: 2020/02/07/14:23:44. [Online]. Available: http://www.osti.gov/servlets/purl/1561273/

[81] A. Proudlove, B. Lips, and D. Sarkisian, "The 50 States of Solar: 2019 Policy Review Q4 2019 Quarterly Report," NC CLEAN ENERGY TECHNOLOGY CENTER, 2020/01// 2020.

[82] P. R. Brown and F. M. O'Sullivan, "Spatial and temporal variation in the value of solar power across United States electricity markets," (in en), *Renewable and Sustainable Energy Reviews*, vol. 121, p. 109594, 2020/04/01/ 2020, doi: 10.1016/j.rser.2019.109594.

[83] K. Siler-Evans, I. L. Azevedo, M. G. Morgan, and J. Apt, "Regional variations in the health, environmental, and climate benefits of wind and solar generation," (in eng), *Proceedings of the National Academy of Sciences of the United States of America*, vol. 110, no. 29, pp. 11768-11773, 2013 2013, doi: 10.1073/pnas.1221978110.

[84] D. Millstein, R. Wiser, M. Bolinger, and G. Barbose, "The climate and air-quality benefits of wind and solar power in the United States," (in en), *Nat Energy*, vol. 2, no. 9, p. 17134, 2017/09// 2017, doi: 10.1038/nenergy.2017.134.

[85] R. Wiser *et al.*, "The environmental and public health benefits of achieving high penetrations of solar energy in the United States," (in en), *Energy*, vol. 113, pp. 472-486, 2016/10/15/ 2016, doi: 10.1016/j.energy.2016.07.068.

[86] C. v. Möllendorff and H. Welsch, "Measuring Renewable Energy Externalities: Evidence from Subjective Well-being Data," (in en), *Land Economics*, vol. 93, no. 1, pp. 109-126, 2017/02/01/ 2017, doi: 10.3368/le.93.1.109.

[87] D. Abel *et al.*, "Potential air quality benefits from increased solar photovoltaic electricity generation in the Eastern United States," (in en), *Atmospheric Environment*, vol. 175, pp. 65-74, 2018/02/01/ 2018, doi: 10.1016/j.atmosenv.2017.11.049.

[88] E. W. Prehoda and J. M. Pearce, "Potential lives saved by replacing coal with solar photovoltaic electricity production in the U.S," (in en), *Renewable and Sustainable Energy Reviews*, vol. 80, pp. 710-715, 2017/12/01/ 2017, doi: 10.1016/j.rser.2017.05.119.

[89] S. Borenstein, "The Market Value and Cost of Solar Photovoltaic Electricity Production," (in en), *escholarship*, p. 39, 2008/01/14/ 2008. [Online]. Available: https://escholarship.org/uc/item/3ws6r3j4.

[90] US EIA, "Annual Energy Outlook 2015," U.S. Energy Information Administration, Technical Report 2015 2015. [Online]. Available: https://www.eia.gov/outlooks/aeo/pdf/0383(2015).pdf

[91] California Energy Commission, "Heat Rates," *Heat Rates*, 2020/03/06/16:06:07 2020. [Online]. Available: https://ww2.energy.ca.gov/almanac/electricity_data/web_qfer/Heat_Rates_cms.php.

[92] P. Deaver, I. Rhyne, S. Bender, and R. P. Oglesby, "Estimating Burner Tip Prices, Uses, and Potential Issues," California Energy Commission, Technical Report CEC-200-2013-006, 2013/11// 2013. [Online]. Available: https://ww2.energy.ca.gov/2013publications/CEC-200-2013-006/CEC-200-2013-006.pdf

[93] E. Baker, M. Fowlie, D. Lemoine, and S. S. Reynolds, "The Economics of Solar Electricity," *Annual Review of Resource Economics*, vol. 5, no. 1, pp. 387-426, 2013 2013, doi: 10.1146/annurev-resource-091912-151843.

[94] I. Hacerola and I. Liberman, "Comparing a Value of Solar (VOS) Tariff to Net Metering," Master, Duke University, 2015. [Online]. Available: https://dukespace.lib.duke.edu/dspace/handle/10161/9703

[95] "FERC FORM No. 1: Annual Report of Major Electric Utilities, Licensees and Others and Supplemental," ed: Department of Energy, 2020.

[96] D. J. Gotham *et al.*, "MISO Energy and Peak Demand Forecasting for System Planning," Technical Report 2018 2018.

[97] G. Butts, "Escalation: How Much is Enough?," presented at the 2007 Space Visions Congress, 2007/04/26/, 2007. [Online]. Available: https://ntrs.nasa.gov/api/citations/20130011639/downloads/20130011639.pdf.

[98] D. Sivaraman and M. R. Moore, "Economic performance of grid-connected photovoltaics in California and Texas (United States): The influence of renewable energy and climate policies," (in en), *Energy Policy*, vol. 49, pp. 274-287, 2012/10/01/ 2012, doi: 10.1016/j.enpol.2012.06.019.

[99] "Technical Support Document: -Technical Update of the Social Cost of Carbon for Regulatory Impact Analysis -Under Executive Order 12866," ed: Interagency Working Group on Social Cost of Greenhouse Gases, United States Government, 2016.

[100] US BLS, "Consumer Price IndexU.S. City AverageAll Urban Consumers (CPI-U): All Items, 1982-84," (in en), U.S. Bureau Of Labor and Statistics 2020/04/04/10:45:33 2020. [Online]. Available: https://www.bls.gov/regions/midwest/data/consumerpriceindexhistorical_us_table.pdf.

[101] J. L. Sorrels and T. G. Walton, "Chapter 2 - Cost Estimation: Concepts and Methodology," U.S. Environmental Protection Agency, Technical Report 2017/11// 2017.

[102] S. H. L. Yim and S. R. H. Barrett, "Public Health Impacts of Combustion Emissions in the United Kingdom," *Environ. Sci. Technol.*, vol. 46, no. 8, pp. 4291-4296, 2012/04/17/ 2012, doi: 10.1021/es2040416.

[103] F. Caiazzo, A. Ashok, I. A. Waitz, S. H. L. Yim, and S. R. H. Barrett, "Air pollution and early deaths in the United States. Part I: Quantifying the impact of major sectors in 2005," (in en), *Atmospheric Environment*, vol. 79, pp. 198-208, 2013/11/01/ 2013, doi: 10.1016/j.atmosenv.2013.05.081.

[104] I. C. Dedoussi and S. R. H. Barrett, "Air pollution and early deaths in the United States. Part II: Attribution of PM2.5 exposure to emissions species, time, location and sector," (in en), *Atmospheric Environment*, vol. 99, pp. 610-617, 2014/12/01/ 2014, doi: 10.1016/j.atmosenv.2014.10.033.

[105] M. Jerrett *et al.*, "Long-Term Ozone Exposure and Mortality," *N Engl J Med*, vol. 360, no. 11, pp. 1085-1095, 2009/03/12/ 2009, doi: 10.1056/NEJMoa0803894.

[106] N. Z. Muller, R. Mendelsohn, and W. Nordhaus, "Environmental Accounting for Pollution in the United States Economy," (in en), *American Economic Review*, vol. 101, no. 5, pp. 1649-1675, 2011/08// 2011, doi: 10.1257/aer.101.5.1649.

[107] *Hidden costs of energy : unpriced consequences of energy production and use*. Washington, D.C: National Academies Press (in eng), 2010, p. 506.

[108] A. Rabl and J. V. Spadaro, "Public Health Impact of Air Pollution and Implications for the Energy System," *Annual Review of Energy and the Environment*, vol. 25, no. 1, pp. 601-627, 2000 2000, doi: 10.1146/annurev.energy.25.1.601.

[109] B. Machol and S. Rizk, "Economic value of U.S. fossil fuel electricity health impacts," (in en), *Environment International*, vol. 52, pp. 75-80, 2013/02/01/ 2013, doi: 10.1016/j.envint.2012.03.003.

[110] C. P. Carlarne, "U.S. Climate Change Law: A Decade of Flux and an Uncertain Future," (in en), *SSRN Journal*, 2019 2019, doi: 10.2139/ssrn.3493812.

[111] D. C. Jordan and S. R. Kurtz, "Reliability and Geographic Trends of 50,000 Photovoltaic Systems in the USA: Preprint," presented at the European Photovoltaic Solar Energy Conference and Exhibition, Amsterdam, Netherlands, 2014/09//, 2014. [Online]. Available: https://www.osti.gov/biblio/1159380.

[112] A. Phinikarides, N. Kindyni, G. Makrides, and G. E. Georghiou, "Review of photovoltaic degradation rate methodologies," (in en), *Renewable and Sustainable Energy Reviews*, vol. 40, pp. 143-152, 2014/12// 2014, doi: 10.1016/j.rser.2014.07.155.

[113] US EIA, "Capital Cost Estimates for Utility Scale Electricity Generating Plants," U.S. Energy Information Administration, 2016/11// 2016. [Online]. Available: https://www.eia.gov/analysis/studies/powerplants/capitalcost/pdf/capcost_assumption.pdf

[114] "The Heat Rate of Power Generators," (in en), *Sciencing*, 2017/04/24/ 2017. [Online]. Available: https://sciencing.com/heat-rate-power-generators-7958684.html.

[115] US EIA, "SAS Output," *Table 8.2. Average Tested Heat Rates by Prime Mover and Energy Source, 2008 - 2018 (Btu per Kilowatthour)*, 2020/03/04/ 2020. [Online]. Available: https://www.eia.gov/electricity/annual/html/epa_08_01.html.

[116] US EIA, "Electricity generator cost data from survey form EIA-860," *Construction cost data for electric generators installed in 2017*, 2020/03/30/ 2020. [Online]. Available: https://www.eia.gov/electricity/generatorcosts/.

[117] N. W. Council, "Seventh Northwest Conservation and Electric Power Plan," NW Council, Technical Report 2020/03/30/ 2020. Accessed: 2020/03/30/15:30:18. [Online]. Available: https://www.nwcouncil.org/sites/default/files/7thplanfinal_chap07_demandforecast.pdf

[118] US EIA, "Reserve electric generating capacity helps keep the lights on - Today in Energy - U.S. Energy Information Administration (EIA)," 2012/06/01/ 2012. [Online]. Available: https://www.eia.gov/todayinenergy/detail.php?id=6510.

[119] "Transmission Cost Management | Commercial." https://www.aepenergy.com/2018/03/08/february-2018-edition/ (accessed 2020-03-30 13:52:43.

[120] M. A. Mian, *Project Economics and Decision Analysis*, 2nd ed. Tulsa: PennWell Corporation (in English), 2011, p. 481.

[121] State Of Minnesota Public Utilities Commission, "NOTICE OF UPDATED ENVIRONMENTAL EXTERNALITY VALUES," ed: STATE OF MINNESOTA PUBLIC UTILITIES COMMISSION, 2017.

[122] M. F. Akorede, H. Hizam, and E. Pouresmaeil, "Distributed energy resources and benefits to the environment," (in en), *Renewable and Sustainable Energy Reviews*, vol. 14, no. 2, pp. 724-734, 2010/02/01/ 2010, doi: 10.1016/j.rser.2009.10.025.

[123] J. M. Pearce, "Towards Quantifiable Metrics Warranting Industry-Wide Corporate Death Penalties," *Social Sciences*, vol. 8, no. 2, 2019, doi: 10.3390/socsci8020062.

[124] J. A. Burney, "The downstream air pollution impacts of the transition from coal to natural gas in the United States," (in en), *Nature Sustainability*, vol. 3, no. 2, pp. 152-160, 2020/02// 2020, doi: 10.1038/s41893-019-0453-5.

[125] M. Allen, "Liability for climate change," *Nature*, vol. 421, no. 6926, pp. 891-2, Feb 27 2003, doi: 10.1038/421891a.

[126] N. Heidari and J. M. Pearce, "A review of greenhouse gas emission liabilities as the value of renewable energy for mitigating lawsuits for climate change related damages," *Renewable and Sustainable Energy Reviews*, vol. 55, pp. 899-908, 2016, doi: 10.1016/j.rser.2015.11.025.

[127] D. Šebalj, J. Mesarić, and D. Dujak, "Predicting Natural Gas Consumption – A Literature Review," 2017 2017, Varazdin, Croatia, Varazdin: Faculty of Organization and Informatics Varazdin, pp. 293-300.

[128] US EIA, "Factors affecting natural gas prices - U.S. Energy Information Administration (EIA)," *Natural gas explained*, Government Agency 2020/04/04/14:10:55 2020. [Online]. Available: https://www.eia.gov/energyexplained/natural-gas/factors-affecting-natural-gas-prices.php.

[129] M. A. Cohen, P. A. Kauzmann, and D. S. Callaway, "Economic Effects of Distributed PV Generation on California's Distribution System," (in en), *Energy Institute at Haas*, p. 26, 2015/06// 2015. [Online]. Available: https://haas.berkeley.edu/wp-content/uploads/WP260.pdf.

[130] D. P. Brown and D. E. M. Sappington, "Designing Compensation for Distributed Solar Generation:Is Net Metering Ever Optimal?," (in en), *EJ*, vol. 38, no. 3, 2017/07/01/ 2017, doi: 10.5547/01956574.38.3.dbro.

[131] NREL, "Texas | Solar Research | NREL," *NREL Solar Research*, 2020/07/23/ 2020. [Online]. Available: https://www.nrel.gov/solar/rps/tx.html.

[132] Maine Public Utilities Commission, "MPUC: Net Energy Billing," 2020/07/23/ 2020. [Online]. Available: https://www.maine.gov/mpuc/electricity/renewables/neb/index.shtml.

[133] NREL, "Pennsylvania | Midmarket Solar Policies in the United States | Solar Research | NREL," *NREL Solar Research*, 2020/07/23/ 2020. [Online]. Available: https://www.nrel.gov/solar/rps/pa.html.

[134] R. Kenny, C. Law, and J. M. Pearce, "Towards real energy economics: Energy policy driven by life-cycle carbon emission," (in en), *Energy Policy*, vol. 38, no. 4, pp. 1969-1978, 2010/04// 2010, doi: 10.1016/j.enpol.2009.11.078.

[135] Y. Riffonneau, S. Bacha, F. Barruel, and S. Ploix, "Optimal Power Flow Management for Grid Connected PV Systems With Batteries," *IEEE Transactions on Sustainable Energy*, vol. 2, no. 3, pp. 309-320, 2011, doi: 10.1109/tste.2011.2114901.

[136] Y. Ru, J. Kleissl, and S. Martinez, "Storage Size Determination for Grid-Connected Photovoltaic Systems," *IEEE Transactions on Sustainable Energy*, vol. 4, no. 1, pp. 68-81, 2013, doi: 10.1109/tste.2012.2199339.

[137] B. Lu and M. Shahidehpour, "Short-Term Scheduling of Battery in a Grid-Connected PV/Battery System," *IEEE Transactions on Power Systems*, vol. 20, no. 2, pp. 1053-1061, 2005, doi: 10.1109/tpwrs.2005.846060.

[138] G. Mulder, F. D. Ridder, and D. Six, "Electricity storage for grid-connected household dwellings with PV panels," *Solar Energy*, vol. 84, no. 7, pp. 1284-1293, 2010, doi: 10.1016/j.solener.2010.04.005.

[139] B. Preston, "The Influence of Climate Change Litigation on Governments and the Private Sector," Social Science Research Network, Rochester, NY, SSRN Scholarly Paper ID 2345988, 2011/08/11/ 2011. Accessed: 2021/01/14/16:49:37. [Online]. Available: https://papers.ssrn.com/abstract=2345988

[140] D. A. Farber, "Basic Compensation for the Victims of Climate Change," Social Science Research Network, Rochester, NY, SSRN Scholarly Paper ID 954357, 2006/12/01/ 2006. Accessed: 2021/01/14/16:52:07. [Online]. Available: https://papers.ssrn.com/abstract=954357.

[141] D. A. Farber, "The Case for Climate Compensation: Justice for Climate Change Victims in a Complex World," *Utah L. Rev.*, vol. 2008, p. 377, 2008 2008. [Online]. Available: https://heinonline.org/HOL/LandingPage?handle=hein.journals/utahlr2008&div=18&id=&page=.

[142] E. E. Hancock, "Red Dawn, Blue Thunder, Purple Rain: Corporate Risk of Liability for Global Climate Change and the SEC Disclosure Dilemma," (in English), *Georgetown International Environmental Law Review*, vol. 17, no. 2, pp. 233-251, 2005 Winter 2005. [Online]. Available: http://search.proquest.com/docview/225505632/abstract/F74589941093475FPQ/1.

[143] J. K. Healy and J. M. Tapick, "Climate Change: It's Not Just a Policy Issue for Corporate Counsel - It's a Legal Problem," *Colum. J. Envtl. L.*, vol. 29, p. 89, 2004 2004. [Online]. Available: https://heinonline.org/HOL/LandingPage?handle=hein.journals/cjel29&div=7&id=&page=.

[144] D. A. Grossman, "Warming up to a Not-So-Radical Idea: Tort-Based Climate Change Litigation," *Colum. J. Envtl. L.*, vol. 28, p. 1, 2003 2003. [Online]. Available: https://heinonline.org/HOL/LandingPage?handle=hein.journals/cjel28&div=6&id=&page=.

[145] J. Kilinsky, "International Climate Change Liability: A Myth or a Reality," *J. Transnat'l L. & Pol'y*, vol. 18, p. 377, 2008 2009 2008. [Online]. Available: https://heinonline.org/HOL/LandingPage?handle=hein.journals/jtrnlwp18&div=18&id=&page=.

[146] D. A. Farber, "Tort Law in the Era of Climate Change, Katrina and 9/11: Exploring Liability for Extraordinary Risks," Social Science Research Network, Rochester, NY, SSRN Scholarly Paper ID 1121125, 2008/04/13/ 2008. Accessed: 2021/01/14/17:03:48. [Online]. Available: https://papers.ssrn.com/abstract=1121125

[147] R. Schwarze, "Liability for Climate Change: The Benefits, the Costs, and the Transaction Costs," *University of Pennsylvania Law Review*, vol. 155, no. 6, pp. 1947-1952, 2007/06/01/ 2007. [Online]. Available: https://scholarship.law.upenn.edu/penn_law_review/vol155/iss6/16.

[148] D. A. Farber, "Apportioning Climate Change Costs," (in en), *UCLA Journal of Environmental Law and Policy*, vol. 26, no. 1, pp. 21-54, 2008 2008. [Online]. Available: https://escholarship.org/uc/item/0772r66f.

[149] J. Krane, "Climate change and fossil fuel: An examination of risks for the energy industry and producer states," *MRS Energy & Sustainability*, vol. 4, 2017, doi: 10.1557/mre.2017.3.

[150] N. Arnell, "Climate change and global water resources," (in en), *Global Environmental Change*, vol. 9, pp. S31-S49, 1999/10// 1999, doi: 10.1016/S0959-3780(99)00017-5.

[151] M. Kummu, P. J. Ward, H. de Moel, and O. Varis, "Is physical water scarcity a new phenomenon? Global assessment of water shortage over the last two millennia," *Environmental Research Letters*, vol. 5, no. 3, p. 034006, 2010/07// 2010, doi: 10.1088/1748-9326/5/3/034006.

[152] E. D. Coyle, Ed. *Understanding the global energy crisis* (Purdue studies in public policy). West Lafayette, Indiana: Purdue University Press, 2014, p. 304.

[153] L. R. Brown, *Full planet, empty plates: the new geopolitics of food scarcity*, First Edition ed. New York: W.W. Norton & Company, 2012, p. 144.

[154] S. D. Baum, D. C. Denkenberger, and J. Pearce, "Alternative Foods as a Solution to Global Food Supply Catastrophes," (in eng), *Solutions*, vol. 7, no. 4, pp. 31-35, 2016/07// 2016.

[155] J. Rockström, M. Falkenmark, L. Karlberg, H. Hoff, S. Rost, and D. Gerten, "Future water availability for global food production: The potential of green water for increasing resilience to global change: WATER AVAILABILITY FOR FOOD PRODUCTION," (in en), *Water Resources Research*, vol. 45, no. 7, 2009/07// 2009, doi: 10.1029/2007WR006767.

[156] A. K. Misra, "Climate change and challenges of water and food security," (in en), *International Journal of Sustainable Built Environment*, vol. 3, no. 1, pp. 153-165, 2014/06// 2014, doi: 10.1016/j.ijsbe.2014.04.006.

[157] J. Cook *et al.*, "Consensus on consensus: a synthesis of consensus estimates on human-caused global warming," *Environmental Research Letters*, vol. 11, no. 4, p. 048002, 2016/04/01/ 2016, doi: 10.1088/1748-9326/11/4/048002.

[158] S. Solomon, C. Intergovernmental Panel on Climate, and C. Intergovernmental Panel on Climate, Eds. *Climate change 2007: the physical science basis: contribution of Working Group I to the Fourth Assessment Report of the Intergovernmental Panel on Climate Change*. Cambridge ; New York: Cambridge University Press, 2007, p. 996.

[159] W. W. Kellogg and R. Schware, *Climate Change and Society: Consequences of Increasing Atmospheric Carbon Dioxide*, 1 ed. New York: Routledge (in en), 2019, p. 192.

[160] B. Bates, Z. W. Kundzewicz, S. Wu, and J. P. Palutikof, Eds. *Climate change and water. Technical Paper of the Intergovernmental Panel on Climate Change* (IPCC Technical Paper; 6). Geneva: IPCC Secretariat (in eng), 2008, p. 210.

[161] M. de Wit, "Changes in Surface Water Supply Across Africa with Predicted Climate Change," (in en), *Science*, vol. 311, no. 5769, pp. 1917-1921, 2006/03/31/ 2006, doi: 10.1126/science.1119929.

[162] IPCC, O. Edenhofer *et al.*, Eds. *Climate change 2014: mitigation of climate change: Working Group III contribution to the Fifth Assessment Report of the Intergovernmental Panel on Climate Change*. New York, NY: Cambridge University Press, 2014, p. 1435.

[163] J. M. Pearce, "Photovoltaics — a path to sustainable futures," (in en), *Futures*, vol. 34, no. 7, pp. 663-674, 2002/09// 2002, doi: 10.1016/S0016-3287(02)00008-3.

[164] F. Creutzig, P. Agoston, J. C. Goldschmidt, G. Luderer, G. Nemet, and R. C. Pietzcker, "The underestimated potential of solar energy to mitigate climate change," (in en), *Nat Energy*, vol. 2, no. 9, p. 17140, 2017/09// 2017, doi: 10.1038/nenergy.2017.140.

[165] SEIA, "Siting, Permitting & Land Use for Utility-Scale Solar," (in en), *SEIA*, Industry 2020/11/13/ 2020. [Online]. Available: https://www.seia.org/initiatives/siting-permitting-land-use-utility-scale-solar.

[166] J. G. Groesbeck and J. M. Pearce, "Coal with Carbon Capture and Sequestration is not as Land Use Efficient as Solar Photovoltaic Technology for Climate Neutral Electricity Production," (in en), *Sci Rep*, vol. 8, no. 1, p. 13476, 2018/12// 2018, doi: 10.1038/s41598-018-31505-3.

[167] FAO, Ed. *How does international price volatility affect domestic economies and food security?* (The state of food insecurity in the world, no. 2011). Rome: FAO (in eng), 2011, p. 50.

[168] M. Rosa-Clot, P. Rosa-Clot, G. M. Tina, and P. F. Scandura, "Submerged photovoltaic solar panel: SP2," (in en), *Renewable Energy*, vol. 35, no. 8, pp. 1862-1865, 2010/08// 2010, doi: 10.1016/j.renene.2009.10.023.

[169] G. M. Tina, M. Rosa-Clot, P. Rosa-Clot, and P. F. Scandura, "Optical and thermal behavior of submerged photovoltaic solar panel: SP2," (in en), *Energy*, vol. 39, no. 1, pp. 17-26, 2012/03/01/ 2012, doi: 10.1016/j.energy.2011.08.053.

[170] S. A. Abdulgafar, O. S. Omar, and K. M. Yousif, "Improving the efficiency of polycrystalline solar panel via water immersion method," *IJIRSET*, vol. 3, no. 1, pp. 96-101, 2014/01// 2014.

[171] S. Mehrotra, P. Rawat, M. Debbarma, and K. Sudhakar, "Performance of a solar panel with water immersion cooling technique," *International Journal of Science, Environment and Technology*, vol. 3, no. 3, pp. 1161-1172, 2014 2014.

[172] M. Rosa-Clot, G. M. Tina, and S. Nizetic, "Floating photovoltaic plants and wastewater basins: an Australian project," (in en), *Energy Procedia*, vol. 134, pp. 664-674, 2017/10/01/ 2017, doi: 10.1016/j.egypro.2017.09.585.

[173] L. Liu, Q. Wang, H. Lin, H. Li, Q. Sun, and R. wennersten, "Power Generation Efficiency and Prospects of Floating Photovoltaic Systems," (in en), *Energy Procedia*, vol. 105, pp. 1136-1142, 2017/05// 2017, doi: 10.1016/j.egypro.2017.03.483.

[174] D. Mittal, B. K. Saxena, and K. V. S. Rao, "Floating solar photovoltaic systems: An overview and their feasibility at Kota in Rajasthan," in *2017 International Conference on Circuit ,Power and Computing Technologies (ICCPCT)*, 2017/04// 2017, Kollam, India: IEEE, pp. 1-7, doi: 10.1109/ICCPCT.2017.8074182. [Online]. Available: http://ieeexplore.ieee.org/document/8074182/

[175] D. Mittal, B. Kumar Saxena, and K. V. S. Rao, "Potential of floating photovoltaic system for energy generation and reduction of water evaporation at four different lakes in Rajasthan," in *2017 International Conference On Smart Technologies For Smart Nation (SmartTechCon)*, 2017/08// 2017, pp. 238-243, doi: 10.1109/SmartTechCon.2017.8358376. [Online]. Available: https://ieeexplore.ieee.org/document/8358376

[176] M. Abid, Z. Abid, J. Sagin, R. Murtaza, D. Sarbassov, and M. Shabbir, "Prospects of floating photovoltaic technology and its implementation in Central and South Asian Countries," (in en), *Int. J. Environ. Sci. Technol.*, vol. 16, no. 3, pp. 1755-1762, 2019/03// 2019, doi: 10.1007/s13762-018-2080-5.

[177] L. E. Teixeira, J. Caux, A. Beluco, I. Bertoldo, J. A. S. Louzada, and R. C. Eifler, "Feasibility Study of a Hydro PV Hybrid System Operating at a Dam for Water Supply in Southern Brazil," *JPEE*, vol. 03, no. 09, pp. 70-83, 2015 2015, doi: 10.4236/jpee.2015.39006.

[178] G. Vasco, J. S. Silva, and A. Beluco, "Feasibility Study of a PV Hydro Hybrid System, With Photovoltaic Panels on Floating Structures," *IOP Conf. Ser.: Mater. Sci. Eng.*, vol. 366, p. 012011, 2018/06// 2018, doi: 10.1088/1757-899X/366/1/012011.

[179] W. Charles Lawrence Kamuyu, J. Lim, C. Won, and H. Ahn, "Prediction Model of Photovoltaic Module Temperature for Power Performance of Floating PVs," (in en), *Energies*, vol. 11, no. 2, p. 447, 2018/02/18/ 2018, doi: 10.3390/en11020447.

[180] P. Ranjbaran, H. Yousefi, G. B. Gharehpetian, and F. R. Astaraei, "A review on floating photovoltaic (FPV) power generation units," (in en), *Renewable and Sustainable Energy Reviews*, vol. 110, pp. 332-347, 2019/08// 2019, doi: 10.1016/j.rser.2019.05.015.

[181] A.-K. Lee, G.-W. Shin, S.-T. Hong, and Y.-K. Choi, "A study on development of ICT convergence technology for tracking-type floating photovoltaic systems," *SGCE*, vol. 3, no. 1, pp. 80-87, 2014 2014, doi: 10.12720/sgce.3.1.80-87.

[182] J. Song and Y. Choi, "Analysis of the Potential for Use of Floating Photovoltaic Systems on Mine Pit Lakes: Case Study at the Ssangyong Open-Pit Limestone Mine in Korea," (in en), *Energies*, vol. 9, no. 2, p. 102, 2016/02/10/ 2016, doi: 10.3390/en9020102.

[183] Y. K. Choi, W. S. Choi, and J. H. Lee, "Empirical Research on the Efficiency of Floating PV Systems," (in en), *sci adv mater*, vol. 8, no. 3, pp. 681-685, 2016/03/01/ 2016, doi: 10.1166/sam.2016.2529.

[184] J. D. Stachiw, "Performance of Photovoltaic Cells in Undersea Environment," (in en), *Journal of Engineering for Industry,* vol. 102, no. 1, pp. 51-59, 1980/02/01/ 1980, doi: 10.1115/1.3183829.

[185] M. K. Rathod and J. Banerjee, "Thermal stability of phase change materials used in latent heat energy storage systems: A review," (in en), *Renewable and Sustainable Energy Reviews,* vol. 18, pp. 246-258, 2013/02/01/ 2013, doi: 10.1016/j.rser.2012.10.022.

[186] C. J. Ho, W.-L. Chou, and C.-M. Lai, "Thermal and electrical performance of a water-surface floating PV integrated with a water-saturated MEPCM layer," (in en), *Energy Conversion and Management,* vol. 89, pp. 862-872, 2015/01// 2015, doi: 10.1016/j.enconman.2014.10.039.

[187] C. J. Ho, W.-L. Chou, and C.-M. Lai, "Thermal and electrical performances of a water-surface floating PV integrated with double water-saturated MEPCM layers," (in en), *Applied Thermal Engineering,* vol. 94, pp. 122-132, 2016/02// 2016, doi: 10.1016/j.applthermaleng.2015.10.097.

[188] P. Mayville, N. V. Patil, and J. M. Pearce, "Distributed Manufacturing of After Market Flexible Floating Photovoltaic Modules," *Journal of Cleaner Production,* pp. in-press, 2020 2020.

[189] M. T. Moreo and A. Swancar, "Evaporation from Lake Mead, Nevada and Arizona, March 2010 through February 2012," in "Scientific Investigations Report," U.S. Geological Survey, Scientific Investigations Report 2013-5229, 2013 2013. [Online]. Available: https://pubs.usgs.gov/sir/2013/5229/pdf/sir2013-5229.pdf

[190] NPS, "Overview of Lake Mead - Lake Mead National Recreation Area (U.S. National Park Service)," (in en), *National Park Service,* 2019/12/06/ 2019. [Online]. Available: https://www.nps.gov/lake/learn/nature/overview-of-lake-mead.htm.

[191] J. L. Monteith, "Evaporation and environment," (in eng), *Symp. Soc. Exp. Biol.,* vol. 19, pp. 205-234, 1965 1965. [Online]. Available: http://www.ncbi.nlm.nih.gov/pubmed/5321565.

[192] R. G. Allen and Fao, *Crop evapotranspiration: guidelines for computing crop water requirements* (FAO irrigation and drainage paper, no. 56). Rome: Food and Agriculture Organization of the United Nations, 1998, p. 300.

[193] K. S. Hayibo and J. M. Pearce, "Calculations for Water Conservation Potential of Self-funded Foam-Based Flexible Surface-Mounted Floatovoltaics," (in en), *OSF,* 2020/10/13/ 2020, doi: None.

[194] World Bank Group, Esmap, and Seris, "Where Sun Meets Water: Floating Solar Handbook for Practitioners," World Bank Group, Washington, D.C, Technical Report 143112, 2019/10/28/ 2019. [Online]. Available: https://openknowledge.worldbank.org/handle/10986/32804

[195] N. O. A. A. US Department of Commerce, "NDBC Station Page," (in En-us), 2020/06/22/14:32:31 2020. [Online]. Available: https://www.ndbc.noaa.gov/station_page.php?station=nbba3.

[196] Weather Underground, "Las Vegas, NV Weather History | Weather Underground," 2020/06/22/14:36:01 2020. [Online]. Available: https://www.wunderground.com/history/daily/us/nv/las-vegas/KLAS/date/2018-2-28.

[197] SOLCAST, "Solar Irradiance Data," ed: The Australian National University Data Commons, 2020.

[198] NPS, "Storage Capacity of Lake Mead - Lake Mead National Recreation Area (U.S. National Park Service)," (in en), *National Park Service*, 2019/08/05/ 2019. [Online]. Available: https://www.nps.gov/lake/learn/nature/storage-capacity-of-lake-mead.htm.

[199] N. O. A. A. US Department of Commerce, "NDBC Station History Page," (in En-us), 2020/03/16/ 2020. [Online]. Available: https://www.ndbc.noaa.gov/station_history.php?station=nbba3.

[200] *soul-ash/floating-pv: Lake Mead Data Cleaning Code*. (2020). Zenodo. Accessed: 2020/07/26/19:01:32. [Online]. Available: https://zenodo.org/record/3960777

[201] L. Zotarelli, M. D. Dukes, C. C. Romero, and K. W. Migliaccio, "Step by Step Calculation of the Penman-Monteith Evapotranspiration (FAO-56 Method)," ed: Agricultural and Biological Engineering Department, UF/IFAS Extension, 2018.

[202] A. Weiss and C. J. Hays, "Calculating daily mean air temperatures by different methods: implications from a non-linear algorithm," (in en), *Agricultural and Forest Meteorology*, vol. 128, no. 1-2, pp. 57-65, 2005/01// 2005, doi: 10.1016/j.agrformet.2004.08.008.

[203] T.-T. Shi, D.-X. Guan, J.-B. Wu, A.-Z. Wang, C.-J. Jin, and S.-J. Han, "Comparison of methods for estimating evapotranspiration rate of dry forest canopy: Eddy covariance, Bowen ratio energy balance, and Penman-Monteith equation," (in en), *Journal of Geophysical Research: Atmospheres*, vol. 113, no. D19, 2008 2008, doi: 10.1029/2008JD010174.

[204] Sunpower, "SunPower Flexible Solar Panels | SPR-E-Flex-110," (in en), *Sunpower*, Company 2018/09// 2018. [Online]. Available: https://us.sunpower.com/sites/default/files/110w-flexible-panel-spec-sheet.pdf.

[205] Foam Factory, "Foam Factory Data Sheets | Foam Factory, Inc," *Form Factory*, 2020 2020. [Online]. Available: https://www.foambymail.com/datasheets.html.

[206] M. A. L. Domany, L. Touchart, P. Bartout, and R. Nedjai, "THE EVAPORATION FROM PONDS IN THE FRENCH MIDWEST," (in en), *Lakes reservoirs and ponds*, vol. 7, no. 2, pp. 75-88, 2013 2013. [Online]. Available: http://www.limnology.ro/Lakes/2013/201307206.pdf.

[207] W. Abtew and A. Melesse, *Evaporation and Evapotranspiration*. Dordrecht: Springer Netherlands (in en), 2013.

[208] M. E. Jensen, A. Dotan, and R. Sanford, "Penman-Monteith Estimates of Reservoir Evaporation," presented at the World Water and Environmental Resources Congress 2005, 2005/07//, 2005. [Online]. Available: http://ascelibrary.org/doi/10.1061/40792%28173%29548.

[209] J. W. Finch, R. L. Hall, B. Great, and A. Environment, *Estimation of open water evaporation: a review of methods*. Bristol: Environment Agency (in en), 2005.

[210] D. L. McJannet, I. T. Webster, and F. J. Cook, "An area-dependent wind function for estimating open water evaporation using land-based meteorological data," (in en), *Environmental Modelling & Software*, vol. 31, pp. 76-83, 2012/05// 2012, doi: 10.1016/j.envsoft.2011.11.017.

[211] S. B. Idso and R. D. Jackson, "Thermal radiation from the atmosphere," (in en), *J. Geophys. Res.*, vol. 74, no. 23, pp. 5397-5403, 1969/10/20/ 1969, doi: 10.1029/JC074i023p05397.

[212] M. M. Mekonnen and A. Y. Hoekstra, "The blue water footprint of electricity from hydropower," (in en), *Hydrol. Earth Syst. Sci.*, vol. 16, no. 1, pp. 179-187, 2012/01/20/ 2012, doi: 10.5194/hess-16-179-2012.

[213] O. O. Jegede, E. O. Ogolo, and T. O. Aregbesola, "Estimating net radiation using routine meteorological data at a tropical location in Nigeria," (in en), *International Journal of Sustainable Energy*, vol. 25, no. 2, pp. 107-115, 2006/06// 2006, doi: 10.1080/14786450600593261.

[214] R. Niclòs, E. Valor, V. Caselles, C. Coll, and J. M. Sánchez, "In situ angular measurements of thermal infrared sea surface emissivity—Validation of models,"

(in en), *Remote Sensing of Environment*, vol. 94, no. 1, pp. 83-93, 2005/01/15/ 2005, doi: 10.1016/j.rse.2004.09.002.

[215] H. A. R. de Bruin, "Temperature and energy balance of a water reservoir determined from standard weather data of a land station," (in en), *Journal of Hydrology*, vol. 59, no. 3, pp. 261-274, 1982/11/01/ 1982, doi: 10.1016/0022-1694(82)90091-9.

[216] J. W. Finch, "A comparison between measured and modelled open water evaporation from a reservoir in south-east England," (in en), *Hydrol. Process.*, vol. 15, no. 14, pp. 2771-2778, 2001/10/15/ 2001, doi: 10.1002/hyp.267.

[217] D. McJannet, I. T. Webster, M. Stenson, and B. S. Sherman, "Estimating open water evaporation for the Murray-Darling Basin," (in English), *CSIRO: Water for a Healthy Country National Research Flagship*, p. 58, 2008 2008, doi: https://doi.org/10.4225/08/5859742b67eb8.

[218] J. A. Duffie and W. A. Beckman, "Chapter 23 - Design of Photovoltaic Systems," in *Solar engineering of thermal processes / John A. Duffie, William A. Beckman*, 4th ed ed. Hoboken: John Wiley, 2013.

[219] S. Shaari, K. Sopian, N. Amin, and M. N. Kassim, "The Temperature Dependence Coefficients of Amorphous Silicon and Crystalline Photovoltaic Modules Using Malaysian Field Test Investigation," (in en), *American Journal of Applied Sciences*, vol. 6, no. 4, pp. 586-593, 2009/04/30/ 2009, doi: 10.3844/ajassp.2009.586.593.

[220] P. Kamkird, N. Ketjoy, W. Rakwichian, and S. Sukchai, "Investigation on Temperature Coefficients of Three Types Photovoltaic Module Technologies under Thailand Operating Condition," (in en), *Procedia Engineering*, vol. 32, pp. 376-383, 2012/01/01/ 2012, doi: 10.1016/j.proeng.2012.01.1282.

[221] MathWorks, "Multiple linear regression - MATLAB regress," *MathWorks Help Center*, 2020/07/30/13:16:18 2020. [Online]. Available: https://www.mathworks.com/help/stats/regress.html.

[222] M. R. Maghami, H. Hizam, C. Gomes, M. A. Radzi, M. I. Rezadad, and S. Hajighorbani, "Power loss due to soiling on solar panel: A review," (in en), *Renewable and Sustainable Energy Reviews*, vol. 59, pp. 1307-1316, 2016/06/01/ 2016, doi: 10.1016/j.rser.2016.01.044.

[223] M. M. Fouad, L. A. Shihata, and E. I. Morgan, "An integrated review of factors influencing the perfomance of photovoltaic panels," (in en), *Renewable and Sustainable Energy Reviews*, vol. 80, pp. 1499-1511, 2017/12/01/ 2017, doi: 10.1016/j.rser.2017.05.141.

[224] M. Z. Jacobson and V. Jadhav, "World estimates of PV optimal tilt angles and ratios of sunlight incident upon tilted and tracked PV panels relative to horizontal panels," (in en), *Solar Energy*, vol. 169, pp. 55-66, 2018/07/15/ 2018, doi: 10.1016/j.solener.2018.04.030.

[225] M. E. Taboada, L. Cáceres, T. A. Graber, H. R. Galleguillos, L. F. Cabeza, and R. Rojas, "Solar water heating system and photovoltaic floating cover to reduce evaporation: Experimental results and modeling," (in en), *Renewable Energy*, vol. 105, pp. 601-615, 2017/05/01/ 2017, doi: 10.1016/j.renene.2016.12.094.

[226] Las Vegas Valley Water District, "Water rates," *Las Vegas Valley Water District*, 2020/10/16/ 2020. [Online]. Available: https://www.lvvwd.com/customer-service/pay-bill/water-rates.html.

[227] S. Karambelkar, "Hydropower Operations in the Colorado River Basin: Institutional Analysis of Opportunities and Constraints," Hydropower Foundation, Technical Report 1638690, 2018/09/10/ 2018. Accessed: 2020/11/14/03:01:52. [Online]. Available: https://www.osti.gov/biblio/1638690-hydropower-operations-colorado-river-basin-institutional-analysis-opportunities-constraints

[228] H. K. Trabish, "Hoover Dam, the drought, and a looming energy crisis," (in en-US), *Utility Dive*, 2014 2014. [Online]. Available: https://www.utilitydive.com/news/hoover-dam-the-drought-and-a-looming-energy-crisis/281133/.

[229] C. L. Westenburg, G. A. DeMeo, and D. J. Tanko, "Evaporation from Lake Mead, Arizona and Nevada, 1997–99," U.S. Geological Survey, VA, USA, Scientific Investigations Report 2006-5252, 2006 2006. Accessed: 2020/06/26/17:50:27. [Online]. Available: https://pubs.usgs.gov/sir/2006/5252/pdf/sir20065252.pdf

[230] US EPA, "Statistics and Facts," (in en), *US EPA*, Overviews and Factsheets 2017/01/23/T15:16:53-05:00 2017. [Online]. Available: https://www.epa.gov/watersense/statistics-and-facts.

[231] US Census Bureau, "U.S. Census Bureau QuickFacts: Los Angeles city, California," (in en), *QuickFacts Los Angeles city, California*, Government Agency 2020/10/10/16:32:28 2020. [Online]. Available: https://www.census.gov/quickfacts/losangelescitycalifornia.

[232] US Census Bureau, "U.S. Census Bureau QuickFacts: Nevada," (in en), *QuickFacts Nevada*, Government Agency 2020/10/13/18:19:00 2020. [Online]. Available: https://www.census.gov/quickfacts/NV.

[233] US Census Bureau, "U.S. Census Bureau QuickFacts: Reno city, Nevada; Las Vegas city, Nevada; Henderson city, Nevada," (in en), *QuickFacts Reno city, Nevada; Las Vegas city, Nevada; Henderson city, Nevada*, Government Agency 2020/10/13/18:22:24 2020. [Online]. Available: https://www.census.gov/quickfacts/fact/table/renocitynevada,lasvegascitynevada,hendersoncitynevada/PST045219.

[234] J. J. Barsugli, K. Nowak, B. Rajagopalan, J. R. Prairie, and B. Harding, "Comment on "When will Lake Mead go dry?" by T. P. Barnett and D. W. Pierce: COMMENTARY," (in en), *Water Resources Research*, vol. 45, no. 9, 2009/09// 2009, doi: 10.1029/2008WR007627.

[235] B. Rajagopalan *et al.*, "Water supply risk on the Colorado River: Can management mitigate?," (in en), *Water Resources Research*, vol. 45, no. 8, 2009 2009, doi: 10.1029/2008WR007652.

[236] T. P. Barnett and D. W. Pierce, "When will Lake Mead go dry?," (in en), *Water Resources Research*, vol. 44, no. 3, 2008 2008, doi: 10.1029/2007WR006704.

[237] US EIA, "Frequently Asked Questions (FAQs) - U.S. Energy Information Administration (EIA)," *How much electricity does an American home use?*, Government Agency 2020/10/09/ 2020. [Online]. Available: https://www.eia.gov/tools/faqs/faq.php?id=97&t=3.

[238] US EIA, "Electric Power Annual 2018," U.S. Energy Information Administration, Washington, D.C, Technical Report 2019/10// 2019. [Online]. Available: https://www.eia.gov/electricity/annual/pdf/epa.pdf

[239] G. D. Thurston *et al.*, "Ischemic Heart Disease Mortality and Long-Term Exposure to Source-Related Components of U.S. Fine Particle Air Pollution," (in eng), *Environ Health Perspect*, vol. 124, no. 6, pp. 785-794, 2016//06/ 2016, doi: 10.1289/ehp.1509777.

[240] D. Krewski *et al.*, "Extended Follow-Up and Spatial Analysis of the American Cancer Society Study Linking Particulate Air Pollution and Mortality," Health Effects Institute, Boston, MA, Research Report Report 140, 2009 2009. [Online]. Available: https://www.healtheffects.org/publication/extended-follow-and-spatial-analysis-american-cancer-society-study-linking-particulate

[241] R. S. Spencer, J. Macknick, A. Aznar, A. Warren, and M. O. Reese, "Floating Photovoltaic Systems: Assessing the Technical Potential of Photovoltaic Systems on Man-Made Water Bodies in the Continental United States," (in en), *Environ. Sci. Technol.*, vol. 53, no. 3, pp. 1680-1689, 2019/02/05/ 2019, doi: 10.1021/acs.est.8b04735.

[242] S. Gorjian, H. Sharon, H. Ebadi, K. Kant, F. B. Scavo, and G. M. Tina, "Recent technical advancements, economics and environmental impacts of floating photovoltaic solar energy conversion systems," (in en), *Journal of Cleaner Production,* vol. 278, p. 124285, 2021/01// 2021, doi: 10.1016/j.jclepro.2020.124285.

[243] H. Dinesh and J. M. Pearce, "The potential of agrivoltaic systems," (in en), *Renewable and Sustainable Energy Reviews,* vol. 54, pp. 299-308, 2016/02/01/ 2016, doi: 10.1016/j.rser.2015.10.024.

[244] A. M. Pringle, R. M. Handler, and J. M. Pearce, "Aquavoltaics: Synergies for dual use of water area for solar photovoltaic electricity generation and aquaculture," (in en), *Renewable and Sustainable Energy Reviews,* vol. 80, pp. 572-584, 2017/12/01/ 2017, doi: 10.1016/j.rser.2017.05.191.

[245] K. Moustafa, "Toward Future Photovoltaic-Based Agriculture in Sea," (in en), *Trends in Biotechnology,* vol. 34, no. 4, pp. 257-259, 2016/04/01/ 2016, doi: 10.1016/j.tibtech.2015.12.012.

[246] D. Sica, O. Malandrino, S. Supino, M. Testa, and M. C. Lucchetti, "Management of end-of-life photovoltaic panels as a step towards a circular economy," (in en), *Renewable and Sustainable Energy Reviews,* vol. 82, pp. 2934-2945, 2018/02/01/ 2018, doi: 10.1016/j.rser.2017.10.039.

[247] C. C. Farrell *et al.*, "Technical challenges and opportunities in realising a circular economy for waste photovoltaic modules," (in en), *Renewable and Sustainable Energy Reviews,* vol. 128, p. 109911, 2020/08/01/ 2020, doi: 10.1016/j.rser.2020.109911.

[248] R. Contreras Lisperguer, E. Muñoz Cerón, J. de la Casa Higueras, and R. D. Martín, "Environmental Impact Assessment of crystalline solar photovoltaic panels' End-of-Life phase: Open and Closed-Loop Material Flow scenarios," (in en), *Sustainable Production and Consumption,* vol. 23, pp. 157-173, 2020/07/01/ 2020, doi: 10.1016/j.spc.2020.05.008.

[249] J. M. Pearce, "Industrial symbiosis of very large-scale photovoltaic manufacturing," (in en), *Renewable Energy,* vol. 33, no. 5, pp. 1101-1108, 2008/05/01/ 2008, doi: 10.1016/j.renene.2007.07.002.

[250] N. C. McDonald and J. M. Pearce, "Producer responsibility and recycling solar photovoltaic modules," (in en), *Energy Policy,* vol. 38, no. 11, pp. 7041-7047, 2010/11/01/ 2010, doi: 10.1016/j.enpol.2010.07.023.

[251] E. T. Kabamba and D. Rodrigue, "The effect of recycling on LDPE foamability: Elongational rheology," (in en), *Polymer Engineering & Science,* vol. 48, no. 1, pp. 11-18, 2008 2008, doi: 10.1002/pen.20807.

[252] M. Bedell, M. Brown, A. Kiziltas, D. Mielewski, S. Mukerjee, and R. Tabor, "A case for closed-loop recycling of post-consumer PET for automotive foams," (in en), *Waste Management,* vol. 71, pp. 97-108, 2018/01/01/ 2018, doi: 10.1016/j.wasman.2017.10.021.

[253] A. M. Al-Sabagh, F. Z. Yehia, G. Eshaq, A. M. Rabie, and A. E. ElMetwally, "Greener routes for recycling of polyethylene terephthalate," (in en), *Egyptian Journal of Petroleum,* vol. 25, no. 1, pp. 53-64, 2016/03/01/ 2016, doi: 10.1016/j.ejpe.2015.03.001.